SISSA - SCUOLA INTERNAZIONALE SUPERIORE DI STUDI AVANZATI
TRIESTE
Strada Costiera 11

ISAS - INTERNATIONAL SCHOOL FOR ADVANCED STUDIES

Andrzej Fleszar

DIELECTRIC RESPONSE IN SEMICONDUCTORS:

THEORY AND APPLICATIONS

Supervisor: Prof. R. Resta

Academic Year 1984/1985

TRIESTE

International School for Advanced Studies

Trieste

Andrzej Fleszar

DIELECTRIC RESPONSE IN SEMICONDUCTORS:

THEORY AND APPLICATIONS

Supervisor: Prof. R. Resta

Academic Year 1984/1985

ACKNOWLEDGMENTS

I would like to express my gratitude to Professor Raffaele Resta for his courageous decision to cooperate with me as well as his extremely friendly and helpful supervision of this work.

I am also indebted to Professor Alfonso Baldereschi for his idea, at the very begining, to give me a small exercise which pushed me into the field of band structure calculations and gave me a "fulcrum" to do also this work.

I am grateful to Professor Erio Tosatti for several of his ideas that have found their realization in this work, for his invitations to Trieste and his belief that I will succeed...

I would like also to thank Professor Karel Kunc for his very helpful cooperation during many parts of this work as well as for his moral encouragement.

CONTENTS

I. INTRODUCTION

This work is concerned with the static screening properties of crystalline solids. When an external perturbation is applied to a solid, the particles of it (ions and electrons) rearrange themselves into a relaxed configuration which (at zero temperature) minimizes the total energy of the system. This process results in the polarization of the medium and in the screening of the perturbation in the way that will be described in the second chapter of this work. On the microscopic level this means that the system assumes new quantum states in agreement with the laws of quantum mechanics and (possibly) thermodynamics.

The microscopic description of the many-body system is by itself an extremly complex problem, manageable however after a series of approximations which work surprisingly well in a large class of materials. The very first one in the context of our work is the adiabatic approximation [1-3]. Within this approximation the motion of electrons is "decoupled" from the motion of ions of the system, or in other words, the electrons assume their own quantum states as if the ions were classical particles in a given fixed configuration. The purely electronic response to the external perturbation becomes then the basic quantity which in turn determines, via lattice dynamics, the response of ions.

The many-electron problem we are left with is still a formidable problem. This is usually treated within some selfconsistent scheme, like for example local density functional approximation (LDA) to functional density formalism [4-6], which has recently proved to work very well for many solids.

When the external perturbation is weak the electronic response is linear in perturbation and a linear response operator in $\vec{r}$-space can be defined. This operator when

transformed to Fourier space in crystals assumes the form of a matrix, like e.g. so called polarizability, dielectric, etc. matrices. The first-principle calculation of static electronic polarizability and dielectric matrices in semiconductors is the main subject of this work.

When the response matrices are known the effect induced by the presence of a weak external perturbation can be calculated. One of the perturbations which have been commonly treated in this framework, has been the motion of the ions of the solid themselves. The electronic dielectric response to ionic displacements in a given phonon mode determines in fact lattice dynamics of the solid [7-9]. Some other problems studied recently in this way from first principles concerned the macroscopic dielectric properties of semiconductors [10], the internal microscopic polarization in a crystal induced from a constant electric field [11] or from ion displacements from equilibrium in a phonon mode [12,13] and related subjects. It should be noticed however that the complete knowledge of dielectric matrices in a crystal allows to study the response to any weak perturbation.

The present work overcomes in a sense some important technical limitations which existed previously in this kind of calculations: as a consequence, first-principle results which are qualitatively new have been achieved here.

The calculation of a first-principle dielectric matrix through the usual techniques [30,31,10] is computationally very costly and mostly situations of high symmetry have been considered so far. By proposing some new practical ideas (Ref. [14] and the third part of chapter III) we were able to show the feasibility of accurate ab-initio evaluation of response matrices in semiconductors at any point of the Brillouin zone. As an important demonstration of the power of the method for "non-symmetric" problems we have calculated the interatomic force constants in germanium. The interatomic forces in a crystal involve two atoms only or - in other words - correspond to geometry when only one atom is displaced, while we measure

the forces on all other kept at rest. Such a problem is clearly non periodic and the state-of-art "direct" methods for theoretical lattice dynamics were not able to treat it up to now. As a second novel application we present here also the first ab-initio calculation of the screening of Coulombic impurity potentials in germanium. We believe that nowadays it is practically possible to study within first principles any kind of a weak perturbation in semiconductors and we expect the interest in the theoretical methods of solid state physics we are going to describe here will be growing. Some perspective applications are proposed in the last chapter of this work, where the capabilities of the method are discussed.

The second chapter of this work is devoted to general definitions and formulation of the problem. In the third one we will discuss the practical methods for calculating the response operators in semiconductors together with a short survey of recent achievements in the field. The subject of this chapter are also the novel techniques we have developed and which underlie our calculations in germanium. In the fourth chapter we shall give the technical details concerning mostly band structure methods used in this work. There we shall also illustrate one of the possible applications of the dielectric matrix concept in the acceleration of the band structure selfconsistent iterations. In the fifth chapter the results of different calculations of dielectric matrices in germanium are presented and compared. The sixth chapter deals with phonons. Apart from giving there some new results for phonon frequencies at various points of the Brillouin zone, we discuss the effects of exchange correlation and local fields on the lattice dynamics and stability of crystal. The cruciality of these effects is pointed out by us for the first time. Then we present our calculation of interplanar and interatomic force constants in germanium. The latter ones are calculated for the first time in this work and, as said above, are out of reach of different computational techniques for first-principles lattice dynamics. Phonon dispersion curves are also shown and compared to

experience. In chapter seven some of our recent results concerning realistic screening of impurities, with full inclusion of local-field effects, are given. Conclusions and perspectives close our work in chapter eight.

CHAPTER II

RESPONSE MATRICES IN CRYSTALLINE SOLIDS: THEORY

In the first part of this chapter we shall give the basic definitions concerning the problem of linear electronic screening in crystals. These will be the exact formulations not connected to any particular many-electron scheme. The differentiations and adoptation of general notions to a given selfconsistent scheme will be studied in the second part, while some important analytical properties of response functions and related sum rules will be analized in the last part of the chapter.

II. 1. Exact Formulations.

A static electric field in electrodynamics can be described completely by a scalar time-independent potential. In order to discuss external static perturbation in crystal we can assume the presence of the external electrostatic potential φ^{ext}. Let the unperturbed all-electron Hamiltonian be:

$$H^{\circ}(\vec{r}_1,\vec{r}_2,\ldots) = \sum_i \frac{p_i^2}{2m} + \frac{1}{2}\sum_{i\neq j}\frac{e^2}{|\vec{r}_i-\vec{r}_j|} + \sum_i V_I(\vec{r}_i) \qquad (II-1)$$

where V_I is the potential energy due to all the ions. The electrostatic potential φ^{ext} gives rise to a perturbation H' to this Hamiltonian coupled with the electron density operator $\hat{\rho}$:

$$H'(\vec{r}_1,\vec{r}_2,\ldots) = -\sum_i e\,\varphi^{ext}(\vec{r}_i) = -e\int d\vec{r}\;\hat{\rho}(\vec{r})\,\varphi^{ext}(\vec{r}) \qquad (II-2)$$

where

$$\hat{\rho}(\vec{r}) = \sum_i \delta(\vec{r}-\vec{r}_i) \qquad (II-3)$$

Suppose φ^{ext} (and H') is small. Then by means of perturbation theory we have a new ground state of the system given up to the first order in H' by:

$$|\tilde{0}\rangle = |0\rangle + \sum_{m\neq 0}\frac{\langle m|H'|0\rangle}{E_0-E_m}|m\rangle \qquad (II-4)$$

and a new electronic density:

$$\tilde{n}(\vec{r}) = \langle\tilde{0}|\hat{\rho}(\vec{r})|\tilde{0}\rangle \cong n^{\circ}(\vec{r}) - e\int\sum_{m\neq 0}\frac{\rho_{m0}(\vec{r}')\rho_{0m}(\vec{r}) + \rho_{m0}(\vec{r})\rho_{0m}(\vec{r}')}{E_0-E_m}\varphi^{ext}(\vec{r}') \qquad (II-5)$$

where $|\tilde{0}\rangle$ and $|0\rangle$ are perturbed and unperturbed ground states respectively and we made use of (II-2). The change in electron density $\delta n = \tilde{n} - n^{\circ}$, up to first order in φ^{ext} defines the density response function χ [15-18]:

$$\delta n(\vec{r}) = -e\int d\vec{r}'\;\chi(\vec{r},\vec{r}')\,\varphi^{ext}(\vec{r}') \qquad (II-6)$$

where $\chi(\vec{r},\vec{r}')$ is given by [9]:

$$\chi(\vec{r},\vec{r}') = \sum_{m\neq 0}\frac{\rho_{m0}(\vec{r}')\rho_{0m}(\vec{r}) + \rho_{m0}(\vec{r})\rho_{0m}(\vec{r}')}{E_0-E_m} \qquad (II-7)$$

The change in electron density δn originates the electrostatic polarization potential $\delta\varphi$ through the Poisson equation:

$$\delta\varphi(\vec{r}) = -e\int d\vec{r}'\;\frac{\delta n(\vec{r}')}{|\vec{r}'-\vec{r}|} \qquad (II-8)$$

To linear order in φ^{ext} the total (or screened) perturbation potential $\varphi^{ext}+\delta\varphi$ is written, using Eq. (II-7), as:

$$\varphi^{ext}(\vec{r}) + \delta\varphi(\vec{r}) = \int d\vec{r}''\left[\delta(\vec{r}''-\vec{r}) + e^2\int d\vec{r}'\,\frac{\chi(\vec{r}',\vec{r}'')}{|\vec{r}-\vec{r}'|}\right]\varphi^{ext}(\vec{r}'') \qquad (II-9)$$

The above equation defines the inverse dielectric response

operator, which gives the relationship between the external potential φ^{ext} and the total screened electrostatic potential $\varphi^{ext} + \delta\varphi$ as:

$$\varphi(\vec{r}) \equiv \varphi^{ext}(\vec{r}) + \delta\varphi(\vec{r}) = \int d\vec{r}' \; \epsilon^{-1}(\vec{r},\vec{r}')\,\varphi^{ext}(\vec{r}') \qquad (II-10)$$

By (II-9) ϵ^{-1} is equal to:

$$\epsilon^{-1}(\vec{r},\vec{r}') = \delta(\vec{r}-\vec{r}') + e^2 \int d\vec{r}'' \frac{\chi(\vec{r}'',\vec{r}')}{|\vec{r}-\vec{r}''|} \qquad (II-11)$$

or in compact notation:

$$\epsilon^{-1} = 1 + v_c\,\chi \qquad (II-11')$$

where v_c stays for the Coulomb interaction.

The operators χ and ϵ^{-1} satisfy the requirements of crystal translational and rotational symmetry invariance:

$$\chi(\vec{r}+\vec{R}_l,\vec{r}'+\vec{R}_l) = \chi(\vec{r},\vec{r}') \;;\quad \epsilon^{-1}(\vec{r}+\vec{R}_l,\vec{r}'+\vec{R}_l) = \epsilon^{-1}(\vec{r},\vec{r}') \qquad (II-12)$$

$$\chi(\mathcal{R}\vec{r}+\vec{f}_{\mathcal{R}},\mathcal{R}\vec{r}'+\vec{f}_{\mathcal{R}}) = \chi(\vec{r},\vec{r}') \;;\; \epsilon^{-1}(\mathcal{R}\vec{r}+\vec{f}_{\mathcal{R}},\mathcal{R}\vec{r}'+\vec{f}_{\mathcal{R}}) = \epsilon^{-1}(\vec{r},\vec{r}') \qquad (II-13)$$

where $\vec{R}_l$ is an arbitrary lattice vector, $\mathcal{R}$ – a symmetry operation from the point group of the crystal and $\vec{f}_{\mathcal{R}}$ is a fractional translation associated with $\mathcal{R}$.

It follows from (II-12) that in a homogeneous system the operators ϵ^{-1} and χ depend only on the difference $\vec{r}-\vec{r}'$:

$$\chi(\vec{r},\vec{r}') = \chi(\vec{r}-\vec{r}') \;;\qquad \epsilon^{-1}(\vec{r},\vec{r}') = \epsilon^{-1}(\vec{r}-\vec{r}') \qquad (II-12')$$

while for homogeneous and isotropic medium (II-12) and (II-13) give:

$$\chi(\vec{r},\vec{r}') = \chi(|\vec{r}-\vec{r}'|) \;;\qquad \epsilon^{-1}(\vec{r},\vec{r}') = \epsilon^{-1}(|\vec{r}-\vec{r}'|) \qquad (II-13')$$

Real crystals are neither homogeneous nor isotropic systems and (II-12') (II-13') are only approximations. In some applications however the crystal can be treated as homogeneous and isotropic and (II-12') (II-13') are assumed. This concerns mostly metals [15], but in semiconductors some well known model dielectric functions [19-21] are based on (II-13') as well.

All of the above equations can be expressed in Fourier space. Let our definition of Fourier transform be:

$$\varphi(\vec{r}) = \frac{\Omega_0}{(2\pi)^3} \int d\vec{k}\; \varphi(\vec{k})\, e^{-i\vec{k}\vec{r}} \qquad (II-14)$$

where Ω_0 is the unit cell volume. The Eq. (II-10) becomes:

$$\varphi(\vec{k}) = \int d\vec{k}\; \epsilon^{-1}(\vec{k},\vec{k}')\;\varphi^{ext}(\vec{k}') \qquad (II-15)$$

where

$$\epsilon^{-1}(\vec{k},\vec{k}') = \frac{1}{(2\pi)^3} \int d\vec{r} \int d\vec{r}'\; e^{i\vec{k}\vec{r}}\, \epsilon^{-1}(\vec{r},\vec{r}')\, e^{-i\vec{k}'\vec{r}'} \qquad (II-16)$$

Similarly $\chi(\vec{r},\vec{r}')$ can be transformed to Fourier space.

Lattice translations invariance condition (II-12) has an important consequence on the Fourier transforms of response functions: $\epsilon^{-1}(\vec{k},\vec{k}')$ and $\chi(\vec{k},\vec{k}')$ vanish unless $\vec{k}$ and $\vec{k}'$ differ by a reciprocal lattice vector. This fact stays at the origin of our nomenclature as well. If we represent $\vec{k}$ and $\vec{k}'$ as:

$$\vec{k} = \vec{q} + \vec{G} \quad ; \qquad \vec{k}' = \vec{q} + \vec{G}' \tag{II-17}$$

where $\vec{q}$ is from the first Brillouin zone and $\vec{G}$, $\vec{G}'$ are reciprocal lattice vectors, the response operators ϵ^{-1} and χ in Fourier space will have the form of matrices. For example:

$$\epsilon^{-1}(\vec{k},\vec{k}') \equiv \epsilon^{-1}(\vec{q}+\vec{G},\vec{q}+\vec{G}') \equiv \epsilon^{-1}_{\vec{G}\vec{G}'}(\vec{q}) \tag{II-18}$$

where different kinds of notations used in the literature are given. The response functions in Fourier representation are then the matrices of infinite order in reciprocal lattice vectors parametrized by $\vec{q}$ vectors from the first Brillouin zone. The equation (II-15) takes then a physically transparent form:

$$\varphi(\vec{q}+\vec{G}) = \sum \epsilon^{-1}(\vec{q}+\vec{G},\vec{q}+\vec{G}')\ \varphi^{ext}(\vec{q}+\vec{G}') \tag{II-19}$$

It is easy to verify that for a homogeneous system the response matrices are diagonal and Eq. (II-19) simplifies to:

$$\varphi(\vec{q}+\vec{G}) = \epsilon^{-1}(\vec{q}+\vec{G})\ \varphi^{ext}(\vec{q}+\vec{G}) \tag{II-20}$$

The physical message of (II-19) is that if a perturbation of a given $\vec{q}$-vector acts in the crystal, the electronic response

has the same wave-vector $\vec{q}$, but also all other wave-vectors different from $\vec{q}$ by reciprocal lattice vectors (Umklapp process). In real space it will mean that, say, a macroscopic perturbation of a wavelength λ ($\lambda >>$ lattice spacing a) will produce in crystal the response of the same wavelength, but also microscopic oscillations, which are called local-field effects. These oscillations will be around a macroscopic mean value given by the diagonal part of ϵ^{-1}:

$$\vec{\varphi}(\vec{q}) = \epsilon^{-1}(\vec{q},\vec{q})\ \varphi^{ext}(\vec{q}) \tag{II-21}$$

It is clear from (II-20) that in a homogeneous medium local-fields do not exist and the system responds only at the wavelength of the perturbation.

The macroscopic dielectric constant ε in electrostatics is defined by the relation:

$$\vec{E} = \frac{\vec{D}}{\varepsilon} \tag{II-22}$$

where $\vec{E}$ and $\vec{D}$ are contant electric and displacement fields respectively. Since the constant electric field can be treated as a limiting case with $\vec{q} \longrightarrow 0$ of an oscillating field, we arrive from (II-21) to the following microscopic expression for ε :

$$\varepsilon = \frac{1}{\lim\limits_{\vec{q}\to 0} \epsilon^{-1}(\vec{q},\vec{q})} \tag{II-23}$$

It should be noticed that the dielectric matrix ϵ^{-1} describes only the electronic response of a crystal, so ε from (II-23) will be in general not equal to the macroscopic dielectric constant, but to the so called "high frequency" or

"electronic" dielectric constant ε_∞ . In non polar materials however the ions do not contribute to the macroscopic dielectric constant and there these two constants are equivalent while in polar crystals the ionic response is determined in adiabatic approximation by electronic response via lattice dynamics [8], being the last one then a fundamental quantity.

The condition (II-13) which expresses the invariance of ϵ^{-1} and χ with respect to the operations $\mathcal{R}$ of the point group of the crystal in Fourier space takes the form:

$$\epsilon^{-1}(\mathcal{R}\vec{k}\,,\mathcal{R}\vec{k}') = e^{i\mathcal{R}(\vec{k}-\vec{k}')\vec{f}_{\mathcal{R}}}\ \epsilon^{-1}(\vec{k}\,,\vec{k}') \qquad \text{(II-24)}$$

Matrices ϵ^{-1} and χ are of infinite order but in practical calculations only a part of them is retained, which corresponds to truncate at a given shell of $\vec{G}$ - vectors. Since first-principle computations of these matrices are very elaborate, it is convenient to evaluate only the independent matrix elements, using then Eq. (II-24).

From Eq. (II-16) it follows that:

$$\epsilon^{-1}(-\vec{k}\,,-\vec{k}') = \epsilon^{-1}(\vec{k}\,,\vec{k}')^* \qquad \text{(II-25)}$$

It is easy to prove on the basis of Eq. (II-25) and Eq. (II-24), that in crystals having a centre of inversion a proper choise of the origin can give $\epsilon^{-1}(\vec{k},\vec{k}')$ real. This situation is found for example in diamond structure when the origin is placed at the centre of the bond.

The matrix $\chi(\vec{q}+\vec{G},\vec{q}+\vec{G}')$ is hermitian, while the matrix $\epsilon^{-1}(\vec{q}+\vec{G},\vec{q}+\vec{G}')$ is not such. An hermitian matrix closely related to ϵ^{-1} can be defined as [10]:

$$\tilde{\epsilon}^{-1}(\vec{q}+\vec{G}\,,\vec{q}+\vec{G}') = \frac{|\vec{q}+\vec{G}|}{|\vec{q}+\vec{G}'|}\ \epsilon^{-1}(\vec{q}+\vec{G}\,,\vec{q}+\vec{G}') \qquad \text{(II-26)}$$

which in compact notation takes the form:

$$\tilde{\epsilon}^{-1} = v_c^{-1/2}\,\epsilon^{-1}\,v_c^{1/2} \qquad \text{(II-26')}$$

There are several advantages in dealing with hermitian dielectric matrices. The matrix elements of both ϵ^{-1} and $\tilde{\epsilon}^{-1}$ are in general non analytic for $\vec{q}\longrightarrow 0$. But in insulators and semiconductors the matrix elements of $\tilde{\epsilon}^{-1}$ for a given $\vec{q}$ - direction are all of zero order in $\vec{q}$, thus simplifying the evaluation of long-wavelength limits (see Sec. II.3.). Furthermore, hermitian matrices are more easily stored and diagonalized.

The matrices ϵ^{-1} and $\tilde{\epsilon}^{-1}$ have the same real eigenvalues, which together with eigenvectors give the so called "dielectric band structure" (DBS). This concept introduced by A. Baldereschi and E. Tosatti in 1979 [23] proved to be useful in the analysis of the symmetry properties of screening and in the comparison of different matrices. Matrix ϵ^{-1} is invariant with respect to the operations of the point group of $\vec{q}$, so its eigenvalues and eigenvectors can be labeled by the irreducible representations of the point group of $\vec{q}$ and have well defined symmetry properties. By DBS analysis we can select for example the symmetry of the most screened perturbations. Moreover, when the perturbation is proportional to a given eigenvector of $\tilde{\epsilon}^{-1}$, screening by a matrix reduces to the multiplication of this perturbation by a corresponding eigenvalue, as if the crystal were homogeneous:

$$\sum_{\vec{G}'} \tilde{\epsilon}^{-1}(\vec{q}+\vec{G}\,,\vec{q}+\vec{G}')\,\varphi_\nu(\vec{q}+\vec{G}') = \frac{1}{\varepsilon_\nu(\vec{q})}\,\varphi_\nu(\vec{q}+\vec{G}) \qquad \text{(II-27)}$$

Eq. (II-7) gives the microscopic expression for χ in terms of exact quantum many-electron states. Through (II-11) analogous expression for ϵ^{-1} can be easily derived. They are however, in a sense, impractical: we do not know the exact many-body eigenstates in crystals. The best we can do nowadays is to use some selfconsistent scheme to describe many-electron system. In the following part of this chapter we shall discuss the expressions for response matrices within selfconsistent schemes.

II. 2. Response within Selfconsistent Schemes.

Many-electron systems in a selfconsistent scheme are described by a kind of Schrödinger-like equation for one-particle states φ_i in which the potential energy of an electron is a sum of external potential V_I (in our case due to all the ions) plus the selfconsistent field V_S coming from all other electrons [24]:

$$H^o\varphi_i = \left(\frac{p^2}{2m} + V_I + V_S\right)\varphi_i = \mathcal{E}_i\,\varphi_i \qquad \text{(II-28)}$$

The parameters $\mathcal{E}_i$ in some schemes are treated as one-particle energies. The many-electron system in its ground state occupies all one-particle states for which $\mathcal{E}_i \leq \mathcal{E}_F$, where $\mathcal{E}_F$ is Fermi energy. In general, the selfconsistent field V_S depends on occupied one-particle states, so equations (II-28) are in fact a set of coupled integrodifferential equations. Within the Hartree and LDA schemes however V_S depends only on the electron density $n(\vec{r})$:

$$V_S(\vec{r}) = e^2\int d\vec{r}'\,\frac{n(\vec{r}')}{|\vec{r}-\vec{r}'|} \equiv V_H(\vec{r}) \qquad \text{, (Hartree)} \qquad \text{(II-29)}$$

$$V_S(\vec{r}) = e^2\int d\vec{r}'\,\frac{n(\vec{r}')}{|\vec{r}-\vec{r}'|} + V_{xc}(\vec{r}) = V_H(\vec{r}) + V_{xc}(\vec{r}), \text{ (LDA)} \qquad \text{(II-30)}$$

where V_{xc} is the exchange-correlation part of the selfconsistent potential energy. An equation analogous to Eq. (II-30) can be written for the exact many-body case within the density functional theory [4-6], but the exact form of V_{xc} is unknown. A valuable approximation to the density functional is LDA, where

the assumed form of V_{xc} is taken over from some electron-gas results. The most popular choises assume for V_{xc} the results of Wigner [25], Slater [26] or the recent ones of Ceperley-Alder [27-28]. Following the computational scheme of Ref. [29, 62, 65] we have performed our calculations with Slater form on V_{xc} with 0.8 factor:

$$V_{xc}(\vec{r}) = -0.8 \cdot \frac{3}{2} \frac{e^2}{\pi} \left(3\pi^2 n(\vec{r})\right)^{1/3} \qquad \text{(II-31)}$$

When an external potential φ^{ext} is applied, the change in the electron density will induce a change in the selfconsistent potential energy V_s and the perturbed Hamiltonian will be:

$$H = \frac{p^2}{2m} + V_I + V_s + \delta V = H^0 + \delta V \qquad \text{(II-32)}$$

where

$$\delta V = -e\varphi^{ext} + v_c \delta n = V^{ext} + \delta V_H \qquad \text{(Hartree)} \qquad \text{(II-33)}$$

$$\delta V = V^{ext} + \delta V_H + \delta V_{xc} \qquad (\text{ LDA }) \qquad \text{(II-34)}$$

Suppose φ^{ext} is small, then δV will also be small. It is useful to introduce the notion of independent-particle polarizability χ_0 through the equation:

$$\delta n(\vec{r}) = \int d\vec{r}' \, \chi_0(\vec{r},\vec{r}') \, \delta V(\vec{r}') \qquad \text{(II-35)}$$

It should be noticed that χ_0 is fundamentally different object from χ defined in (II-6), since it gives the response in electron density to the total perturbation selfconsistent potential δV, while χ gives the response to external

potential $-e\varphi^{ext}$.

Since δV is a weak perturbation to the Hamiltonian H^0 we can calculate δn in usual way by means of perturbation theory. It is easy to verify the following expression for χ_0 :

$$\chi_0(\vec{r},\vec{r}') = \sum_{v,c} \frac{f_c - f_v}{\varepsilon_c - \varepsilon_v} \varphi_c^*(\vec{r}') \varphi_c(\vec{r}) \varphi_v^*(\vec{r}) \varphi_v(\vec{r}') \qquad \text{(II-36)}$$

Here f_c , f_v mean occupation numbers of states c and v respectively. In the zero-temperature case (II-36) reduces to:

$$\chi_0(\vec{r},\vec{r}') = -4 \sum_{c,v} \frac{\varphi_c^*(\vec{r}') \varphi_c(\vec{r}) \varphi_v^*(\vec{r}) \varphi_v(\vec{r}')}{\varepsilon_c - \varepsilon_v} \qquad \text{(II-37)}$$

and now c, v stay for empty and occupied one-electron states respectively.

Let us now specify our considerations to the Hartree scheme. Using compact notation we can write:

$$\delta V^{ext} = \delta V - v_c \delta n = (1 - v_c \chi_0) \delta V \qquad \text{(II-38)}$$

We thus obtain the expression for the dielectric operator (which is the inverse of ϵ^{-1}) in Hartree approximation in terms of independent-particle polarizability χ_0 as:

$$\epsilon = 1 - v_c \chi_0 \qquad \text{(II-39)}$$

A dielectric response in this approximation is called also the RPA dielectric response. Strictly speaking RPA approximation in response is equivalent to Hartree one; in the literature however it is used to call RPA or SCF all dielectric functions obtained from χ_0 via (II-39), even if the system eigenvalues and

eigenvectors had been calculated within some other scheme (for example LDA). The numerical results for ϵ_{RPA} which will be presented in chapter IV of this work have been obtained via (II-39) within LDA scheme in band structure calculation.

Equations (II-37,39) in Fourier space, first derived by Adler [30] and Wiser [31], are:

$$\epsilon(\vec{q}+\vec{G},\vec{q}+\vec{G}') = \delta_{\vec{G},\vec{G}'} + \frac{2e^2}{\pi^2\Omega_0|\vec{q}+\vec{G}|^2}\sum_{vc}\int_{BZ} d\vec{k}\,\frac{\langle\vec{k}+\vec{q},c|e^{i(\vec{q}+\vec{G})\vec{r}}|\vec{k},v\rangle\langle\vec{k},v|e^{-i(\vec{q}+\vec{G}')\vec{r}}|\vec{k}+\vec{q},c\rangle}{\varepsilon_c(\vec{k}+\vec{q}) - \varepsilon_v(\vec{k})} \qquad (II-40)$$

(II-40) as applied to fully homogeneous system results in the famous Lindhard expression [32], while in its diagonal form for crystals has been also derived by Ehrenreich and Cohen [33].

At the Hartree level ϵ_{RPA} is the "true" test charge-test charge response function: it relates two electrostatic potentials φ^{ext} and $\delta V/-e$. It is not the case when we work at LDA scheme. There δV is not only the electrostatic potential energy, but is built up also from exchange-correlation part of selfconsistent field:

$$\delta V = \delta V^{ext} + \delta V_H + \delta V_{xc} \qquad (II-41)$$

For this reason the relation between χ_0 and ϵ in LDA scheme will look differently.

δV_H is linear in δn and the same concerns also δV_{xc}. To fined δV_{xc} let us write $V_{xc}[n]$ (which is a functional of n) up to the first order in δn. We get:

$$\delta V_{xc}[n] = V_{xc}[n_0+\delta n] - V_{xc}[n_0] \simeq \frac{\delta V_{xc}}{\delta n}[n_0]\,\delta n \equiv f_{xc}[n_0]\,\delta n \qquad (II-42)$$

where $f_{xc}[n_0]$ is the functional derivative of $V_{xc}[n]$ taken at the unperturbed particle density n_0. In the case of (II-31) expression for V_{xc}, f_{xc} has the following form:

$$f_{xc}(\vec{r},\vec{r}') = -\delta(\vec{r}-\vec{r}')\cdot 0.4\, e^2\left(\frac{3}{\pi}\right)^{1/3} n(\vec{r})^{-2/3} \qquad (II-43)$$

Rewriting equation (II-35) in LDA scheme we get:

$$\delta n = \chi_0\,\delta V = \chi_0\left(V^{ext} + v_c\,\delta n + f_{xc}\,\delta n\right) \qquad (II-35')$$

and we arrive to the relation:

$$V^{ext} = (1 - v_c\chi_0 - f_{xc}\chi_0)\,\delta V \qquad (II-44)$$

We shall call the operator in parenthesis the "electronic" or test charge-electron dielectric function:

$$\epsilon_e = 1 - v_c\chi_0 - f_{xc}\chi_0 \qquad (II-45)$$

ϵ_e^{-1} gives the total selfconsistent potential produced by an external electrostatic potential φ^{ext}. This potential is therefore the one felt in LDA scheme by the electrons of the system and which affects their motion. The dielectric response (II-45) should be used in problems such as the determination of impurity potentials or calculation of electron-phonon interaction.

The dielectric function ϵ_e of (II-45) is not yet the test charge - test charge dielectric response of (II-11). To obtain the latter one we have to extract from δV only its electrostatic part:

$$V^{ext} + \delta V_H = \delta V - f_{xc}\,\delta n = (1 - f_{xc}\,\chi_0)\,\delta V \qquad \text{(II-46)}$$

Replacement of Eq. (II-44) into (II-46) yields the expression we were looking for:

$$V^{ext} + \delta V_H = (1 - f_{xc}\,\chi_0)(1 - v_c\,\chi_0 - f_{xc}\,\chi_0)^{-1}\,V^{ext} \qquad \text{(II-47)}$$

This is the relation between two electrostatic potentials: the external and the induced ones. It defines the "true" response function on LDA level which we shall call LDA dielectric response. We give it in (II-48) in three alternative forms.

$$\begin{aligned}\epsilon_{LDA} &= 1 - v_c\,\chi_0\,(1 - f_{xc}\,\chi_0)^{-1} = (1 - v_c\,\chi_0 - f_{xc}\,\chi_0)(1 - f_{xc}\chi_0)^{-1} \\ &= 1 - v_c\,(\chi_0^{-1} - f_{xc})^{-1}\end{aligned} \qquad \text{(II-48)}$$

Putting $f_{xc}=0$ in (II-48) we obtain again the RPA response. The inclusion of exchange-correlation corrections corresponds therefore to assume $f_{xc}=0$. These "corrections" however are quite large and essential in important physical problems in real semiconductors. In chapter IV we shall demonstrate that RPA and LDA matrices are very different. The same conclusion brings about chapter V: phonons in Germanium calculated within RPA response are worse (and even unphysical) than when LDA response is used.

II.3. Analytical Properties and Acoustic Sum Rules

Dielectric matrices are non-analytic in $\vec{q}\longrightarrow 0$ limit. This fact is a direct consequence of the long-rangeness of Coulomb interactions. Different elements of these matrices however behave in a different way. To trace the analytical properties of response matrices let us define as the "head" of a matrix the $\vec{G}=0$, $\vec{G}'=0$ element; the "wings" let be $\vec{G}=0$ and $\vec{G}'\neq 0$ or vice versa; and the "body" all elements with $\vec{G},\vec{G}'\neq 0$.

A constant potential (i.e. $V^{ext}(\vec{G}\neq 0)=0$) applied to the crystal does not produce obviously any polarization. Since local fields are due to the DM wings, as explained above, these wings at $\vec{q}=0$ should be strictly equal to zero, while the head should be one. In screening of perturbations which have lattice periodicity only the body of the DM is involved and the inverse dielectric matrix at $\vec{q}=0$ must be used.

The $\vec{q}\longrightarrow 0$ limiting values of $\tilde{\epsilon}$ are however non analytic and in the case of ϵ_{RPA} or ϵ_{LDA} they can be easily obtained from (II-39), (II-40) (II-48) as:

$$\tilde{\epsilon}(\vec{q},\vec{q}) \longrightarrow 1 + \sum_{\alpha\beta} \frac{q^\alpha B^{\alpha\beta} q^\beta}{q^2} \qquad \text{(II-49)}$$

$$\tilde{\epsilon}(\vec{q}+\vec{G},\vec{q}) \longrightarrow \sum_{\alpha} \frac{q^\alpha C^\alpha(\vec{G})}{q} \qquad \text{(II-49')}$$

The body of $\tilde{\epsilon}$ is analytic in $\vec{q}\longrightarrow 0$. The above relations are given for hermitian dielectric matrix $\tilde{\epsilon}$; it is straightforward to get from (II-49) those for ϵ. Moreover, as was shown by Pick, Cohen and Martin [8], rules (II-49) are general and are satisfied also by the exact dielectric matrix independently of selfconsistent schemes.

Following PCM [8] paper we can derive the analytical

properties of inverse hermitian dielectric matrix:

$$\frac{1}{\tilde{\epsilon}^{-1}(\vec{q},\vec{q})} \longrightarrow \sum_{\alpha\beta} \frac{q^\alpha B'^{\alpha\beta} q^\beta}{q^2} \qquad \text{(II-50)}$$

$$\frac{\tilde{\epsilon}^{-1}(\vec{q},\vec{q}+\vec{G})}{\tilde{\epsilon}^{-1}(\vec{q},\vec{q})} \longrightarrow \sum_{\alpha} \frac{q^\alpha C'^{\alpha}(\vec{G})}{q} \quad ,\vec{G}\neq 0 \qquad \text{(II-51)}$$

$$\epsilon^{-1}(\vec{q}+\vec{G},\vec{q}+\vec{G}') \longrightarrow \tilde{\epsilon}^{-1}(\vec{G},\vec{G}')+\left[\sum_{\alpha}\frac{q^\alpha C'^{\alpha}}{q}\right]\epsilon(\vec{q},\vec{q})\left[\sum_{\beta}\frac{q^\beta C'^{\beta}}{q}\right] \quad ,\vec{G},\vec{G}'\neq 0 \qquad \text{(II-52)}$$

when $\tilde{\epsilon}^{-1}(\vec{G},\vec{G}')$ is the inverse of the body of $\tilde{\epsilon}$ at $\vec{q}=0$. In cubic materials tensor products like the one appearing in Eq. (II-50) are analytic, so according to (II-23) we put $\varepsilon_\infty = 1/\lim_{\vec{q}\to 0}\tilde{\epsilon}^{-1}(\vec{q},\vec{q}')$. In contrast with HDM χ_0 is always analytic with wings and head going to zero when $\vec{q}\longrightarrow 0$.

From the properties (II-49) to (II-52) and the invariance of the system with respect to infinitesimal translations an important restriction on dielectric matrix elements can be derived. It is called "acoustic sum rule" (ASR) and was first presented by PCM [8] in the context of lattice dynamics as the condition on microscopic dielectric response to give acoustc phonon frequencies vanishing as $\vec{q}\longrightarrow 0$. Here we shall derive it in a somewhat different way. Suppose we have moved the crystal rigidly by an infinitesimal vector $\vec{u}$. Since the charged ions have been moved by the same amount, this gives rise to the appearance of a lattice periodical perturbation of the form:

$$V_b(\vec{G}) = i\sum_s \vec{u}\cdot\vec{G}\, V_s(\vec{G})\, e^{i\vec{G}\vec{R}_s} \quad ,\vec{G}\neq 0 \qquad \text{(II-53)}$$

$$V_b(0) = 0$$

where subscript "b" stays for "bare" or "external" and subscript "s" enumerates different ions in the unit cell. The detailed proof of (II-53) is given in Appendix A. Bare potential (II-53) should be multiplied by the inverse dielectric matrix at $\vec{q}=0$ (according to what was stated above) to produce the screened potential δV :

$$\delta V(\vec{G}) = \sum_{\vec{G}'\neq 0}\frac{|\vec{G}'|}{|\vec{G}|}\,\tilde{\epsilon}^{-1}(\vec{G},\vec{G}')\, V_b(\vec{G}') \qquad \text{(II-54)}$$

The same screened potential (so the same physical effect) should be obtained as the long wavelength limit if we impose on the ions the displacement with a given vector $\vec{q}$ (a phonon). We illustrate these two displacement patterns in Fig. II. 1.

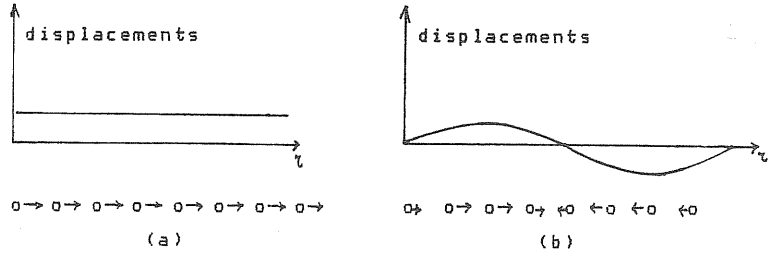

Fig. II. 1. Two displacement patterns imposed on ions: a) uniform, b) phonon-like with $\vec{q}\longrightarrow 0$.

Again according to Appendix A we can write the bare perturbing potential as:

$$V_b(\vec{q}+\vec{G}) = i\sum_s \vec{u}(\vec{q}+\vec{G})\, V_s(\vec{q}+\vec{G})\, e^{i\vec{G}\vec{R}_s} \qquad \text{(II-55)}$$

and the screened potential is:

$$\delta V(\vec{q}+\vec{G}) = \sum_{\vec{G}'} \frac{|\vec{q}+\vec{G}'|}{|\vec{q}+\vec{G}|}\, \tilde{\epsilon}^{-1}(\vec{q}+\vec{G},\vec{q}+\vec{G}')\, V_b(\vec{q}+\vec{G}') \qquad \text{(II-56)}$$

The equality of (II-54) with the $\vec{q}\longrightarrow 0$ limit of (II-56)

$$\delta V(\vec{G}) = \lim_{\vec{q}\to 0} \delta V(\vec{q}+\vec{G}) = 0 \qquad \text{(II-57)}$$

gives two conditions on the $\tilde{\epsilon}^{-1}$:

$$\lim_{\vec{q}\to 0} \sum_{\vec{G}} \frac{|\vec{q}+\vec{G}|}{|\vec{q}|}\, \tilde{\epsilon}^{-1}(\vec{q},\vec{q}+\vec{G})\, V_b(\vec{q}+\vec{G}) = 0 \qquad \text{(II-58)}$$

and

$$\lim_{\vec{q}\to 0} \sum_{\vec{G}'} \frac{|\vec{q}+\vec{G}'|}{|\vec{q}+\vec{G}|} \left[\sum_{\alpha} \frac{q^{\alpha} C^{\prime\alpha\alpha}(\vec{G})}{|\vec{q}|}\right] \frac{1}{\epsilon_\infty} \left[\sum_{\alpha} \frac{q^{\alpha} C^{\prime\alpha\alpha}(\vec{G}')}{|\vec{q}|}\right] V_b(\vec{q}+\vec{G}') = 0\,; \quad \vec{G}\neq 0 \qquad \text{(II-59)}$$

(II-58) comes from equating $\vec{G}=0$ terms in (II-57), while (II-59) is given by $\vec{G}\neq 0$ terms of (II-57). In deriving (II-59) we made use of (II-52).

Let us focus our attention on (II-58). It can be rewritten in the following way:

$$\lim_{\vec{q}\to 0} i\vec{u} \sum_{s} \left[\frac{\vec{q}\, V_s(\vec{q})}{\epsilon_\infty} + \sum_{\vec{G}\neq 0} \frac{\vec{G}\,|\vec{G}|}{|\vec{q}|}\, \tilde{\epsilon}^{-1}(\vec{q},\vec{q}+\vec{G})\, V_s(\vec{G})\, e^{i\vec{G}\vec{R}_s}\right] = 0 \qquad \text{(II-60)}$$

V_s is the ionic pseudopotential, for if the ion has charge $Z_s e$ it should have the limiting behaviour:

$$V_s(\vec{q}) \longrightarrow -\frac{4\pi Z_s e^2}{\Omega_0 q^2} \qquad \text{(II-61)}$$

Putting (II-61) into (II-60) and noticing that $\vec{u}$ is an arbitrary constant we arrive after some manipulations to the expression, which we shall call (after PCM [8]) the acoustic sum rule (ASR):

$$\lim_{\vec{q}\to 0} \sum_{s} \left[\frac{\vec{q}\, Z_s e^2}{q^2} - \frac{\Omega_0 \epsilon_\infty}{4\pi} \sum_{\vec{G}\neq 0} \vec{G}\, \frac{|\vec{G}|}{|\vec{q}|}\, \tilde{\epsilon}^{-1}(\vec{q},\vec{q}+\vec{G})\, V_s(\vec{G})\, e^{i\vec{G}\vec{R}_s}\right] = 0 \qquad \text{(II-62)}$$

Passing to the usual in the literature forms of ASR we multiply (II-62) by $\vec{q}$ and recast in term of ϵ^{-1}. We obtain:

$$\sum_{s} \left[Z_s e^2 - \frac{\Omega_0 \epsilon_\infty}{4\pi} \lim_{\vec{q}\to 0} \sum_{\vec{G}\neq 0} \vec{q}\,\vec{G}\, \epsilon^{-1}(\vec{q},\vec{q}+\vec{G})\, V_s(\vec{G})\, e^{i\vec{G}\vec{R}_s}\right] = 0 \qquad \text{(II-63)}$$

If V_s is not a pseudopotential but the Coulomb potential, (II-63) becomes:

$$\sum_{s} \left[Z_s + Z_s \epsilon_\infty \lim_{\vec{q}\to 0} \sum_{\vec{G}\neq 0} \frac{\vec{q}\cdot\vec{G}}{G^2}\, \epsilon^{-1}(\vec{q},\vec{q}+\vec{G})\, e^{i\vec{G}\vec{R}_s}\right] = 0 \qquad \text{(II-64)}$$

Relations (II-62) to (II-65) are very important in lattice dynamics and up to now they have met there the major interest. They are however the general conditions, which dielectric matrices should satisfy and can serve either as a check of the accuracy of calculations [34] or as a constraint to determine the values of fitting parameters. In first-principle calculations the ASR is usually not satisfied with very good accuracy. As far as our results are concerned we shall discuss this point in chapter V.

The value in parenthesis in (II-62) defines the so called transverse or Born effective charge tensor, which in cubic crystals is diagonal and takes the form:

$$Z_s^{*} e = Z_s e - \frac{\Omega_0 \epsilon_\infty}{4\pi e} \lim_{\vec{q}\to 0} \sum_{\vec{G}\neq 0} \vec{q}\cdot\vec{G}\, \epsilon^{-1}(\vec{q},\vec{q}+\vec{G})\, V_s(\vec{G})\, e^{i\vec{G}\vec{R}_s} \qquad \text{(II-65)}$$

The ASR can be also formulated in the form:

$$\sum_s Z_s^* = 0 \qquad \text{(II-66)}$$

It is clear then, that in elemental cubic crystals with symmetry equivalent positions of atoms in the basis $Z_s^*=0$. Such a situation is for example in diamond type semiconductors.

Effective charges Z_s^* are macroscopic quantities which are in principle measurable and whose physical meaning is the charge the ions are "worn" when they are displaced. Bare ions have ionic charge Z_s, but when they move, electrons follow somehow their displacements screening their charge. When a macroscopic electric field is applied to the crystal, the force felt by the ions is as if their charge were Z_s^*. So in building up the ionic part of the dielectric response the effective charges are an essential ingredient.

CHAPTER III

METHODS OF CALCULATION OF RESPONSE MATRICES IN SEMICONDUCTORS

III. 1. Perturbative Method.

According to the definitions of chapter II, the independent-particle polarizability matrix, which describes the response of electrons of a crystal to the total screened potential, can be written in terms of wave-functions and energies of unperturbed system as:

$$\chi_0(\vec{q}+\vec{G},\vec{q}+\vec{G}') = -\frac{4}{(2\pi)^3}\sum_{cv}\int_{BZ} d\vec{k}\,\frac{\langle \vec{k}+\vec{q}c|e^{i(\vec{q}+\vec{G})\vec{r}}|\vec{k}v\rangle\langle\vec{k}v|e^{-i(\vec{q}+\vec{G}')\vec{r}}|\vec{k}+\vec{q}c\rangle}{\varepsilon_c(\vec{k}+\vec{q}) - \varepsilon_v(\vec{k})} \qquad \text{(III-1)}$$

The RPA dielectric matrix will be then:

$$\epsilon_{RPA}(\vec{q}+\vec{G},\vec{q}+\vec{G}') = \delta_{\vec{G},\vec{G}'} + \frac{4\pi e^2}{|\vec{q}+\vec{G}|^2}\,\chi_0(\vec{q}+\vec{G},\vec{q}+\vec{G}') \qquad \text{(III-2)}$$

The approach to the problem of electronic screening in crystals for several years was going along the line of evaluation of Eqs. (III-1) and (III-2). Recently completely new approaches have been proposed to calculate independent-particle polarizabilities and density response matrices in crystals [29, 14]. These are so called "direct" methods, which we shall discuss later on in this chapter.

The complexity and length of the numerical evaluation of (III-1) is connected basically to the integration over the Brillouin zone and the summation over empty conduction states. One must compute the wave-functions and energies of unperturbed crystal at a dense enough mesh of $\vec{k}$-points in BZ and sum over many conduction bands to obtain satisfactory convergence of the results. These were the reasons why the calculations of screening properties of crystals at the "ab-initio" level (i.e. based on an accurate band structure scheme) proved rather difficult for several years. For these

reasons as well, a number of models of models of dielectric matrices appeard in the literature [35-40]. Those models have been proposed for a given, well defined, purpose (say, lattice dynamics or screening of impurities) and their overall utility is up to now rather poor. This situation is likely to change nowadays however, when the accuracy of a model can be improved by a confrontation with several already existing first-principle calculations of dielectric matrices and fitting parameters of models can be better determined.

Due to above mentioned complexity, the early calculations of dielectric matrices (in crystals having high symmetry, like diamond, silicon, aluminium) were done mostly in $\vec{q} \longrightarrow 0$ limit for a static or dynamic response [41-51]. Dielectric matrices of rather small sizes ($\sim 27x27$ or $\sim 59x59$) have been computed summing up only a few conduction bands and in some cases with the use of additional approximations to overcome the problem of slow convergence with respect to the number of conduction bands ("closure approximation" or moment expansion) [51-53]. A noticeable progress in dielectric matrix calculations and their applications to various problems from the late seventies on was a consequence of a general progress in band structure calculations caused by the use of better and better computers and the development of several useful concepts. Among the concepts that influenced these calculations probably the most, we mention the concepts of mean-value points [54-56] and pseudopotentials [3, 57, 58].

In 1978 A. Baldereschi and E. Tosatti have shown [10], that the mean-value point technique, known for some time as a powerful tool to calculate charge and energy densities of semiconductors or insulators is very useful in the evaluation of Eq. (III-1) as well. Instead of computing band structure of a crystal on a fine mesh of $\vec{k}$-points in BZ (say, several hundreds in the irreducible part of BZ), it is enough (to a very good accuracy) to do it at a few only, but chosen in a special way. These authors have come to the conclusion, that for $\epsilon(0,0)$ element of the static DM at $\vec{q} \longrightarrow 0$ one needs as many as 10 mean-value points in the

irreducible part of BZ, for the "wings" i.e. $\epsilon(0,\vec{G})$ or $\epsilon(\vec{G},0)$ elements with $\vec{G} \neq 0$ two mean-value points give already good approximation, while for the "body" of DM i.e. $\epsilon(\vec{G},\vec{G}')$ elements with $\vec{G} \neq 0$, $\vec{G}' \neq 0$, the single Baldereschi point could be enough.

We have reexamined the above results finding indeed stronger than expected before dependence of $\epsilon(0,0)$ on the number of mean-value points. Our values for $\epsilon(\vec{q},\vec{q})$ in the limit $\vec{q} \longrightarrow 0$ for silicon and germanium obtained with the same band structure scheme [59] as in Ref. [10] and in the case of germanium also with the local Berkeley pseudopotential [60-62] discussed in the next chapter are presented in Tab. III-1. The values obtained within 10 mean-value points are of course very close to those reported in Ref. [10], the small difference is due to a different number of basis functions or/and different number of conduction bands which enter the summation in (III-1).

Number of special points	1	2	10	28	60
a	4.79	18.94	12.12	11.50	11.43
b	5.20	29.47	15.93	14.33	14.06
c	5.54	73.77	31.14	24.78	23.13

Tab. III-1. Values of $\epsilon(\vec{q},\vec{q})$ in the limit $\vec{q} \rightarrow 0$. In first row the number of mean-value points in the irreducible part of BZ. a) silicon with band structure [59]; b) germanium with band structure [59]; c) germanium-Berkeley pseudopotential [62].

It is easy to understand why the $\epsilon(0,0)$ element of $\vec{q} \longrightarrow 0$ dielectric matrix has the strongest dependence on the number of mean-value points. This technique replaces the BZ integral with a sum over representative points: the smoother is the function, the better does the approximation perform. As is proved in the Appendix B, to get the $\epsilon(0,0)$ element of DM in the limit $\vec{q} \longrightarrow 0$ we need to integrate over BZ the function which is in fact varying on $\vec{k}$ in the strongest way. In Appendix B as well we give

the practical expressions to implement in computer program for evaluation of "head" and "wings" of DM in $\vec{q} \longrightarrow 0$ limit.

The authors of Ref. [10] have presented accurate calculations of static dielectric matrices at $\vec{q}=0$ and $\vec{q} \longrightarrow 0$ for several semiconducting and insulating materials like C, Si, Ge, α-Sn, MgO, NaCl. The ionicity trends reflected in dielectric matrix elements have been examined. It was proved that more ionic material is, more important role play off-diagonal elements of its DM with respect to diagonal ones.

In subsequent papers [11-13] polarization charges inside the crystal resulting from the constant electric displacement field or periodic perturbation due to some phonons have been investigated. P. E. Van Camp, V. E. Van Doren and J. T. Devreese in 1979 [52] used the dielectric matrix approach to calculate the phonon frequency spectrum in Si, while R. Resta and A. Baldereschi [34] obtained within the same method Born-effective charges and phonon frequencies at Γ point in Si, Ge, GaAs and ZnSe.

Most of the above mentioned calculations have been performed on the basis of a pseudopotential scheme, being it empirical or selfconsistent. This confirms the trend of increasing success from the sixties to present day for pseudopotential methods as applied to structural, dynamical, screening etc. problems in semiconductors. In the context of screening the pseudopotential approximation is a very good one, because the polarization of the valence electrons is in most cases dominant in the electronic response and the core polarization can be neglected. The matrix elements in (III-1) are obtained in the simplest and natural way when working in plane-wave representation, that is why the choice of a plane-wave pseudopotential scheme seems to be the most suited. Nevertheless works have been done in this field using basis sets of localized functions as well [45-47, 63, 64].

III. 2. "Direct" Methods.

The "direct" approach in dielectric matrix calculations is basically related to the "direct" approach in ab-initio lattice dynamics [51, 70, 76-88]. This is a natural consequence of the similarity of problems and of the successes of "direct" approaches in the computations of phonons. The approach consists in computing the ground state of a given system of electrons both in the presence of a perturbation and without it, extracting then the relevant informations from the resulting differencies in charge densities, potentials or total energies. In the case of phonons this means that one must calculate the total energy of a crystal with a "frozen phonon" i. e. with atoms in suitable positions determined by a particular phonon mode under consideration. The evaluation of small differences in energies resulting from small displacements of atoms with respect to equilibrium was possible owing to the great accuracy achieved by LDA together with the power of band structure methods developed over the last two decades.

Two "direct" methods have been proposed in order to calculate dielectric matrices in semiconductors and insulators [29, 14]. They differ both in the perturbation applied and in the quantity which is computed. In one of these methods [14] basically the independent-particle polarizability matrix χ_0 is calculated, in the other one [29] the quantity which is evaluated is the density response χ or directly the inverse dielectric matrix ϵ^{-1}. The two methods are very similar in technical detailes and are equivalent in the sense, that should in principle yield the same results.

Suppose we have a set of Kohn-Sham equations describing electrons in a crystal:

$$\left[\frac{p^2}{2m} + V_{cr}(\vec{r})\right] \psi_i(\vec{r}) = \varepsilon_i \psi_i(\vec{r}) \qquad \text{(III-3)}$$

where V_{cr} is the total selfconsistent crystal potential:

$$V_{cr} = V_{ext}(\vec{r}) + V_H(\vec{r}) + V_{xc}(\vec{r}) \qquad \text{(III-4)}$$

If we now add to V_{cr} a monochromatic small (screened) potential $\delta V_{tot} = c\ \exp(i(\vec{q}+\vec{G})*\vec{r})$ and we calculate the electron density δn induced by such a perturbation, we immediately obtain the whole row of the independent-particle polarizability matrix χ_o. Since we prefer to deal with hermitian Hamiltonians and $c\ \exp(i(\vec{q}+\vec{G})*\vec{r})$ is not hermitian, we can solve twice Kohn-Sham equations with the perturbation $c\ \sin((\vec{q}+\vec{G})*\vec{r})$ and $c\ \cos((\vec{q}+\vec{G})*\vec{r})$ respectively:

$$\left[\frac{p^2}{2m} + V_{cr}(\vec{r}) + c\sin(\vec{q}+\vec{G})\vec{r}\right]\psi_i(\vec{r}) = \varepsilon_i\,\psi_i(\vec{r}) \qquad \text{(III-5)}$$

$$\left[\frac{p^2}{2m} + V_{cr}(\vec{r}) + c\cos(\vec{q}+\vec{G})\vec{r}\right]\psi_i(\vec{r}) = \varepsilon_i\,\psi_i(\vec{r})$$

Summing over all occupied states in (III-5) we obtain $n^{\sin}_{\vec{q}+\vec{G}}(\vec{r})$ and $n^{\cos}_{\vec{q}+\vec{G}}(\vec{r})$ as well as:

$$\delta n^{\sin}_{\vec{q}+\vec{G}}(\vec{r}) = n^{\sin}_{\vec{q}+\vec{G}}(\vec{r}) - n^{o}(\vec{r}) \qquad \text{(III-6)}$$

$$\delta n^{\cos}_{\vec{q}+\vec{G}}(\vec{r}) = n^{\cos}_{\vec{q}+\vec{G}}(\vec{r}) - n^{o}(\vec{r})$$

where n^0 is the electron density of unperturbed crystal. Since χ_o gives the relation between the total screened perturbation potential and the induced density δn:

$$\delta n^{\sin}_{\vec{q}+\vec{G}}(\vec{r}) = \int d\vec{r}'\,\chi_o(\vec{r},\vec{r}')\,c\sin(\vec{q}+\vec{G})\vec{r}' \qquad \text{(III-7)}$$

$$\delta n^{\cos}_{\vec{q}+\vec{G}}(\vec{r}) = \int d\vec{r}'\,\chi_o(\vec{r},\vec{r}')\,c\cos(\vec{q}+\vec{G})\vec{r}'$$

which in Fourier space reads:

$$\delta n^{\sin}_{\vec{q}+\vec{G}}(\vec{q}+\vec{G}') = \frac{c}{2i}\left[\chi_o(\vec{q}+\vec{G}',\vec{q}+\vec{G}) - \chi_o(\vec{q}+\vec{G}',-\vec{q}-\vec{G})\right] \qquad \text{(III-8)}$$

$$\delta n^{\cos}_{\vec{q}+\vec{G}}(\vec{q}+\vec{G}') = \frac{c}{2}\left[\chi_o(\vec{q}+\vec{G}',\vec{q}+\vec{G}) + \chi_o(\vec{q}+\vec{G}',-\vec{q}-\vec{G})\right]$$

we arrive to the following expression for χ_o :

$$\chi_o(\vec{q}+\vec{G}',\vec{q}+\vec{G}) = \left[\delta n^{\cos}_{\vec{q}+\vec{G}}(\vec{q}+\vec{G}') + i\,\delta n^{\sin}_{\vec{q}+\vec{G}}(\vec{q}+\vec{G}')\right]/c \qquad \text{(III-9)}$$

In (III-8) we have made use of the fact that the wave-vector of the response differs from the wave-vector of the perturbation by a reciprocal lattice vector ("umklapp"). Through (III-2) we immediately get ϵ_{RPA} and through (I-48) ϵ_{LDA}. Let us call this method the "direct-RPA" method.

It should be stressed that in the above approach one does not need to iterate equations (III-5) up to the selfconsistency as if $c\ \sin(\ldots)$ and $c\ \cos(\ldots)$ were additional external potentials. A selfconsistent solution of the unperturbed crystal is assumed at the begining in order to get the unperturbed V_{cr}. $c\ \sin(\ldots)$ or $c\ \cos(\ldots)$ are the total screened excess potentials and solves equations (III-5) only once for each $\vec{q}+\vec{G}$.

When $c\ \sin(\ldots)$ and $c\ \cos(\ldots)$ are taken as perturbing external potentials and a new selfconsistent solution is searched for (III-5), one deals with the second alternative "direct" approach, which we shall call the "direct-LDA" method [29] and one in this way the density response χ :

$$\delta n(\vec{r}) = \int d\vec{r}'\,\chi(\vec{r},\vec{r}')\,\delta V_{ext}(\vec{r}') \qquad \text{(III-10)}$$

Eq. (III-9) must be replaced by a similar one, where χ_0 is substituted by χ . Through (I-11) one gets ϵ^{-1}_{LDA}.

The "direct" methods for dielectric matrix calculations have several fundamental and practical advantages over "traditional" perturbative approach based on (III-1) and one basic disadvantage. The most important fundamental advantage is the fact, that the matrices χ_0 or χ and ϵ_{RPA} or ϵ_{LDA} calculated in the "direct" approach contain the "full" response to the external perturbation up to all orders; not only the linear one as Eq. (III-1) does. In order to obtain χ_0 and χ in linear regime (equivalent to (III-1) formulation) one should put c in (III-5) small enough. It was chacked [14,29], that in the case of Si, Ge, GaAs, the value for c of the order of 1 mRyd already ensures the linear response.

Another important advantage of "direct" methods is the elimination of lengthy and slowly convergent summation over conduction bands in (III-1). The problem of evaluation of matrix elements in (III-1) between all valence and conduction states is substituted by very fast electron density calculation. Moreover the whole row of $\chi(\vec{q}+\vec{G},\vec{q}+\vec{G}')$ (or χ_0) for a given $\vec{G}'$ is calculated at a time while the number of independent applied perturbations c sin(...) and c cos(...) can be severely reduced by symmetry.

The basic disadvantage of "direct" approach is their limitation to high symmetry $\vec{q}$-points only at which response matrices can be calculated. Hamiltonians (III-5) with built-in perturbation should have translational symmetry in order to be able to use the standard band structure schemes. It will preserve its translational symmetry if $\vec{q}$ in the perturbation is at the centre of Brillouin zone. The supercells yet of managable sizes can be constructed and lower translational symmetry is preserved if $\vec{q}$ lies on the border of BZ, in the mid-way between the border and the centre or even in 1/4 of this distance. The problem is in the fact, that increasing n-times the number of atoms in the unit cell of the crystal, we increase raughly n-times the number

of basis functions used to solve (III-5). In Ref. [14] RPA dielectric matrices of the order 108x108 at X and L points in Si and GaAs together with those at Γ point of order 113x113 have been calculated, while some sample elements of ϵ^{-1}_{LDA} of Ge and GaAs in Γ , X, 1/2 X and 1/4 X points have been presented in Ref. [29]. Here 1/2 X and 1/4 X mean $\vec{q}$-points on Δ-direction in the mid-way between Γ and X and in 1/4 of this distance from Γ .

Another disadvantage of "direct" methods as described above is their inapplicability to calculate dielectric matrix elements in the limit $\vec{q}\longrightarrow 0$, which corresponds to screening of a constant electric field. This however can be done, as shown by K. Kunc and R. Resta [65] in a very similar "direct" way. They have applied periodic but "saw-like" external perturbation to Ge and GaAs, simulating successfully locally constant displacement field $\vec{D}$, and have obtained macroscopic dielectric constants as well as Born-effective charge of GaAs. In the same way in principle the "head" and "wings" of dielectric matrices in the limit $\vec{q}\longrightarrow 0$ could be calculated.

III. 3. Perturbative Scheme Using Fast Fourier Transforms.

In the present work a small technical innovation to traditional perturbative approach is also proposed, which however accelerates significantly the calculations. The idea consists in evaluating the matrix elements in the numerator of (III-1) not in $\vec{k}$-space, as is usually done (summing over all $\vec{G}$-vectors in the basis), but rather in $\vec{r}$-space with the aid of Fast Fourier Transform, as is often done in electron density calculations. We are doing the following:

$$\langle v\vec{k} \mid e^{-i(\vec{q}+\vec{G})\vec{r}} \mid c\vec{k}+\vec{q} \rangle \longrightarrow \sum_{\vec{r}_i} u^*_{v\vec{k}}(\vec{r}_i)\, u_{c\vec{k}+\vec{q}}(\vec{r}_i)\, e^{-i\vec{G}\vec{r}_i} \qquad \text{(III-11)}$$

where $\vec{r}_i$ is a suitable mesh of points in the elementary cell (determined by the number of basis functions and vector $\vec{G}$ in (III-11)), while $u_{v\vec{k}}$, $u_{c\vec{k}+\vec{q}}$ are the periodic parts of Bloch functions of the valence and conduction bands respectively. Fast Fourier Transform is performed twice consecutively, first direct to get $u_{v\vec{k}}(\vec{r}_i)$, $u_{c\vec{k}+\vec{q}}(\vec{r}_i)$, then inverse starting from products $u^*_{v\vec{k}}(\vec{r}_i)\,u_{c\vec{k}+\vec{q}}(\vec{r}_i)$ to get at a time matrix elements for all $\vec{G}$ vectors.

In the calculations presented in chapter V of this work we have used essentially this last approach, because - as will be seen - we have computed dielectric matrices in many highly nonsymmetric points over the Brillouin zone.

CHAPTER IV

COMPUTATIONAL DETAILS

In this chapter we shall describe the technical methods used in the present work to obtain dielectric matrices in germanium. These include the kind of band structure scheme, the techniques of integration over the Brillouin zone, the acceleration of iterations methods, etc.

The calculations have been performed iterating up to selfconsistency Kohn-Sham equations (II-28) with a local ionic Berkeley pseudopotential of the form [60-62, 66]:

$$V_{ion}(q) = \frac{a_1[\cos(a_2 q) + a_3]}{q^2} e^{a_4 q^4} \qquad \text{(IV-1)}$$

Part of the results have been obtained with the empirical Cohen-Bergstresser pseudopotential [59] as well. We have chosen the pseudopotential (IV-1) in order to be able to compare our results with some of existing data for electronic screening or lattice dynamics based on the same band structure scheme. Another reason is the lack of a theory describing lattice dynamics of a crystal within dielectric matrix formulation based on non-local, norm-conserving pseudopotentials [67-69]. This is because dielectric matrices deal with the response to a local perturbation, while ionic displacements are a non-local perturbation to the system of electrons, when working in non-local pseudopotential scheme. In principle however a generalization of the dielectric matrix theory to describe the response to non-local potentials is possible. It is possible as well, that the most useful representation of dielectric operators in some circumstances is not the Fourier representation, which we are mostly concerned with in the present work. When not working in a pseudopotential scheme, localized basis could prove their usefulness. To the best of our knowledge this possibility has not been explored in the literature yet.

In previous ab-initio calculations of lattice-dynamical and screening properties of germanium [29, 62, 65, 70] based on the same band structure approach it was claimed, that better structural properties of germanium are obtained, when the ionic pseudopotential of Ge is taken as the average of ionic pseudopotentials of the form (IV-1) of arsenic and gallium. The recipe, which we took over from Ref. [29, 62], is then:

$$V_{Ge}(\vec{q}) = \begin{cases} \frac{1}{2}\left[V_{Ga}(\vec{q}) + V_{As}(\vec{q}) \right] & \text{for } q < 3 \text{ a.u.} \\ \frac{1}{2} V_{As}(\vec{q}) & \text{otherwise} \end{cases} \qquad \text{(IV-2)}$$

The lattice constant of Ge obtained with the choice (IV-2) is quite close to experiment [62] (-1.6 % difference), while the gaps between occupied and empty states are reproduced rather badly (-50 % difference for direct gap at Γ and -80 % for absolute gap Γ-L). Because of the wrong gaps the pseudopotential (IV-2) gives, the "head" of RPA dielectric matrix presented in Tab. II-1. has much too great value. This fact will be also reflected in the - not too accurate - calculation of the macroscopic dielectric constant (see Tab. IV-2.). The effect of the gap is the strongest however for the "head" of DM, while for other elements (specially "body") is a minor one. That is why we believe that this point should not be too important for structural and lattice-dynamical properties of germanium.

In our calculation we impose the lattice constant of Ge equal to 5.66 A. If $\vec{q}$ is given in atomic units and pseudopotentials, given in Rydbergs, are normalized to the unit cell volume, the values of parameters to be used in (IV-1) are given in Tab. IV-1.

	a_1	a_2	a_3	a_4
Ga	-.1692	1.3305	.4566	.0071
As	-.3521	1.0448	.1662	-.0151

Tab. IV-1. Values of parameters a_1, a_2, a_3, a_4 in (IV-1) if q in a.u. and potentials (in Ryd.) normalized to unit cell volume

In order to describe the response of the electrons to an external periodic perturbation of wavelength λ one must use plane-waves of wavelengths rather smaller than λ in the decomposition of Bloch functions. Since it has been already shown [34, 51-53], that for phonon calculations in semiconductors like Si, Ge, GaAs it is essential to operate with dielectric matrices of the order of 100~200, we have computed dielectric matrices in different $\vec{q}$-points using the cutoff $|\vec{q}+\vec{G}|^2 \leq 32(2\pi/a)^2$. According to $\vec{q}$-point in the Brillouin zone our matrices were of the size 180~190 (181 at Γ, 190 at X, 180 at L, etc.). In order to get reliable values of DM elements corresponding to large $\vec{G}$ vectors, we have used even greater basis of plane-waves in the solution of Kohn-Sham equations (II-28). The condition $|\vec{q}+\vec{G}|^2 \leq 35(2\pi/a)^2$ gave us about 220 plane-waves to expand Bloch functions.

The electron density is calculated with the aid of Fast Fourier Transform technique on the grid of points (16, 16, 16) in elementary cell and the mean-value points in Brillouin zone as given by (4, 4, 4) division of Monkhorst and Pack [56] are used. Starting from the electron density the Hartree potential is obtained according to:

$$V_H(\vec{G}) = \frac{4\pi e^2 n(\vec{G})}{|\vec{G}|^2} \qquad \text{(IV-3)}$$

and the exchange-correlation potential in real space is:

$$V_{xc}(\vec{r}) = -0.8 \cdot \frac{3}{2} e^2 \left(\frac{3 n(\vec{r})}{\pi} \right)^{1/3} \qquad \text{(IV-4)}$$

The selfconsistent solution of the Kohn-Sham equations is obtained with a convergence in each Fourier component of crystal potential better then $.5 \times 10^{-5}$ Ryd. The acceleration of iterations scheme based on Anderson extrapolation method [71] as well as the dielectric matrix scheme of Ho, Ihm and Joannopoulos [72] have been used. For the input to the first iteration electron density from Cohen - Bergstresser [59] Hamiltonian had been computed.

The Ho, Ihm and Joannopoulos method [72] is itself one of the illustrations of usefulness of the concept of dielectric matrix. The underlying idea of this method is the observation, that close to selfconsistency the difference between the total potential of a given iteration and the selfconsistent one can be treated as a small perturbation to the Hamiltonian and well approximated via the "electronic" dielectric matrix at $\vec{q}=0$. Ho et al. have shown that:

$$\delta V_{in}(\vec{G}) = \sum_{\vec{G}'} \epsilon_e^{-1}(\vec{G}, \vec{G}') \left[V_{out}(\vec{G}') - V_{in}(\vec{G}') \right] \qquad \text{(IV-5)}$$

where δV_{in} is the difference between the input potential of i'th iteration and a selfconsistent one, V_{out} is the output potential of this iteration and $\epsilon_e(\vec{G}, \vec{G}')$ is given by:

$$\epsilon_e = 1 - v_c \chi_0 - f_{xc} \chi_0 \qquad \text{(IV-6)}$$

We recognize in ϵ_e of (IV-6) the test charge - electron dielectric response defined in chapter II (II-45). The use of $\delta V_{in}(\vec{G})$ in the iteration scheme greatly improves the convergence speed.

In order to compare the effectiveness of different methods of acceleration in iterations we have repeated selfconsistency runs four times within different schemes: dielectric matrix, diagonal dielectric matrix, Anderson's scheme and usual constant mixing of input and output potentials. In all of these calculations we have used the same number of plane-waves in the basis, namely the cutoff $|\vec{q}+\vec{G}|^2 \leq 27(2\pi/a)^2$ and the same charge density from Cohen - Bergstresser [59] pseudopotential as the input to the first iteration. Selfconsistent solution has been assumed if the difference between the output and input crystal potentials was less than 10^{-5} Ryd in each Fourier component. In the calculations within Ho, Ihm and Joannopoulos scheme dielectric matrices of the order 59x59 have been obtained summing up about 60 conduction bands in Eq. (III-1). In Tab. IV-2 the input crystal potential for a few shortest shells of $\vec{G}$-vectors and each iteration is presented. This potential is obtained by mixing according to a given prescription the input and output potentials of the last iteration. The input to the first iteration is in all four calculations the same.

As results from Tab. IV-2 the dielectric matrix scheme of acceleration seems to be the most efficient one. The selfconsistency limit is achieved after three iterations only. In the calculation with the diagonal dielectric matrix the diagonal part was taken after inverting the full ϵ_e. This calculation does not have then a practical importance, but rather shows the relative effect of the off-diagonal to diagonal elements of dielectric matrix in this context. In the choice of a scheme to accelerate selfconsistency runs one should take however into account the simplicity in the implementation of a given scheme as well as the computer time it consumes. The Ho, Ihm and Joannopoulos method is more time consuming than the other schemes, because of the need of calculating Bloch functions of conduction states and the matrix elements in (III-1). This concernes specially the cases when the symmetry can not be used to simplify the problem. Because of this fact, the method based on the Anderson's extrapolation scheme seems to be the most practical and effective one: it does not take much time and is

easy to implement even in "nonsymmetric" cases.

Response matrices which we have calculated in the present work are quite large as well as obtained from a large basis set. In chapter V, while discussing phonons at point L in germanium, we give some arguments why these matrices should be even larger for the application in lattice dynamics. The increase of size of matrices should however go together with the general increase of the level of "sophistication" of calculations (finer mesh of mean-value points, better pseudopotentials, etc.). We would like to mention here two very recent calculations of macroscopic dielectric constant in silicon [73] and Raman tensor [74] from dielectric formalism done with non-local, norm-conserving pseudopotentials and a large basis set.

Tab.III-2. Comparative study of different acceleration methods in selfconsistency iterations. Input potential in Ryd. Shown for a prototype vector of each of 3 shells for each reciprocal lattice vector assumed when the difference between the output and input potentials was less than 10^{-5} Ryd in each Fourier component.

G	ITERATION 1	2	3	4	5	6	7
	Inverse dielectric matrix calculated in each iteration - Ho,Ihm,Joannopoulos scheme Ref.72						
(1 1 1)	.144364	.149542	.149533	.149535			
(2 2 0)	-.015092	-.014666	-.014788	-.014780			
(3 1 1)	-.028681	-.028748	-.028658	-.028664			
(2 2 2)	.005361	.004676	.004755	.004749			
(4 0 0)	-.043147	-.045621	-.045650	-.045654			
(3 3 1)	.026944	.027790	.027841	.027841			
(4 2 2)	.022607	.023202	.023195	.023196			
(3 3 3)	.005699	.006115	.006106	.006107			
(5 1 1)	.005854	.005905	.005883	.005883			
	Diagonal part of the inverse dielectric matrix calculated in each iteration						
(1 1 1)	.144364	.149253	.149436	.149522	.149530		
(2 2 0)	-.015092	-.014492	-.014769	-.014775	-.014779		
(3 1 1)	-.028681	-.028692	-.028664	-.028664	-.028664		
(2 2 2)	.005361	.004516	.004750	.004746	.004749		
(4 0 0)	-.043147	-.045621	-.045653	-.045655	-.045655		
(3 3 1)	.026944	.027790	.027843	.027841	.027841		
(4 2 2)	.022607	.023202	.023196	.012196	.023196		
(3 3 3)	.005699	.006115	.006105	.006108	.006107		
(5 1 1)	.005854	.005905	.005883	.005883	.005883		

Tab.III-2. Cont.

G	ITERATION						
	1	2	3	4	5	6	7
	Anderson`s extrapolation scheme, Ref. 71						
(1 1 1)	.144364	.147836	.149570	.149539	.149532		
(2 2 0)	-.015092	-.014795	-.014712	-.014781	-.014781		
(3 1 1)	-.028681	-.028686	-.028677	-.028665	-.028664		
(2 2 2)	.005361	.004961	.004750	.004746	.004748		
(4 0 0)	-.043147	-.044384	-.045332	-.045653	-.045653		
(3 3 1)	.026944	.027367	.027712	.027841	.027841		
(4 2 2)	.022607	.022905	.023127	.023197	.023196		
(3 3 3)	.005699	.005907	.006060	.006107	.006107		
(5 1 1)	.005854	.005879	.005889	.005884	.005883		
	Constant mixing of output and input potentials with mixing parameter 0.3						
(1 1 1)	.144364	.149225	.149512	.149530	.149531	.149532	.149532
(2 2 0)	-.015092	-.014676	-.014736	-.014766	-.014776	-.014779	-.014780
(3 1 1)	-.028681	-.028688	-.028674	-.028668	-.028665	-.028664	-.028664
(2 2 2)	.005361	.004801	.004755	.004750	.004749	.004749	.004750
(4 0 0)	-.043147	-.044879	-.045403	-.045572	-.045627	-.045646	-.045654
(3 3 1)	.026944	.027537	.027742	.027809	.027831	.027838	.027841
(4 2 2)	.022607	.023024	.023143	.023179	.023191	.023194	.023196
(3 3 3)	.005699	.005991	.006070	.006095	.006103	.006106	.006107
(5 1 1)	.005854	.005890	.005887	.005885	.005884	.005883	.005883

CHAPTER V

DIELECTRIC MATRICES IN GERMANIUM: RESULTS

In this chapter we shall present some of the results obtained for RPA and LDA dielectric matrices in germanium at Γ, X and L points. The matrices have been calculated within the perturbative scheme with Fast Fourier Transform exept for point Γ, where both perturbative and "direct-LDA" methods were used. The comparison of the two calculations at Γ made us sure, that up to accuracy better than 0.01 (in absolute units for inverse DM's) both results were equal. The small difference is due to the selfconsistency criterion, finite value of the monochromatic perturbation in the "direct" method and the finite size of DM which must be inverted in perturbative scheme.

In Tab. V-1 some of the matrix elements of symmetrized $\tilde{\varepsilon}_{LDA}$ and $\tilde{\varepsilon}_{RPA}$ of Ge in the limit $\vec{q}\longrightarrow 0$, $\vec{q} \parallel (100)$ are shown. The matrix obtained with the selfconsistent pseudopotential (IV-2) was of the order 181x181, while that from Cohen-Bergstresser empirical pseudopotential [59] was of the size 113x113. The most striking feature of these results is the fact, that the elements of $\tilde{\varepsilon}$ differ more because of exchange-correlation corrections than because of different band structure schemes. We shall come back to discuss this point later on in this chapter. The "heads" of dielectric matrices at Γ are very different in all three schemes. This is mainly the direct consequence of the value of the gap, which largely differs for the two pseudopotentials used. "Wings" and "body" elements however are not so different and here exchange correlation has the most important influence. The above results confirm the hypothesis, that the values of gap between valence and conduction bands affects mostly (0,0) element of $\vec{q}\longrightarrow 0$ dielectric matrix, while "body" and "wings" are less affected.

$\vec{G}$	$\vec{G}'$	Cohen – Bergstresser	Berkeley	
		RPA	RPA	LDA
(0,0,0)	(0,0,0)	14.060	23.128	27.379
(0,0,0)	(1,1,1)	-.430	-.473	-.767
(0,0,0)	(2,2,0)	.169	.280	.402
(0,0,0)	(3,1,1)	.200	.252	.388
(0,0,0)	(1,1,3)	.101	.155	.239
(0,0,0)	(2,2,2)	.176	.226	.362
(0,0,0)	(4,0,0)	.125	.123	.198
(0,0,0)	(1,3,3)	.019	.030	.047
(0,0,0)	(3,3,1)	.010	.009	.017
(1,1,1)	(1,1,1)	1.702	1.753	2.133
(1,1,$\bar{1}$)	($\bar{1}$,$\bar{1}$,1)	-.163	-.181	-.379
(2,0,0)	(1,1,1)	.111	.118	.187
(2,2,0)	(1,1,1)	.088	.089	.134
(2,0,0)	(2,0,0)	1.556	1.599	1.896
(2,0,0)	($\bar{2}$,0,0)	-.060	-.039	-.102
(3,1,$\bar{1}$)	($\bar{2}$,0,0)	.071	.071	.108
($\bar{1}$,1,3)	($\bar{2}$,0,0)	.020	.019	.033
(2,2,0)	(2,2,0)	1.235	1.248	1.348
(1,$\bar{3}$,1)	(2,$\bar{2}$,0)	.051	.053	.078
(3,1,1)	(3,1,1)	1.127	1.132	1.173
($\bar{2}$,2,$\bar{2}$)	($\bar{3}$,1,$\bar{1}$)	.036	.037	.052
(2,2,2)	(2,2,2)	1.105	1.111	1.143
(4,0,0)	(4,0,0)	1.047	1.054	1.064

Tab. V-1. Sample elements of symmetrized RPA or LDA DM of Ge in $\vec{q}\rightarrow 0$ limit $\vec{q} \parallel (100)$, obtained with Cohen-Bergstresser [59] and Berkeley pseudopotentials (IV-2).

From the calculated matrices at $\vec{q}\rightarrow 0$ the electronic macroscopic dielectric constant ε_∞ can be obtained according to (II-23). The values for ε_∞ got with the Berkeley and the Cohen-Bergstresser pseudopotentials are reported in Tab. V-2.

	Cohen – Bergstresser	Berkeley	
	RPA	RPA	LDA
ε_∞	12.521	20.700	22.435

Tab. V-2. Electronic macroscopic dielectric constant of Ge obtained with Cohen-Bergstresser [59] and Berkeley (IV-2) pseudopotentials

All these results are quite far from experiment (ε^{exp}=15.4). Cohen-Bergstresser pseudopotential at least with original form-factors [59] turns out to work not too well in germanium. Such a great difference between the theoretical and experimental values has not been noticed so far because the convergence with respect to BZ integration in the calculation of (0,0) element of DM has not been achieved previously [10] (see Tab. III-1). In the inaccurate result for ε_∞ that Berkeley pseudopotential gives the problem of gaps mentioned in the last chapter is reflected. Remembering the values of the "head" of RPA dielectric matrices (Tab. III-1) we see, that the inclusion of local-fields effects pushes down ε_∞ (from 23.13 to 20.70 for the Berkeley pseudopotential and from 14.06 to 12.52 for empirical one), while exchange correlation pulls it up. K. Kunc and R. Resta have got [65] within the "direct" method and the same pseudopotential the value of 19.08 for ε_∞. It should be compared with the last column (LDA) of Tab. V-2. The difference is most probably due to different computational methods, supercell size in in Ref. [65], the number of basis functions in the Kohn-Sham equations and the way these equations are solved (Löwdin perturbation scheme used in Ref. [65]).

$\vec{G}$	$\vec{G}'$	Cohen – Bergstresser	Berkeley	
		RPA	RPA	LDA
(0,0,0)	(0,0,0)	3.012	3.215	4.256
($\bar{1}$,$\bar{1}$,1)	(0,0,0)	.133	.159	.188
(1,$\bar{1}$,$\bar{1}$)	(0,0,0)	.183	.181	.275
($\bar{3}$,1,$\bar{1}$)	(0,0,0)	-.062	-.063	-.137
($\bar{1}$,$\bar{1}$,1)	($\bar{1}$,$\bar{1}$,1)	2.089	2.174	2.759
($\bar{1}$,1,$\bar{1}$)	($\bar{1}$,$\bar{1}$,1)	-.166	-.155	-.302
(0,0,2)	($\bar{1}$,$\bar{1}$,1)	-.142	-.146	-.227
(0,$\bar{2}$,2)	($\bar{1}$,$\bar{1}$,1)	.111	.106	.163
(1,$\bar{1}$,$\bar{1}$)	(1,$\bar{1}$,$\bar{1}$)	1.335	1.353	1.505
(0,0,$\bar{2}$)	(1,$\bar{1}$,$\bar{1}$)	.076	.077	.117
(2,0,0)	(1,$\bar{1}$,$\bar{1}$)	-.062	-.063	-.093
(0,0,2)	(0,0,2)	1.425	1.449	1.651
($\bar{1}$,1,3)	(0,0,2)	.065	.065	.095
(2,0,0)	(2,0,0)	1.182	1.190	1.255
(3,$\bar{1}$,$\bar{1}$)	(2,0,0)	.023	.024	.032
(2,$\bar{2}$,0)	(2,$\bar{2}$,0)	1.083	1.088	1.108
(1,$\bar{3}$,1)	(2,$\bar{2}$,0)	.021	.022	.027
(0,$\bar{2}$,$\bar{2}$)	(0,$\bar{2}$,$\bar{2}$)	1.191	1.200	1.276
(0,2,2)	(0,$\bar{2}$,$\bar{2}$)	-.014	-.014	-.028
(1,$\bar{1}$,$\bar{3}$)	(0,$\bar{2}$,$\bar{2}$)	.036	.036	.052
($\bar{1}$,$\bar{1}$,$\bar{3}$)	(0,$\bar{2}$,$\bar{2}$)	.051	.052	.076
(1,$\bar{3}$,1)	(1,$\bar{3}$,1)	1.069	1.075	1.090
($\bar{1}$,1,3)	($\bar{1}$,1,3)	1.153	1.159	1.210

Tab. V-3. Sample elements of symmetrized RPA or LDA DM of Ge at $\vec{q}$=(1,0,0)*(2π/a), obtained with Cohen-Bergstresser [59] and Berkeley pseudopotentials (IV-2).

$\vec{G}$	$\vec{G}'$	Cohen – Bergstresser	Berkeley	
		RPA	RPA	LDA
(0,0,0)	(0,0,0)	3.196	3.435	4.593
($\bar{1}$,$\bar{1}$,$\bar{1}$)	(0,0,0)	.686	.681	1.440
($\bar{1}$,$\bar{1}$,1)	(0,0,0)	.201	.222	.332
($\bar{2}$,$\bar{2}$,$\bar{2}$)	(0,0,0)	-.173	-.187	-.372
($\bar{2}$,0,0)	(0,0,0)	.063	.070	.133
($\bar{1}$,$\bar{1}$,1)	($\bar{1}$,$\bar{1}$,1)	1.817	1.877	2.317
($\bar{2}$,0,0)	($\bar{1}$,$\bar{1}$,1)	.138	.146	-.224
($\bar{2}$,$\bar{2}$,0)	($\bar{1}$,$\bar{1}$,1)	-.109	-.116	-.182
($\bar{2}$,$\bar{2}$,2)	($\bar{1}$,$\bar{1}$,1)	.090	-.087	.133
($\bar{1}$,1,1)	($\bar{1}$,1,1)	1.440	1.464	1.675
(0,0,2)	($\bar{1}$,1,1)	.078	.078	.117
(1,1,1)	(1,1,1)	1.284	1.299	1.426
(0,0,2)	(1,1,1)	.066	.066	.100
(0,0,2)	(0,0,2)	1.290	1.305	1.430
($\bar{1}$,1,3)	(0,0,2)	.039	.040	.056
(2,$\bar{2}$,0)	(2,$\bar{2}$,0)	1.200	1.210	1.288
(1,$\bar{3}$,1)	(2,$\bar{2}$,0)	.050	.051	.076
(1,$\bar{3}$,$\bar{1}$)	(2,$\bar{2}$,0)	-.060	-.061	-.093
(0,2,2)	(0,2,2)	1.087	1.092	1.113
($\bar{1}$,1,3)	(0,2,2)	.020	.021	.026
(1,$\bar{3}$,1)	(1,$\bar{3}$,1)	1.135	1.141	1.187
($\bar{1}$,$\bar{1}$,3)	(1,$\bar{3}$,1)	.014	.010	.017
($\bar{1}$,1,3)	($\bar{1}$,1,3)	1.060	1.066	1.079

Tab. V-4. Sample elements of symmetrized RPA or LDA DM of Ge at $\vec{q}$=(.5,.5,.5)*(2$\sqrt{3}$/a), obtained with Cohen-Bergstresser [59] and Berkeley pseudopotentials (IV-2).

In Tab. V-3,4 we present some of elements of symmetrized dielectric matrices of germanium at points X and L respectively. The calculated matrices were of the size 190x190 for X and 180x180 for L points in the case of Berkeley pseudopotential and of the order 108x108 for both points when empirical pseudopotential was used.

The effect of exchange-correlation on dielectric properties of crystals can be visualized in the best way by calculation of some "global" quantity, or by screening some external perturbation. It is not only because it is difficult to handle one by one elements of a large matrix, but rather because it is difficult to understand the trends governing the behaviour of the off-diagonal elements of DM. The most striking example of the role of exchange-correlation on the electronic screening is given in the next chapter, where phonons in germanium are discussed. Here we will show the effect of exchange correlation on the dielectric band structure of germanium. In Tab. V-5 the greatest eigenvalues of RPA and LDA dielectric matrices at Γ , X and L points are presented.

The trends similar to those of Tab. V-1 and discussed before can be found also in Tab. V-2, 3, 4, 5. We can see, that both DM elements and their eigenvalues are more affected by exchange-correlation effects than by details of band structure scheme. Moreover, there is quite a big difference in response matrices when exchange correlation is included or not. The fact that dielectric eigenvalues are greater in LDA case suggests that XC makes the screening more metallic.

It is also interesting to look at the effect of XC on inverse dielectric matrices. After all, these quantities are the true physical response and through them the effect can be rediscovered in a concrete physical problem (as it is done in the next chapter). In Tab. V-6 our results for the inverse symmetrical dielectric matrix at Γ and X points are shown. Recently the values for some selected elements have been obtained by Kunc and Tosatti [29] within "direct-LDA" scheme and the same pseudopotential as used here; these are also reported

in Tab. V-6. The slight difference between our and Kunc-Tosatti results is due to the reasons discussed just above.

It can be seen from all of the above tables, that off-centre of the Brillouin zone the difference between RPA and LDA responses seems to be more pronounced. While for the inverse dielectric matrix at the Γ point this difference is of the order of 10%, at X or L points it becomes of the order of 25-30%. Another important fact to be noticed in Tab. V-6 is that the exchange-correlation corrections to the inverse dielectric matrix lower its diagonal elements, while off-diagonal ones become larger in absolute value. As it has been discussed in [75], this could be understood in the framework of an "excitonic" picture of exchange-correlation corrections. The inverse dielectric matrix in many-body formulation is given by:

$$\epsilon^{-1}(\vec{q}+\vec{G},\vec{q}+\vec{G}') = \delta_{\vec{G},\vec{G}'} + \frac{8\pi e^2}{\Omega_0 |\vec{q}+\vec{G}|^2} \sum_n \frac{\langle 0|\rho^+_{\vec{q}+\vec{G}}|n\rangle\langle n|\rho_{\vec{q}+\vec{G}'}|0\rangle}{E_n - E_0} \qquad (V-1)$$

where 0 and n refer to the "true" many-body ground and excited states. The inclusion of exchange correlation lowers the excitation energies of the system (excitonic effect) thus - roughly speaking - decreasing diagonal and increasing off-diagonal elements of ϵ^{-1} as an effect of $\delta_{\vec{G},\vec{G}'}$ in Eq. (V-1). Having smaller excitation gap the system becomes more metallic, and the screening is more effective. This is visualized by the comparison of the most important dielectric eigenvalues in both LDA and RPA schemes, as it is done in Tab. V-5. At the same time however the importance of the off-diagonal elements of ϵ^{-1} with respect to diagonal ones is confirmed. This enhancement of local-field effects - which points out on the contrary the ionicity of the system - is responsable for the more directional character of the screening. As it will be shown in the next chapter, this effect turns out to be of a great importance as

the stability condition for the lattice of germanium.

At the end of this chapter we would like to verify how well the acoustic sum rule (ASR) is satisfied. We can do this calculating the Born effective charge Z^* (II-66). In germanium like in any other diamond-structure material Z^* should be zero because of (II-67). LDA calculation yields for Z^* the value -0.29, while RPA one gives +0.69. The LDA approximation results in 7% violation of ASR and is much better than RPA one, which gives 17% error in ASR. Since the response we calculated is the exact (in principle) response within the LDA approximation, this is a test of the accuracy of the numerical procedures. We recall, however, that the ASR is a very crucial and delicate test. Most physical properties are predicted to a better accuracy.

Cohen-Bergstresser		Berkeley			
RPA	symmetry	RPA	symmetry	LDA	symmetry
		$\vec{q}=0$			
2.171	Γ'_2	2.308	Γ'_2	3.251	Γ'_2
1.962	Γ'_{15}	2.014	Γ'_{15}	2.613	Γ'_{15}
1.742	Γ'_{25}	1.780	Γ'_{25}	2.172	Γ'_{12}
1.721	Γ'_{12}	1.749	Γ'_{12}	2.037	Γ'_{25}
		$\vec{q}=\vec{q}_X$			
3.169	X_1	3.378	X_1	4.491	X_1
2.377	X_4	2.445	X_4	3.241	X_4
2.074	X_1	2.156	X_1	2.772	X_1
1.567	X_3	1.607	X_3	1.918	X_3
1.560	X_2	1.562	X_2	1.840	X_2
		$\vec{q}=\vec{q}_L$			
4.097	L_1	4.334	L_1	6.390	L_1
2.676	L'_1	2.911	L'_1	3.426	L'_1
2.112	L_1	2.215	L_1	2.958	L_1
2.019	L'_3	2.068	L'_3	2.573	L'_3
1.892	L_3	1.943	L_3	2.480	L_3

Tab. V-5. The greatest eigenvalues and their symmetries of the symmetrized LDA and RPA DM of Ge in Γ, X and L points.

$\vec{G}$	$\vec{G}'$	RPA	LDA	K-T
		$\tilde{\epsilon}^{-1}(\vec{q}=0)$		
(1,1,1)	(1,1,1)	.5959	.5136	.517
(2,0,0)	(2,0,0)	.6497	.5677	.570
(2,0,0)	(1,1,1)	.0076	.0130	.014
(2,0,0)	(2,0,0)	.0084	.0133	.015
(3,1,1)	(2,0,0)	.0411	.0521	.050
(2,2,0)	(2,2,0)	.8167	.7697	....
(3,1,1)	(2,2,0)	-.0081	-.0110	....
		$\tilde{\epsilon}^{-1}(\vec{q}=\vec{q}_x)$		
(0,0,0)	(0,0,0)	.3311	.2599	....
(1,1,1)	(0,0,0)	-.0401	-.0234	....
(1,1,1)	(1,1,1)	.4887	.4040	....
(0,0,2)	(1,1,1)	.0103	.0114	....
(0,0,2)	(0,0,2)	.7134	.6445	....
(0,0,2)	(0,0,2)	.0038	.0069	....
(1,1,1)	(1,1,1)	.7607	.7027	....
(2,0,0)	(1,1,1)	-.0498	-.0522	....
(0,2,2)	(0,2,2)	.8477	.8115	....
(2,2,2)	(0,2,2)	.0095	.0155	....

Tab. V-6. Sample elements of symmetrized RPA or LDA IDM of Ge at $q=0$ and $\vec{q}=(1,0,0)$ in $(2\pi/a)$ units. K-T means results of Kunc and Tosatti from Ref. [29].

CHAPTER VI

PHONONS FROM DIELECTRIC SCREENING THEORY

One of the most extensively studied applications of dielectric screening matrices in semiconductors has been the lattice dynamics. For the most general external perturbation in the crystal all Fourier components for $\vec{q}$-vectors from and outside the first Brillouin zone are nonvanishing. Thus, in order to screen it, one should basically have available dielectric matrices calculated at all $\vec{q}$-vectors of the BZ. Due to the technical complexity discussed above however, first-principle calculations of dielectric matrices were possible only at high symmetry points up to recently. Phonons have a simplifying feature: when the atoms of a crystal move according to the displacement pattern of a given phonon mode of $\vec{q}$ wavevector, they produce an external perturbation potential in the system of electrons, which involves Fourier components of wave-vector $\vec{q}$ and $\vec{q}+\vec{G}$, where $\vec{G}$ is a reciprocal lattice vector. Such a perturbation within linear regime (and the potential due to a phonon is weak, since the atomic displacements are small) can be screened with the aid of the dielectric matrix calculated at point $\vec{q}$. Having then dielectric matrices calculated in separate points of the BZ, we can use them to obtain phonon dynamical matrices at these points.

A very successful achievement of theoretical semiconductor physics of recent years has been however the "direct" method of phonon calculations [51,70,76-88]. The idea of the "frozen-phonon" concept was to find the vibrational frequencies by calculating in LDA scheme the total energy of the electronic system with and without atomic displacements in a given phonon mode. The results obtained in the "direct" way proved to be very accurate. Anharmonic as well as harmonic phonons are the output of those calculations in contrast to the "perturbative" or "dielectric matrix" approach, which deals with harmonic phonons only. The "direct" methods turned out to be useful also in computing long wavelength properties of crystals, like Born effective charges [70], elastic constants [88-89] or macroscopic

dielectric constants [65]. These methods suffer however from a technical limitation of the size of a supercell, that must be used. Such a supercell limitation is not present in "perturbative" approach. As far as harmonic phonons are concerned, these two methods are in principle equivalent and should give the same results.

The present work can be thought as a "revenge" of "perturbative" approach over "direct" one in their competition of recent years. We prove that the calculations of dielectric matrices across Brillouin zone are feasible and we report some quantities, which could not be - according to our best knowledge - obtained till now in "direct" way. These are for example the interatomic force constants, the basic ingredient of lattice dynamics.

In the first part of this chapter we shall explain how interatomic force constants and dynamical matrices can be obtained via the dielectric matrix approach. In the second part of the chapter we shall present our results for phonon frequencies at a number of points in BZ together with the discussion of the influence of local-field effects and exchange-correlation corrections on lattice dynamics in germanium. Finally we shall pass to the calculation of interatomic and interplanar force constants in Ge.

VI.1. General Theory.

In the adiabatic approximation one first solves the electronic many particle problem with "frozen" ionic positions (as if masses of ions were infinite) and then obtains ionic motion from the equation:

$$\left[\sum_j \frac{P_j}{2M_j} + V(R_j)\right]\Phi(R_j) = E\Phi(R_j) \qquad \text{(VI-1)}$$

where P_j, M_j are momenta and masses of ions and $V(R_j)$ is the sum:

$$V(R_j) = \frac{1}{2}\sum_{j\neq j'} \frac{Z_j Z_{j'} e^2}{|R_j - R_{j'}|} + \mathcal{E}(R_j) \qquad \text{(VI-2)}$$

The first term on the right-hand side in (VI-1) is the Coulombic ion-ion interaction, while $\mathcal{E}(R_j)$ stays for the ground state energy of electronic system with "frozen" ions.

The proper derivation of force constants from electronic contribution to ionic potential energy was the main task of lattice-dynamic theory up to nowadays. The situation was particularly complicated in insulating crystals, where the highly non-homogeneous character of electron density distribution made it difficult to understand and describe the response of electrons to the ionic movement. That is why a number of models have been proposed over last decades in which several aspects of electron behaviour have been exploited. Let us mention at least shell models [90-91], deformation dipole models [92], bond charge models [93,94] or valence force field models [95-97]. Some of them, like for example the adiabatic bond charge model (BCM) [94], give phonon frequencies of covalent materials with surprisingly good accuracy with the use

of a very few fitting parameters only.

We deal with harmonic phonons when interionic interaction potential is quadratic in ion displacements from equilibrium. If those displacements are small, we can approximate $V(R_j)$ by its power series expantion up to second order being thus in harmonic regime. We shall show in the following, that the electronic contribution to lattice dynamics in harmonic approximation is governed by the electronic linear screening of ionic motion.

Let $u_s^\alpha(l)$ be the α-component of a displacement of an s-ion from equlibrium position $\vec{R}^0_{ls}=\vec{R}_l+\vec{R}_s$ in l'th unit cell. Up to the second order in u, we can write (the linear term vanishes when expanding around equilibrium)

$$V(R_j) = V_0 + \frac{1}{2}\sum_{ls\alpha}\sum_{l's'\beta} C^{\alpha\beta}_{ss'}(l,l')\, u_s^\alpha(l)\, u_{s'}^\beta(l') \qquad \text{(VI-3)}$$

where

$$C^{\alpha\beta}_{ss'}(l,l') = \left.\frac{\partial^2 V(R_j)}{\partial R^\alpha_{ls}\,\partial R^\beta_{l's'}}\right|_{R_j=R^0} \qquad \text{(VI-4)}$$

$C^{\alpha\beta}_{ss'}(l,l')$ are by definition the harmonic force constants, they give the force in the α-direction which an ion at position $\vec{R}^0_{ls}$ feels, when another ion at position $\vec{R}^0_{l's'}$ is moved in β-direction by a unit of length. These force constants satisfy several conditions that result from their definition or symmetry properties of crystal or space. They are presented in any text-book [9, 98, 99]; here we would only report one of them, which follows from the invariance of system with respect to infinitesimal rigid translations:

$$\sum_{l,s} C^{\alpha\beta}_{ss'}(l,l') = 0 \qquad \text{(VI-5)}$$

The above condition, which implies that frequencies of acoustic

phonons go to zero for infinite wavelengths, is intimately related to acoustic sum rule [8] (I-62) - the condition on "wing" elements of inverse dielectric matrix at $\vec{q}\longrightarrow 0$.

We shall pass now to the microscopic derivation of $C^{\alpha\beta}_{ss'}(l,l')$.

The electron-ion interaction part of the total Hamiltonian of the system can be written by means of ionic potentials (or pseudopotentials) V_s in the following way:

$$V_{e\text{-}j} = \sum_{i\,ls} V_s(\vec{r}_i - \vec{R}_{ls}) = \sum_{ls}\int d\vec{r}\;\hat{\varrho}(\vec{r})\, V_s(\vec{r}-\vec{R}_{ls}) \qquad \text{(VI-6)}$$

where

$$\hat{\varrho}(\vec{r}) = \sum_i \delta(\vec{r}-\vec{r}_i) \qquad \text{(VI-7)}$$

is the electron density operator. Expanding $V_{e\text{-}j}$ up to the second order in u yields:

$$\begin{aligned} V_{e\text{-}j} &= \sum_{ls}\int d\vec{r}\;\hat{\varrho}(\vec{r})\, V_s(\vec{r}-\vec{R}^0_{ls}) - \sum_{ls\alpha}\int d\vec{r}\;\hat{\varrho}(\vec{r})\,\frac{\partial V_s(\vec{r}-\vec{R}^0_{ls})}{\partial r^\alpha}\, u_s^\alpha(l) \\ &+ \frac{1}{2}\sum_{ls\alpha\beta}\int d\vec{r}\;\hat{\varrho}(\vec{r})\,\frac{\partial V_s(\vec{r}-\vec{R}^0_{ls})}{\partial r^\alpha\,\partial r^\beta}\, u_s^\alpha(l)\, u_s^\beta(l) \qquad \text{(VI-8)} \\ &= \int d\vec{r}\;\hat{\varrho}(\vec{r})\, v^{(0)}(\vec{r}) + \int d\vec{r}\;\hat{\varrho}(\vec{r})\, v^{(1)}(\vec{r}) + \int d\vec{r}\;\hat{\varrho}(\vec{r})\, v^{(2)}(\vec{r}) \end{aligned}$$

where the meaning of $v^{(0)}$, $v^{(1)}$, $v^{(2)}$ is obvious. The second and third term of (VI-8) can be treated as a perturbation to the all-electron Hamiltonian after adiabatic separation from ionic variables. The second order contribution to $\mathcal{E}(R)$ will consist then of the first order perturbation term from $\int d\vec{r}\;\hat{\varrho}\, v^{(2)}$ and the second order perturbation term coming from $\int d\vec{r}\;\hat{\varrho}\, v^{(1)}$.

The expectation value in the ground state of $\int d\vec{\tau}\, \hat{\rho}\, v^{(2)}$ gives the following contribution to force constants:

$$C^{\alpha\beta}_{ss'}(l,l')^{e}_{1} = \delta_{ll'}\,\delta_{ss'} \int d\vec{\tau}\; n^{o}(\vec{\tau})\, \frac{\partial^2 V_s(\vec{\tau}-\vec{R}^{o}_{ls})}{\partial \tau^{\alpha}\,\partial \tau^{\beta}} \qquad \text{(VI-9)}$$

The second-order change of energy due to $\int d\vec{\tau}\, \hat{\rho}\, v^{(1)}$ yields:

$$\Delta \mathcal{E}^{(2)}(R) = -\sum_{m} \frac{\langle 0 | \int d\vec{\tau}\, \hat{\rho}\, v^{(1)} | m \rangle \langle m | \int d\vec{\tau}\, \hat{\rho}\, v^{(1)} | 0 \rangle}{E_m - E_0}$$

$$= -\frac{1}{2} \int d\vec{\tau} \int d\vec{\tau}'\, v^{(1)}(\vec{\tau}) \sum \frac{\varrho_{om}(\vec{\tau})\varrho_{mo}(\vec{\tau}') + \varrho_{om}(\vec{\tau}')\varrho_{mo}(\vec{\tau})}{E_m - E_0}\, v^{(1)}(\vec{\tau}') \qquad \text{(VI-10)}$$

$$= \frac{1}{2} \int d\vec{\tau} \int d\vec{\tau}'\, v^{(1)}(\vec{\tau})\; \chi(\vec{\tau},\vec{\tau}')\; v^{(1)}(\vec{\tau}')$$

where m and o refer to excited and ground states of many-electron system and χ is the density response defined in (I-7). The contribution to force constants coming from (VI-10) is the following:

$$C^{\alpha\beta}_{ss'}(l,l')^{e}_{2} = \int d\vec{\tau} \int d\vec{\tau}'\, \frac{\partial V_s(\vec{\tau}-\vec{R}^{o}_{ls})}{\partial \tau^{\alpha}}\; \chi(\vec{\tau},\vec{\tau}')\; \frac{\partial V_{s'}(\vec{\tau}'-R^{o}_{l's'})}{\partial \tau'^{\beta}} \qquad \text{(VI-11)}$$

It follows from (VI-9), that C^{e}_{1} is the force which an ion feels when it is moved from equilibrium. The infinitesimal translations invariance conditions (VI-5) states, that this force constant must be equal to the sum of force constants from all other ions with opposite sign. We can prove this fact integrating by parts in (VI-9):

$$\int d\vec{\tau}\; n^{(0)}(\vec{\tau})\, \frac{\partial^2 V_s(\vec{\tau}-\vec{R}^{o}_{ls})}{\partial \tau^{\alpha}\,\partial \tau^{\beta}} = -\int d\vec{\tau}\, \frac{\partial\, n^{o}(\vec{\tau})}{\partial \tau^{\alpha}}\; \frac{\partial V_s(\vec{\tau}-\vec{R}^{o}_{ls})}{\partial \tau^{\beta}} \qquad \text{(VI-12)}$$

and then observing that if the whole crystal is moved rigidly by an infinitesimal vector $\vec{u}$, the change in the V_{e-j} potential will be:

$$\vec{u}\, \frac{\partial V_{e-j}(\vec{\tau})}{\partial \vec{\tau}} = \sum \frac{\partial V_s(\vec{\tau}-\vec{R}^{o}_{ls})}{\partial \vec{\tau}}\, \vec{u} \qquad \text{(VI-13)}$$

In the same time the electron density will change by $\vec{u}\,\frac{\partial n^{o}}{\partial \vec{\tau}}$. These two changes should be compatible with each other and the relation between them is established with the aid of χ function:

$$\vec{u}\, \frac{\partial\, n^{o}(\vec{\tau})}{\partial \vec{\tau}} = \int d\vec{\tau}'\, \chi(\vec{\tau},\vec{\tau}')\, \vec{u}\, \frac{\partial V_{e-j}(\vec{\tau}')}{\partial \vec{\tau}'} \qquad \text{(VI-14)}$$

which yields:

$$\frac{\partial\, n^{o}(\vec{\tau})}{\partial \tau^{\alpha}} = \sum_{ls} \int d\vec{\tau}'\, \chi(\vec{\tau},\vec{\tau}')\, \frac{\partial V_s(\vec{\tau}'-\vec{R}^{o}_{ls})}{\partial \tau'^{\alpha}} \qquad \text{(VI-15)}$$

Putting (VI-15) into (VI-12), then into (VI-9) and suming with (VI-11) we obtain the <u>microscopic</u> expression for electronic part of interatomic force constants:

$$C^{\alpha\beta}_{ss'}(l,l')^{e} = C^{\alpha\beta}_{ss'}(l,l')^{e}_{1} + C^{\alpha\beta}_{ss'}(l,l')^{e}_{2} \qquad \text{(VI-16)}$$

$$= \int d\vec{\tau} \int d\vec{\tau}' \left[\frac{\partial V_s(\vec{\tau}-\vec{R}^{o}_{ls})}{\partial \tau^{\alpha}}\, \chi(\vec{\tau},\vec{\tau}')\, \frac{\partial V_{s'}(\vec{\tau}'-\vec{R}^{o}_{ls'})}{\partial \tau'^{\beta}} - \delta_{ll'}\,\delta_{ss'} \sum_{l''s''} \frac{\partial V_s(\vec{\tau}-\vec{R}^{o}_{ls})}{\partial \tau^{\alpha}}\; \chi(\vec{\tau},\vec{\tau}')\, \frac{\partial V_{s''}(\vec{\tau}'-\vec{R}^{o}_{s''l''})}{\partial \tau'^{\beta}} \right]$$

Taking second order in ionic displacements contribution to ion-ion interaction potential one can extract the ionic part of

force constants:

$$C^{\alpha\beta}_{ss'}(l,l')^{I} = -\frac{\partial^2 V_I(\vec{R}^0_{ls} - \vec{R}^0_{l's'})}{\partial\tau^\alpha\,\partial\tau^\beta} + \delta_{ll'}\,\delta_{ss'}\sum_{l''s''}\frac{\partial^2 V_I(\vec{R}^0_{ls} - \vec{R}^0_{l''s''})}{\partial\tau^\alpha\,\partial\tau^\beta} \qquad \text{(VI-17)}$$

where V_I is a Coulomb interaction:

$$V_I(\vec{R}_{ls} - \vec{R}_{l's'}) = \frac{Z_s Z_{s'} e^2}{|\vec{R}_{ls} - \vec{R}_{l's'}|} \qquad \text{(VI-18)}$$

It is easy to see that both $C^{\alpha\beta e}_{ss'}$ and $C^{\alpha\beta I}_{ss'}$ satisfy "in form" the condition (VI-5) of infinitesimal rigid body translations invariance as well as crystal translational symmetry invariance condition:

$$C^{\alpha\beta}_{ss'}(l,l') = C^{\alpha\beta}_{ss'}(l-l',0) = C^{\alpha\beta}_{ss}(0,l'-l) \qquad \text{(VI-19)}$$

For the use in first-principle calculations expression (VI-16) is up to now impractical. It needs density response functions calculated at each possible pair of points in real space - the task too difficult to achieve nowadays, even if reduction from crystal symmetries is applied and the continuum variable $\vec{r}$ is replaced by a grid of discrete points, like in Fast Fourier Transform technique. In this chapter we shall present first-principle calculations of $C^{\alpha\beta}_{ss'}(l,l')$ based not on (VI-16) but on its Fourier representation.

Because of lattice translational symmetry, normal vibrational modes of a harmonic crystal can have plane-wave character with a single $\vec{q}$-vector from the first Brillouin zone:

$$\vec{u}_s(l) = (NM_s)^{-1/2}\,\vec{e}_s(\vec{q})\,e^{-i\vec{q}\,\vec{R}_{ls} + i\omega_q t} \qquad \text{(VI-20)}$$

where M_s is the mass of s-ion, N - the number of unit cells in the crystal in which periodic Born - von Karman conditions are assumed. $\vec{e}$ is called polarization vector and gives the displacement pattern of a given mode. Substituting (VI-20) into the Newton equation:

$$M_s\,\ddot{u}^\alpha_s(l) = \sum_{l's'\beta} C^{\alpha\beta}_{ss'}(l,l')\,u^\beta_{s'}(l') \qquad \text{(VI-21)}$$

we obtain the equations for normal modes in the form:

$$\omega^2_q\,e^\alpha_s(\vec{q}) = \sum_{s'\beta} D^{\alpha\beta}_{ss'}(\vec{q})\,e^\beta_{s'}(\vec{q}) \qquad \text{(VI-22)}$$

where $D^{\alpha\beta}_{ss'}$ is called the <u>dynamical matrix</u> and is essentially the Fourier transform of force constants $C^{\alpha\beta}_{ss'}(l,l')$:

$$D^{\alpha\beta}_{ss'}(\vec{q}) = (M_s M_{s'})^{-1/2}\sum_{l'} C^{\alpha\beta}_{ss'}(0,l')\,e^{-i\vec{q}(\vec{R}_{l'} + \vec{R}_{s'} - \vec{R}_s)} \qquad \text{(VI-23)}$$

Phonon frequencies are then obtained from the diagonalization of the dynamical matrix $D^{\alpha\beta}_{ss'}$. It is convenient to write down the dynamical matrix in form, which shows up its translational invariance:

$$D^{\alpha\beta}_{ss'} = (M_s M_{s'})^{-1/2}\left[\bar{C}^{\alpha\beta}_{ss'}(\vec{q}) - \delta_{ss'}\sum_{s''}\bar{C}^{\alpha\beta}_{ss''}(0)\right] \qquad \text{(VI-24)}$$

where

$$\bar{C}^{\alpha\beta}_{ss'}(\vec{q}) = e^{-i\vec{q}(\vec{R}_{s'} - \vec{R}_s)}\sum_{l'} C^{\alpha\beta}_{ss'}(0,l')\,e^{-i\vec{q}\,\vec{R}_{l'}} \qquad \text{(VI-25)}$$

From (VI-16), (VI-17) and (VI-23) we get the microscopic expression for dynamical matrix, or equvalently, for $\bar{C}^{\alpha\beta}_{ss'}(\vec{q})$:

$$\bar{C}^{\alpha\beta}_{ss'}(\vec{q}) = \frac{4\pi Z_s Z_{s'} e^2}{\Omega_0}\sum_{\vec{G},\vec{G}'}\frac{(\vec{q}+\vec{G})^\alpha(\vec{q}+\vec{G}')^\beta}{|\vec{q}+\vec{G}|\,|\vec{q}+\vec{G}'|}\left[\delta_{\vec{G},\vec{G}'} - C_{ss'}(\vec{q}+\vec{G},\vec{q}+\vec{G}')\right]e^{-i\vec{G}\vec{R}_s + i\vec{G}'\vec{R}_{s'}} \qquad \text{(VI-26)}$$

where

$$G_{ss'}(\vec{q}+\vec{G},\vec{q}+\vec{G}') = \frac{V_s(\vec{q}+\vec{G})\ V_{s'}(\vec{q}+\vec{G}')}{\frac{4\pi Z_s e^2}{\Omega_0|\vec{q}+\vec{G}|^2}\ \frac{4\pi Z_{s'} e^2}{\Omega_0|\vec{q}+\vec{G}'|^2}} \left[\delta_{\vec{G},\vec{G}'} - \tilde{\varepsilon}^{-1}(\vec{q}+\vec{G},\vec{q}+\vec{G}')\right] \qquad \text{(VI-26')}$$

In above expressions $Z_s e^2$ and $\vec{R}_s$ are ionic charges and positions in unit cell of the volume Ω_0, $\vec{G}$ are reciprocal lattice vectors and $\tilde{\varepsilon}^{-1}$ is the inverse symmetrized dielectric matrix related to χ by (I-11) and (I-26). (VI-26) proves that harmonic phonons come out as a result of <u>linear</u> and <u>static</u> response of electrons to ionic displacements. The static response is a direct consequence of adiabatic approximation - the movement of ions is so slow, that in each moment electrons retain their ground state (changing in time however).

Eq. (VI-26) is the basic result due to Pick, Cohen and Martin. We gave here a somewhat different derivation; another derivation can be found in a recent review article by R. Resta and A. Baldereschi [100].

It should be noticed, that $\tilde{\varepsilon}^{-1}$ in (VI-26) is the "true" dielectric response (test charge-test charge) of a system of electrons, or in other words, it is a response in electrostatic potential to the external electrostatic perturbation. Working in the Local Density Approximation it means that one inserts in (VI-26) the $\tilde{\varepsilon}^{-1}_{LDA}$ of Eq. (I-48).

The formalism becomes simpler for the Γ point. It can be shown [8] on the basis of analytical properties of inverse dielectric matrices, that the dynamical matrix in $\vec{q}\longrightarrow 0$ limit takes the form:

$$D^{\alpha\beta}_{ss'}(\vec{q}) = (M_s M_{s'})^{-\frac{1}{2}}\left[\bar{C}^{\alpha\beta}_{ss'}(0) - \delta_{ss'}\sum_{s''}\bar{C}^{\alpha\beta}_{ss''}(0) + \frac{4\pi Z^*_s Z^*_{s'} e^2}{\Omega_0\ \varepsilon_\infty}\ \frac{q^\alpha q^\beta}{q^2}\right] \qquad \text{(VI-27)}$$

where the effective charge Z^*_s is defined in (I-66). $\bar{C}^{\alpha\beta}_{ss'}(0)$ should be calculated here only with "body" elements of the

inverse dielectric matrix at $\vec{q}=0$. The expression (VI-27) determines the particular form of dynamical matrix for zinc-blend and diamond type crystals at the Γ point, from which the following rules can easily be derived:

$$\omega^2_{TO} = -\bar{C}^{\alpha\alpha}_{AC}(0)\left(\frac{1}{M_A} + \frac{1}{M_C}\right) \qquad \text{(VI-28)}$$

$$\omega^2_{LO} = \omega^2_{TO} + \frac{4\pi (Z^*)^2 e^2}{\Omega_0\ \varepsilon_\infty}\left(\frac{1}{M_A} + \frac{1}{M_C}\right) \qquad \text{(VI-29)}$$

Here A and C mean "anion" and "cation" respectively (we use this terminology also for diamond type crystals) and because of acoustic sum rule $Z^* = Z^*_A = -Z^*_C$. The frequency of a transverse acoustic phonon is zero by symmetry, while for longitudinal acoustic mode it vanishes because of ASR (I-67). In first principle calculations ASR is usually not satisfied and ω_{LA} frequency for diamond-type crystals is then given by the calculations as:

$$\omega^2_{LA} = \frac{8\pi (Z^*)^2 e^2}{\Omega_0\ \varepsilon_\infty\ M} \qquad \text{(VI-30)}$$

We believe that the dielectric matrix approach is particularly suitable for calculations of electron-phonon interaction matrix elements. It is because this interaction can involve phonons of wavelengths, which are not simple multiplies of lattice constant and "direct" methods could face great problems in finding a proper supercell size. It is however roughly the same computational efford nowadays to calculate a dielectric matrix in any point of Brillouin zone. Having the dielectric matrix in a given point we can obtain both the dynamical matrix and the polarization potential due to a given phonon having this $\vec{q}$-wavevector. Since a phonon of wave-vector $\vec{q}$ produces a small external potential in the electronic system of the form:

$$\delta V_{ext}(\vec{q}+\vec{G}) = i\sum_s \frac{\vec{e}_s(\vec{q})(\vec{q}+\vec{G})}{\sqrt{M_s}} V_s(\vec{q}_v+\vec{G})\, e^{i\vec{G}\vec{R}_s} \qquad \text{(VI-31)}$$

it is a question of a simple multiplication by a proper dielectric matrix (I-45) (test charge-electron) to have the total perturbing potential due to the phonon, which electrons feel: $\delta V = \delta V_{ext} + \delta V_H + \delta V_{xc}$. Notice that the dielectric matrix to be used in this problem is not the standard (test charge - test charge) one.

VI.2. Phonons in Germanium: Results.

Equation (VI-26) has been up to recently the main tool for calculating phonon frequencies in covalent and ionic solids on the basis of the microscopic theory. Since first-principle calculations of inverse dielectric matrices turned out to be very difficult, in early phonon computations based on (VI-26) simplified band structures have been used. [64], or model dielectric matrices have been proposed [35] to account for the most important screening features of the electronic system. Some of the lattice-dynamical models, like Phillip's, Martin's and Weber's bond charge models [93,94], even if not referring to expression (VI-26) directly, were constructed in the way to mimic charge density of electrons of a covalent solid and their displacements under the perturbing potential of a phonon.

It was known from Martin's paper [93], that the off-diagonal elements of the inverse dielectric matrix in (VI-26) are essential in the lattice dynamics of covalent or ionic materials - the frequencies of transverse acoustic phonons turned out to be imaginary if calculated with diagonal response only. Bertoni et.al. [35] were able to stabilize the silicon crystal including off-diagonal elements of response matrices in a model approach. These works proved, that first-principle calculations of phonons in covalent solids have to deal with the full complexity of dielectric matrix evaluation.

The first ab-initio calculations of phonon frequencies in semiconductors based on Eq. (VI-26) started to appear in the late seventees. S.Louie and M.L.Cohen presented in 1978 [49] the results for phonon frequencies at Γ point in silicon obtained via RPA dielectric matrix of the order 59. The exchange-correlation effects were included in phenomenological way by multiplication of polarizability matrix by a constant adjastable factor [102]. In 1979 the Antwerpen group has published a paper [52] on ab-initio calculation of phonon frequencies in silicon. To circumvent the problem of slowly

convergent summation over conduction bands in (II-1), they proposed the so-called "closure" approximation, i.e. the substitution of the energy difference denominators in (II-1) by a constant term. R.Resta and A.Baldereschi have published in 1981 [34] a calculation of phonons at Γ point in Si, Ge and GaAs. They have used the RPA dielectric matrices obtained from the Cohen-Bergstresser empirical pseudopotential [59] band structure together with the Appelbaum-Hamman [103] ionic pseudopotentials in expression (VI-26). The two choises are not exactly compatible. Their results differ from experiment by about 10% and (since they worked in RPA scheme) reflect the weak dependence of optical modes at Γ on exchange correlation in screening - the fact, that will be demonstrated more clearly from our calculations for Ge.

size of IDM	89	113	137	145	169	181
a	142.1	142.1	142.1	142.1	142.1	142.1
b	-56.4 -56.2	-71.7 -69.2	-66.1	-66.1	-66.1	-66.0
c	23.5 11.1	-1.4 -19.0	6.9	7.7	7.4	7.4
total	-32.9	-73.1	-59.2	-58.4	-58.7	-58.6

Tab.VI-1. Partial contributions to ω^2_{LTO} at Γ in THz^2: a) bare ions; b) diagonal IDM; c) off-diagonal IDM for different sizes of IDM in (VI-26). The lowest row is the total electronic contribution to (VI-26) - sum of b) and c). Numbers below in rows b) and c) taken from Ref. [34].

The phonon frequencies of germanium we shall present in this section have been obtained with larger dielectric matrices and larger basis set of plane waves in Bloch functions expansion than those of Ref. [49, 52, 34]. The ionic pseudopotentials in

(VI-26) was the same as in band structure calculation and exchange-correlation corrections were fully included. The technical details have already been given in chapter III of this work.

In the optical mode at the Γ point different contributions to (VI-26) sum up additively to construct ω^2_{LTO}. It is then feasible to detect their relative importance (this analysis however is valid only for this mode). Tab. VI-1 shows partial contributions to ω^2_{LTO} at Γ coming from: a) bare ions, b) diagonal inverse dielectric matrix (IDM) elements, c) off-diagonal IDM elements as a function of IDM size. The bare ion term has been obtained with the Ewald technique [99] and the number of $\vec{G}$ vectors indicated in first row of Tab. VI-1 concerns only the electronic part of (VI-26).

It follows from Tab. VI-1 that the optical mode at Γ is governed mostly by interionic Coulomb interaction (line a). Because of the negative sign of the total electronic contribution to ω^2_{LTO}, the strong interionic Coulomb interaction is screened and weakened by electrons. It is consistent with what has been already shown [104, 13, 76] in the study of polarization charge induced by the optical phonon at Γ: there is the electron charge transfer from stretched bonds to compressed ones. The relative importance of the off-diagonal to diagonal contribution in ω^2_{LTO} is quite small - of the order of 11%. It is much less than in [34], where this figure was almost three times as large. The other significant fact is, that while the diagonal contributions in both calculations (our and Ref. [34]) are rather similar, the off-diagonal ones are quite different. The reason could be in the small size (113x113) of dielectric matrices used in [34], which didn't guarantee the convergence of results. In fact, the diagonal "tail" contribution from greater $\vec{G}$ vectors in Tab. II of Ref. [34] is almost as large as the off-diagonal from first 113 vectors. The present results seem to be in excellent convergence and, on the contrary to Ref. [34] and [105], no diagonal "tail" is needed.

Our off-diagonal contribution to ω^2_{LTO} apart from being

smaller in absolute value than that in [34] is yet of opposite sign, being positive. It could seem then that off-diagonal IDM elements do not contribute to the charge transfer from stretched to compressed bonds, but - on the contrary - they slightly balance it. An analysis of the polarization charge in $\vec{r}$-space shows however, that this is not true. In Fig. VI.1 we show the polarization charge transfer due to LTO mode at Γ as it results from diagonal, off-diagonal and full response. It can be seen, that both diagonal and off-diagonal IDM elements contribute to the charge transfer in question in roughly the same manner. Moreover, our figure is very similar to the analogous Fig. II of Ref. [13], despite the different band structure and the different screening (LDA versus RPA) used. It follows therefore, that the phonon energy is not transparently connected to the shape of the polarization charge, being a rather complicated function of all the Fourier components of the charge density, pseudopotentials etc. The phonon energy seems to be more determined by the kind of pseudopotential used, than by the polarization charge density, which turns out to be rather insensitive on the details of band structure and response schemes.

Our calculation differs from that in Ref. [34] in the response function used to build up the dynamical matrix. While in [34] the RPA dielectric matrix has been calculated and inserted into (VI-26), this work is performed strictly within the selfconsistent Kohn-Sham sheme; we have been able here to construct the proper test charge - test charge response (ϵ^{-1}_{LDA}) to insert in (VI-26). To find out the effect of exchange correlation in dielectric response on the optical phonon frequency at Γ , we have performed two other calculations. First, we have put into (VI-26) the RPA inverse dielectric matrix, then we have calculated the LDA dielectric matrix corrected by exchange correlation but with diagonal polarizability χ_o . In the latter case the local-field effects are due to exchange correlation only. The results of all these calculations are given in Tab. VI-2.

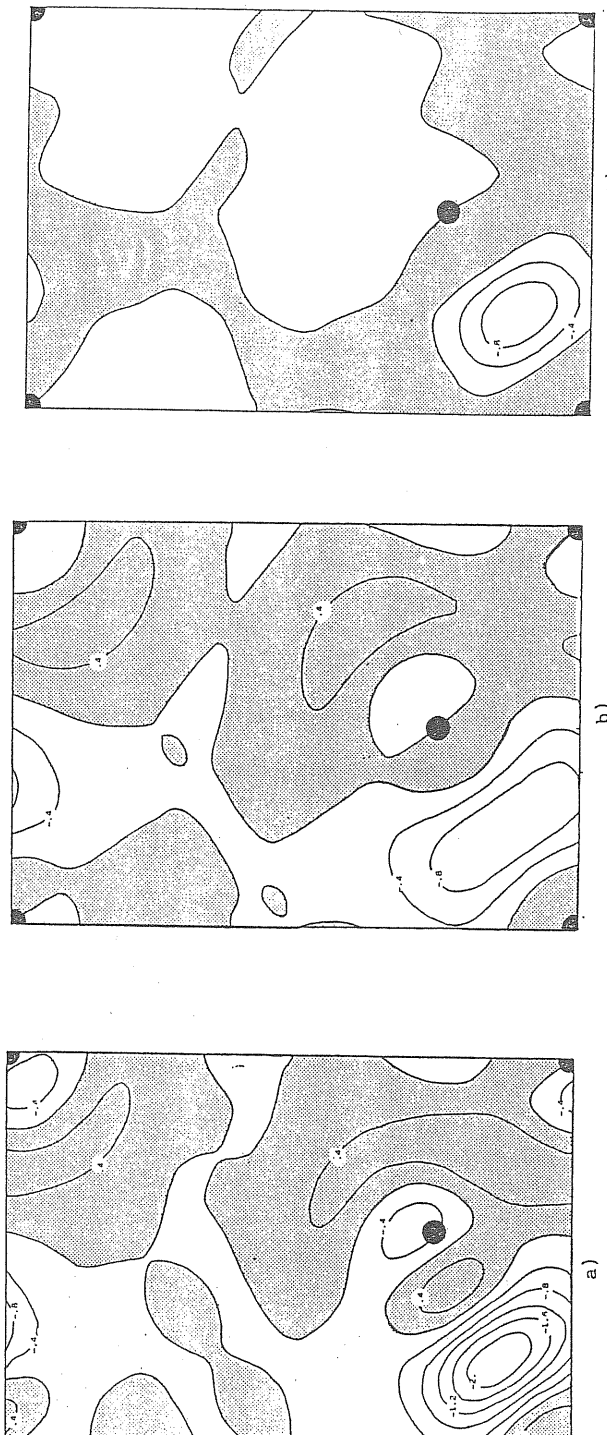

Fig. VI.1. Polarization electron density (in 10^{-1} electrons per cell) in $(1\bar{1}0)$ plane due to LTO phonon at q=0 in Ge: a) full LDA response matrix in dynamical matrix, b) diagonal LDA response, c) off-diagonal response. Shaded areas indicate positive electron density. Black dots show positions of atoms. Atomic displacements in the basis are $\bar{u}=\pm x(1,1,1)$ with x=.005 a.u.

Optical phonon frequencies are in very good agreement with experiment. The role of exchange correlation in this mode is a minor one: the values of frequencies calculated with LDA or RPA dielectric matrices are almost equal (columns a and c in Tab. VI-2). A greater difference for this particular mode - however yet quite small - is made by the diagonal approximation to DM. The comparison of b) and d) of Tab. VI-2 proves, that the values of the off-diagonal elements of DM at Γ point are mostly affected by the off-diagonal polarizability matrix χ_0. As far as the longitudinal acoustic mode at Γ is concerned, the value of .32 THz for its frequency obtained in calculation a) is a direct consequence of 7% violation of ASR as discussed in the preceding chapter. Here the exchange correlation is more important, as results from the value .79 THz obtained from the RPA response and neglecting of local-field effects gives rise to completly wrong results.

THz	Exp	a	b	c	d
LTO(Γ)	9.11	9.13	8.72	9.15	8.82
LA(Γ)	0.0	.32	4.36	.79	4.30

Tab. VI-2. Phonon frequencies at Γ in Ge in THz units; a) full $\tilde{\epsilon}^{-1}_{LDA}$, b) diagonal $\tilde{\epsilon}^{-1}_{LDA}$, c) full RPA and d) LDA constructed from diagonal χ_0 - dielectric matrices in (VI-26).

A completely different situation is dealt with at the point X of Brillouin zone. The importance of local-field effects in stabilizing covalent and ionic crystals against shear was well recognized already for some time [93,35]. It was shown [93,35], that the frequencies of transverse acoustic modes of silicon become imaginary when calculated using diagonal response only. Thus at the origin of transverse forces stabilizing crystal structure of covalent semiconductors is the inhomogeneity of the

electronic charge distribution, which is responsable for local-field effects in screening.

In chapter V of this work it was shown, that exchange correlation plays a greater role in screening at $\vec{q}$-vectors from the border of Brillouin zone in Ge than in the centre and its role is to enhance the importance of the off-diagonal elements of dielectric matrix with respect to diagonal ones. On the ground of above and preceding observations about the stability of covalent crystals, it should be expected that exchange correlation affects significantly the transverse acoustic mode at X.

In Tab. VI-3 we report the results of four different calculations of phonon frequencies at point X in germanium. The ingredients of the calculations are the same as in Tab. VI-2 for point Γ. It is seen that in contrast to the situation at optical mode at Γ the local fields and exchange correlation have dramatic effect on phonon frequencies at X. The transverse acoustic mode becomes unstable if one neglects either exchange correlation or off-diagonal elements of polarizability matrix χ_0 or both. The frequencies of the transverse optic mode are also increased by the neglect of these effects, while longitudinal modes remain almost unaffected. From Tab. VI-3 one could drawn the qualitative conclusion, that off-diagonal screening in χ_0 is somewhat more important than exchange correlation, however both are necessary to stabilize the crystal structure of germanium. When the LDA inverse dielectric matrix is used in (VI-26), the results for all modes at X are in very good agreement with experiment. As in Γ point the convergence with respect to IDM size is reached. To illustrate this fact we present in Tab. VI-4 the phonon frequencies at X obtained with different LDA IDM size.

THz	Exp	a	b	c	d
TO(X)	8.26	8.06	10.36	9.42	10.06
LOA(X)	7.21	7.13	7.26	7.49	7.25
TA(X)	2.40	2.25	4.59i	3.25i	4.10i

Tab. VI-3. Phonon frequencies at point X in Ge in THz. Experimental values from Ref. [106]. a), b), c), d) as in Tab. VI-2.

size of IDM	TA(X)	LOA(X)	TO(X)
92	2.95	6.64	8.63
116	2.15	7.42	8.26
150	2.54	7.23	8.12
174	2.42	7.14	8.10
190	2.25	7.13	8.06

Tab. VI-4. Convergence test on phonon frequencies at X point in Ge. In first column the size of inverse LDA DM used in (VI-26). Phonon frequencies in THz.

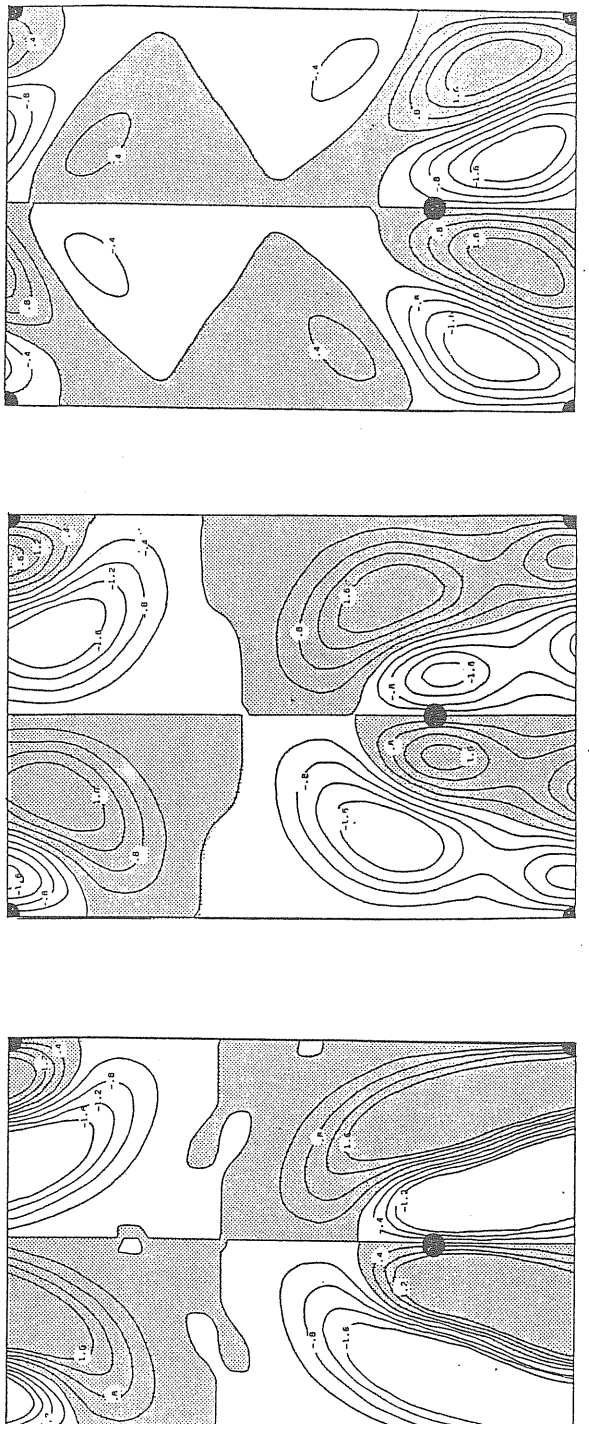

ig VI.2. Polarization electron density in $(O\bar{1}1)$ plane (in electrons per cell) due to TA(X) phonon in Ge:a) full LDA response in dynamical matrix, b) diagonal LDA response, c) off-diagonal LDA response. Shaded areas indicate positive electron density. Atoms, shown as black dots, move horizontally to the right by the amount of .035 of lattice constant.

If we look at the polarization charge density due to the transverse acoustic mode at X, Fig. VI.2, we can state, that electric dipoles perpendicular to bonds are induced. It follows from electrostatics, that these dipoles produce a restoring force on displaced atoms. We have not reported here the analogous picture obtained from the RPA response, since its shape is almost equal to Fig. VI.2. The difference is in numbers however. The induced dipole (the flow of displaced charge) in LDA case is somehow stronger than in RPA case. Again we can state, that our polarization charge is very similar to the one shown in Ref. [104] for silicon and obtained within a different band structure scheme than the one used here.

First-principle frozen-phonon calculations for LTO(Γ) and TA(X) modes in germanium have been published [87], which make use of the same pseudopotential scheme. The results are however a bit different from ours ($\omega_{LTO}(\Gamma)$=9.33 THz, $\omega_{TA}(X)$=1.61 THz) and we believe, this is mostly due to the differences in basis sets used in both calculations and/or possibly different other factors (like for instance the number of mean-value points). In our calculation we are using larger basis set than [87] and we diagonalize the full Hamiltonian matrices without Löwdin perturbation approach, as was done in [87].

The very good agreement of calculated phonon frequencies with experimental ones is no longer found when passing to the L point. In Tab. VI-5 phonon frequencies at L point obtained as previously with LDA and RPA dielectric matrices are reported. As in Γ and X, RPA input gives results much worse than the RPA one. The crucial role of exchange correlation is then again confirmed and the considerations on stability remain valid also here. The TA(L) mode frequency results from the calculation to be three times smaller than experiment. Moreover, the frequency of this particular mode is not in convergence with respect to the size of IDM, as the frequencies of other modes at L do. The addition of a diagonal "tail" to IDM has not improved the results. The possible explanation of above facts could be the following: when we deal with acoustic phonons at X point, the

planes of atoms, which move against each other are in a distance a/4, where a is lattice spacing. To describe properly the induced polarization charge density between planes one needs to use plane waves of wavelengths of the order and smaller than a/4. This distance transformed into Fourier space corresponds to the condition $|\vec{k}| \gg 4$ in $(2\pi/a)$ units. Since we have calculated response matrices for $\vec{G}$ vectors limited by $|\vec{q}_X+\vec{G}|^2 < 32$ in $(2\pi/a)^2$ units, the above condition is well satisfied and at X point our results are in convergence. For acoustic modes at the L point however, the distance between planes which move against each other is smaller - it is equal to a 3/12, which gives the condition $|\vec{q}_L+\vec{G}|^2 \gg 48(2\pi/a)^2$. It is probably far too large to be dealt with by the above cutoff. Notice, that the cutoff used for wave functions is instead $|\vec{q}+\vec{G}|^2 \leq 35(2\pi/a)^2$. The polarization charge density responsable particularly for weak transverse forces is a delicate quantity, which is probably not properly described. We can expect similar problems with the convergence of transverse acoustic phonon frequency for modes along Λ direction.

THz	TA(L)	LA(L)	LO(L)	TO(L)
Exp	1.90	6.66	7.34	8.70
LDA	.59	6.81	6.92	8.52
RPA	2.66i	5.55	8.76	9.18

Tab. VI-5. Phonon frequencies at L point in Ge in THz from LDA or RPA dielectric matrices in (VI-26). Exp. values from [106].

In Tab. VI-6 phonon frequencies calculated at 10 mean-value points of Chadi and Cohen [55] are presented. They have been obtained with exchange correlation included in response (LDA IDM in (VI-26)) and without it (RPA matrices). Since the experimental values of all those frequencies are not available to us, we compare our results with values calculated within the adiabatic bond charge model of Weber [94,107]. This model seems

to work very well in covalent crystals and gives phonon frequencies with average accuracy of about 2%. The input dielectric matrices in the above calculations were of the order determined by the condition $|\vec{q}+\vec{G}|^2 \leq 32(2\pi/a)^2$.

It follows from Tab. VI-6, that values of phonon frequencies obtained within LDA scheme are in general much closer to the bond charge model values. There are some common features of the spectra: i) transverse acoustic phonons become unstable without exchange correlation in screening - the fact noticed already at Γ, X and L points. As expected however, and discussed before, we have problems with stability of the phonons along direction Λ even within LDA; ii) the frequencies in LDA scheme are generally below BCM frequencies, while RPA scheme gives frequencies generally above the model ones. Since the BCM fequencies are close to experiment, this means that the ionic fequencies are close to experiment, this means that the ionic Coulomb interactions are overscreened due to the particular form of exchange-correlation potential (III-5) in Kohn-Sham equations and local ionic pseudopotential used in this work. The RPA dielectric response is in general not effective enough to screen the potential of ionic displacements, while the LDA response gives a much stronger screening.

We have proved in this chapter that first-principle phonon calculations in semiconductors via dielectric matrix method are feasible nowadays with quite a good accuracy, practically in any point of Brillouin zone. To this end one must use the full LDA dielectric matrix with exchange-correlation corrections and the pseudopotential (if used) in expression (VI-26) should be the same as that used in the calculation of DM. The convergence with respect to the size of dielectric matrix is different for different modes. The fundamental limitation of the method comes however from the local form of exchange correlation and - specially for the very sensitive transverse acoustic modes - from the local form assumed for the pseudopotential of the present work. In the next section we will show how to calculate from first principles the interatomic force constants in real space.

$\vec{q}$ in $2\pi/a$ units	type of calc.	1	2	3 THz	4	5	6
$\frac{1}{8}\frac{1}{8}\frac{1}{8}$	LDA	.21	.21	2.11	8.53	8.76	8.76
	RPA	1.21i	1.21i	2.47	8.71	8.93	8.93
	BCM	1.05	1.05	2.07	9.08	9.13	9.13
$\frac{3}{8}\frac{3}{8}\frac{3}{8}$	LDA	.55i	.55i	5.35	7.53	8.50	8.50
	RPA	2.62i	2.62i	4.80	8.63	9.07	9.07
	BCM	1.79	1.79	5.35	7.76	8.73	8.73
$\frac{3}{8}\frac{1}{8}\frac{1}{8}$	LDA	1.25	1.78	3.28	8.11	8.42	8.45
	RPA	1.96i	1.59i	3.70	8.58	8.85	8.96
	BCM	1.88	2.07	3.45	8.58	8.72	8.89
$\frac{5}{8}\frac{1}{8}\frac{1}{8}$	LDA	1.64	2.36	4.70	7.45	8.10	8.34
	RPA	2.84i	2.58i	5.15	8.15	9.11	9.12
	BCM	2.37	2.78	4.83	7.97	8.31	8.48
$\frac{5}{8}\frac{3}{8}\frac{3}{8}$	LDA	1.36	2.27	5.80	6.96	8.17	8.21
	RPA	2.68i	2.20i	4.93	8.18	9.02	9.34
	BCM	2.06	2.55	5.80	7.13	8.53	8.64
$\frac{7}{8}\frac{1}{8}\frac{1}{8}$	LDA	1.67	2.62	6.04	7.21	7.93	7.96
	RPA	3.40i	3.05i	6.48	7.62	9.26	9.32
	BCM	2.47	2.91	6.13	7.21	8.12	8.24
$\frac{3}{8}\frac{3}{8}\frac{1}{8}$	LDA	1.50	2.16	4.08	7.59	8.31	8.38
	RPA	2.00i	1.93i	4.02	8.26	8.86	9.21
	BCM	1.97	2.46	4.31	8.06	8.71	8.73
$\frac{5}{8}\frac{5}{8}\frac{1}{8}$	LDA	1.79	3.15	5.38	6.56	8.09	8.41
	RPA	2.78i	2.40i	5.19	7.58	9.08	9.71
	BCM	2.40	3.47	5.60	6.77	8.30	8.55
$\frac{5}{8}\frac{3}{8}\frac{1}{8}$	LDA	1.97	2.85	4.84	7.22	7.87	8.20
	RPA	2.62i	2.28i	4.76	7.92	8.88	9.47
	BCM	2.50	3.09	5.05	7.36	8.42	8.52
$\frac{7}{8}\frac{3}{8}\frac{1}{8}$	LDA	2.48	3.05	5.60	6.49	7.80	7.95
	RPA	2.89i	2.74i	5.79	7.13	9.15	9.51
	BCM	2.85	3.44	5.78	6.64	8.22	8.35

Tab. VI-6. Phonon frequencies at 10 mean-value points in THz in LDA, RPA schemes or BCM.

VI.3. Interatomic and Interplanar Force Constants

Interatomic force constants are the basic ingredient of lattice dynamics of solids. Their knowledge allows the calculation of phonon frequencies and eigenvectors throughout the Brillouin zone. However they have not been the main object of investigation in lattice dynamics. This was because the interatomic force constants in real space are up to now not accessible experimentally nor it was possible previously to calculate them at the ab-initio level. In a number of lattice dynamical models some force constants are dealt with only as fitting parameters.

A few years ago however first-principle calculations of interplanar force constants in semiconductors appeared [70, 84, 85]. They were based on the observation, that when a monochromatic phonon mode propagates through the crystal having a $\vec{q}$-vector along some symmetry direction, the whole planes of atoms perpendicular to the direction of propagation move as rigid entities. The phonon spectra and eigenvectors along a given high-symmetry line are thus determined by the interplanar force constants. It was suspected and then veryfied in calculations, that interplanar forces in semiconductors decay faster then interatomic ones. In other words, one has to take into account less interactions between planes of atoms in building up the dynamical matrix for phonons along a given line than should take interatomic interactions in construction of the dynamical matrix of the crystal at a general $\vec{q}$-point. This was a technically quite important fact, since it allowed to use manageable supercells in which atoms separated by half a period can be considered as decoupled. We refer to some of the many review articles devoted to this subject [51, 62, 86] for a more detailed account of this method. Roughly speaking one displaces only one atomic plane in a supercell and calculates the Hellman-Fynman force on atoms of the other planes. If the supercell is large enough, the interactions between the

displaced planes and those in other supercells can be neglected. In the recent calculation of Ref. [87] the supercell size was eight times the normal cell size in the direction of propagation of phonons, which means that it contained eight nearest neighbour planes in each (forward and backward) direction, while 4'th neighbour interplanar forces were already of the order of 1-2 % of the first neighbour ones. Phonon spectra along given lines of propagation obtained in such a way proved to be in very good agreement with experiment [87].

The above method belongs to the class of "direct" computational methods in solid state theory. It has similar advantages as for example frozen-phonon technique. One of the most interesting is the possibility of studying the anharmonic effects. The same technique as applied to interatomic forces proved to be up to now impractical. One would have to move a single atom in a supercell much larger than for interplanar needs, since it should be a multiple of the elementary cell in all three dimentions and - what was already mantioned above - the interatomic forces are of relative longer range.

In the following we present our ab-initio calculation of interatomic force constants in a covalent semiconductor. To the best of our knowledge, this is the first calculation of this kind to appear. It has been performed basically in a different way from the existing interplanar force constant calculations. The present one is not "direct", but rather "perturbative". The method follows the path of dielectric matrix scheme in lattice dynamics theory amd makes use of the computational feasibility of reponse matrix calculations at a general $\vec{q}$-point in the Brillouin zone.

It follows from (VI-23), that the phonon dynamical matrix $D^{\alpha\beta}_{ss'}(q)$ is essentially the Fourier transform on the Bravais lattice of interatomic force constants $C^{\alpha\beta}_{ss'}(0,l)$. If the dynamical matrix were available in every point of the Brillouin zone, the inverse Fourier transform would be possible yielding as the output interatomic force constants in real space:

$$C^{\alpha\beta}_{ss'}(0,l) = \frac{\omega\Omega_0}{(2\pi)^3}\int_{BZ} d\vec{q}\,(M_s M_{s'})^{1/2} D^{\alpha\beta}_{ss'}(\vec{q})\, e^{i\vec{q}(\vec{R}_l+\vec{R}_{s'}-\vec{R}_s)} \qquad \text{(VI-32)}$$

Practically the possibility of evaluation of the integral in (VI-32) on an arbitrarily dense grid of points in the Brillouin zone is highly limited by the feasibility of first-principle calculations of dynamical matrices, by no means simple yet. In this context however, the technique of mean-value points – and in particular, the one of Monkhorst and Pack [56] – proves to be very useful.

Mean-value points of Monkhorst and Pack are uniformly distributed points in Brillouin zone according to prescription:

$$\vec{k}_{prs} = u_p\vec{b}_1 + u_r\vec{b}_2 + u_s\vec{b}_3 \qquad \text{(VI-33)}$$

where $\vec{b}_i$ span the reciprocal lattice and fractions u_p, u_r, u_s are:

$$\begin{aligned} u_p &= (2p - q_1 - 1)/2q_1 \qquad (p=1,\ldots,q_1)\\ u_r &= (2r - q_2 - 1)/2q_2 \qquad (r=1,\ldots,q_2)\\ u_s &= (2s - q_3 - 1)/2q_3 \qquad (s=1,\ldots,q_3) \end{aligned} \qquad \text{(VI-34)}$$

The grid of points is determined by three integers (q_1, q_2, q_3). If $\vec{R} = l\vec{t}_1 + m\vec{t}_2 + n\vec{t}_3$, where $\vec{t}_1$, $\vec{t}_2$, $\vec{t}_3$ are primitive translation vectors of Bravais lattice compatible with $\vec{b}_i$ and l, m, n are integers, the summation over $\vec{k}_{prs}$ points of $e^{i\vec{k}_{prs}\vec{R}}$ factorizes:

$$\sum_{prs} e^{i\vec{k}_{prs}\vec{R}} = \left(\sum_{p=1}^{q_1} e^{2\pi i u_p l}\right)\left(\sum_{r=1}^{q_2} e^{2\pi i u_r m}\right)\left(\sum_{s=1}^{q_3} e^{2\pi i u_s n}\right) \qquad \text{(VI-35)}$$

It is now the question of a simple algebra to show, that each of factors on the right hand side of (VI-35) vanishes unless l, m, n are equal to integers times q_1, q_2, q_3 respectively.

Replacing in (VI-32) the integral by the summation over mean-value points yields:

$$C^{\alpha\beta}_{ss'}(0,l) \cong (M_s M_{s'})^{1/2}\frac{1}{N}\sum_{\vec{k}_{prs}} D^{\alpha\beta}_{ss'}(\vec{k}_{prs})\, e^{i\vec{k}_{prs}(\vec{R}_l+\vec{R}_{s'}-\vec{R}_s)} \qquad \text{(VI-36)}$$

10 mean-value points of Chadi and Cohen [55] correspond exactly to the division (8,8,8) of Monkhorst and Pack in the f.c.c. structure (we recall, that according to Appendix A in Ref. [56], (l,m,n) division in f.c.c. lattice is done on the simple cube, which contains the true f.c.c. Brillouin zone; one must pic up only the points, which belong to the first BZ). We can thus plug into (VI-36) the dynamical matrices calculated in the preceding part of this chapter and perform the summation over the (8,8,8) grid of points $\vec{k}_{prs}$. From the above discussion it follows for instance, that the $\vec{R}_l$=0 force constant will be calculated with spurious terms coming from shells with $|l|$, $|m|$, or $|n|$ equal to 8 and onward in $\vec{R}_l = l\vec{t}_1 + m\vec{t}_2 + n\vec{t}_3$. This corresponds to very distant shells for which $C^{\alpha\beta}_{ss'}(0,l)$ could be neglected. It follows as well, that if we take all the shortest $\vec{R}_l$ satisfying condition $|l|<4$, $|n|<4$, $|m|<4$, there are not spurious contributions to force constants of these $\vec{R}_l$ coming from shells that satisfy the same condition. The above limitation cuts off the symmetry shells of neighbors beyond the 16th. The 20 first symmetry shells of neighbors for diamond structure are presented in Tab. VI-7. In other words, our calculation, which makes use of Eq. (VI-36) with the (8,8,8) division, could be exact if force constants from all shells beyond the sixteenth were zero.

N of shell	Prototype vector in a/4	Along (110) chain	Contribution to a given interplanar force constant (100)	(111)
0	(0 0 0)	A	0	0
1	(1 1 1)	B	±1	±1
2	(2 2 0)	C	0, ±2	0, ±2
3	(-1 3 1)		±1, ±3	±1, -3
4	(0 0 0)		0, ±4	±2
5	(3 3 1)	D	±1, ±3	-1, ±3
6	(4 2 2)		±2, ±4	0,-2,4
7	(-4-2-2)		±2, ±4	0,2,-4
8	(5 1 1)		±1, ±5	1, ±3
9	(-3 3 3)		±3	1, -5
10	(4 4 0)	E	0, ±4	0, ±4
11	(5-1 3)		±1,±3,±5	±1,+3,-5
12	(6 2 0)		0,±2,±6	±2, ±4
13	(5 3 3)		±3, ±5	-1,-3,+5
14	(4 4 4)		±4	-2, +6
15	(-4-4-4)		±4	+2,-6
16	(5 5 1)	F	±1, ±5	-1, ±5
17	(-7 1 1)		±1, ±7	±3, -5
18	(6 4 2)		±2,±4,±6	0,-2,-4,+6
19	(-6-4-2)		±2,±4,±6	0,+2,+4,-6
20	(-3 5 5)		±3, ±5	+1,+3,-7

Tab. VI-7. Prototype vectors in a/4 units of 20 shortest symmetry shells in diamond structure. In third column the position in (110) bonding chain indicated. The last two columns give the number of interplanar force constant to which a given shell contributes.

We have performed several calculations of force constants via Eq. (VI-36). They were based either on first-principle dynamical matrices or on those obtained from bond charge model (BCM) [101]. The bond charge model case, easily manageable, apart from giving interesting results by themselves, served us as a guiding tool to the control of approximation introduced by the finite summation in (VI-36). Increasing the number of points up to the division (16,16,16) we could prove that the BCM results from the division (8,8,8) are already in good convergence. In Tab. VI-8 the interatomic force-constants matrices $C_{ss'}^{\alpha\beta}(0,1)$ (with $\alpha,\beta = x,y,z$ and $s=1,2$) for the first 16 symmetry shells from first-principle calculation and BCM are presented. The shells 7th and 15th are not given in Tab. VI-8 because their force constants are connected by symmetry to those of shells 6th and 14th respectively.

The most striking fact resulting from Tab. VI-8 is the long rangeness of forces in germanium - they are of much longer range then expected from previous work [95,108]. The forces coming from 10th shell are greater than those from 3rd, 4th, 6th etc. The same concerns the forces from 16th shell. In the case of first-principle calculation they are more important than forces from 3rd and 4th shells, while for BCM they are about as equal as those of 3rd shell. The most important force constants are those of first and second shells. Then come the forces from 5th, 10th and 16th shells. The striking fact to be noticed is that the strongest interactions propagate along the coplanar bonding chains. Fig. VI.1 presents such a bonding chain in (110) plane. The coordinates of atoms of chain marked by letters A, B, C, D, E, F are given also in Tab. VI-7. The strength of the interatomic force between a given pair of atoms depends on the number of bonds the atoms are joint with together, but depends also strongly on whether these bonds are coplanar or not. It turns out that atoms having a small distance but not lying on the bonding chain of Fig. VI.1 are connected by very weak forces (e.g. 3rd neighbors).

Table VI.8 First-principles versus Bond Charge Model interionic force-constants. in 10^5 dyn/cm.

Num. of shell	Rep. vector in 1/4 a units	First-principles calc. x	y	z	Bond Charge Model x	y	z
		1.7447	0.0	0.0	1.9093	0.0	0.0
0	(0 0 0)	0.0	1.7447	0.0	0.0	1.9093	0.0
		0.0	0.0	1.7447	0.0	0.0	1.9093
		-.4480	-.3145	-.3145	-.4831	-.3334	-.3334
1	(1 1 1)	-.3145	-.4480	-.3145	-.3334	-.4831	-.3334
		-.3145	-.3145	-.4480	-.3334	-.3334	-.4831
		-.0245	-.0240	-.0127	-.0123	-.0153	-.0181
2	(2 2 0)	-.0240	-.0245	-.0127	-.0153	-.0123	-.0181
		.0127	.0127	.0672	.0181	.0181	.0578
		.0042	-.0049	.0048	.0019	-.0008	.0050
3	(-1 3 1)	-.0049	.0069	.0049	-.0008	-.0010	.0008
		.0048	.0049	.0042	.0050	.0008	.0019
		.0075	0.0	0.0	-.0007	0.0	0.0
4	(4 0 0)	0.0	-.0038	0.0	0.0	-.0016	0.0
		0.0	0.0	-.0038	0.0	0.0	-.0016
		-.0010	-.0043	.0056	-.0035	-.0013	.0067
5	(3 3 1)	-.0043	-.0010	.0056	-.0013	-.0035	.0067
		.0056	.0056	-.0288	.0067	.0067	-.0245
		.0009	-.0003	-.0003	.0001	-.0007	-.0007
6	(4 2 2)	.0001	-.0025	.0052	-.0008	-.0008	.0021
		.0001	.0052	-.0025	-.0008	.0021	-.0008

Tab. VI.8. cont.

		-.0063	-.0005	-.0005	-.0001	-.0003	-.0003
8	(5 1 1)	-.0005	.0031	.0011	-.0003	.0008	.0001
		-.0005	.0011	.0031	-.0003	.0001	.0008
		.0016	.0021	.0021	.0004	0.0	0.0
9	(-3 3 3)	.0021	.0016	-.0021	0.0	.0004	0.0
		.0021	-.0021	.0016	0.0	0.0	.0004
		-.0004	-.0007	-.0029	-.0006	-.0015	-.0027
10	(4 4 0)	-.0007	-.0004	-.0029	-.0015	-.0006	-.0027
		.0029	.0029	.0215	.0027	.0027	.0107
		-.0032	.0001	-.0030	.0002	-.0006	.0002
11	(5-1 3)	.0001	.0009	.0028	-.0006	.0003	.0009
		-.0030	.0028	-.0012	.0002	.0009	-.0005
		.0026	.0021	.0005	0.0	-.0001	.0002
12	(6 2 0)	.0021	-.0003	.0012	-.0001	-.0004	0.0
		-.0005	-.0012	-.0006	-.0002	0.0	-.0004
		.0026	.0024	.0024	-.0003	.0003	.0003
13	(5 3 3)	.0024	.0015	-.0056	.0003	.0001	-.0011
		.0024	-.0056	.0015	.0003	-.0011	.0001
		.0016	.0012	.0012	-.0001	.0001	.0001
14	(4 4 4)	.0012	.0016	.0012	.0001	-.0001	.0001
		.0012	.0012	.0016	.0001	.0001	-.0001
		-.0029	.0003	.0002	-.0004	0.0	.0011
16	(5 5 1)	.0003	-.0029	.0002	0.0	-.0004	.0011
		.0002	.0002	-.0102	.0011	.0011	-.0008

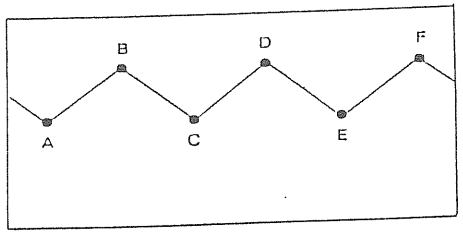

Fig.VI.3. Coplanar bonding chain in (110) plane.

The angular forces between atoms A to D are explicitly included in the valence force field (VVF) model [95,96,109], which however leaves the other atoms in chain decoupled. What we have shown on the ground of first-principle calculation as well as of BCM (which does not explicitly assume such a coupling) is the importance of other interactions in the chain. Kane has recently stressed the role the coplanar bonding chains play in propagating interactions in covalent solids [97,110] and our findings give strong support to his ideas.

It can be noticed in Tab. VI-8 that while the force constants of first few shells have about the same magnitude in both first-principle and BCM calculations, for the more distant shells they differ significantly displaying however the above discussed trends. First-principle forces seem to be stronger than BCM ones from, say, 3rd, 4th shell on. It is difficult to judge the accuracy of BCM forces on the basis only on the phonon frequencies this model gives. As far as first-principle forces are concerned, there are several factors that could have a major effect on the results. We are convinced, that apart from the local approximation for exchange correlation and the locality of the pseudopotential used, the convergence with respect to the size of response matrices and number of mean-value points in the Brillouin zone integration are the factors, which play important role in this calculation. The convergence with respect to the size of dielectric matrices was discussed in the context of

phonon frequencies at point L. As far as the number of mean-value points is concerned, we would like to remind, that this particular pseudopotential required many points for the evaluation of dielectric matrix in $\vec{q} \longrightarrow 0$ limit (60 for the "head" and 10 for "wings"). This fact suggests the necessity of using many mean-value points also in dielectric matrix calculations at least at small $\vec{q}$. For technical reasons we have evaluated all our matrices with two mean-value points only.

Number of shell	Partial sum	Accuracy in %	Number of shell	Partial sum	Accuracy in %
1	1.79	-.27	9	1.81	-3.6
2	1.72	1.5	10	1.73	1.1
3	1.66	5.0	11	1.75	-.5
4	1.66	5.0	12	1.74	-.3
5	1.78	-2.1	13	1.70	2.8
7	1.81	-4.0	15	1.68	3.6
8	1.82	-4.0	16	1.75	-.1

Tab.VI-9. Partial summation of force constants (in 10 dyn/cm) up to ith shell together with the accuracy of satisfying (VI-5).

The internal consistence of our calculations can be veryfied by looking how well the condition (VI-5) of infinitesimal rigid translations invariance is satisfied. This condition states, that the force constant of zeroth shell is equal to the sum with opposite sign of all other force constants. In our method the zeroth force constant is an independent output of the calculation and the condition can be veryfied. In Tab. VI-9 we give the partial summation of forces from first up to ith shell together with the level (in %) of (VI-5) satisfaction. Despite (VI-5) condition with 16 shells is very well satisfied, it is not fair to say we are in convergence. We could rather conclude, that the high disagreement in 13th to 15th shells comes from

overestimating the forces due to the reasons discussed just above.

Having obtained the interatomic force constants we can calculate the phonon spectra at any point or along any line in the Brillouin zone. Fig. VI.2 shows such spectra for some directions obtained with ab-initio LDA force constants of Tab. VI-8. To ensure the vanishing frequency of the acoustic modes for $\vec{q} \longrightarrow 0$ we have taken as the 0th shell force constant the sum with a minus sign of all other ones from 1th to 16th shell. The black circles in Fig. VI.2 give experimental values taken from Ref. [106] and white squares are the results for Γ, X and L points from the preceding part of this work.

The greatest discrepancy between theory and experiment is found in the vicinity of point L. This fact has been already discussed before. At point L however, the results now are somewhat better than from the diagonalization of the dynamical matrix constructed via the "perturbative" approach, while at X they become a bit worse. This is not strange, because using force constants from calculations of dynamical matrices at different points with different accuracies "smears" the accuracy all over the Brillouin zone. It can be noticed also, that while the frequencies of longitudinal acoustic modes are reproduced very well, in general our calculation predicts smaller phonon energies than experiment gives. We guess, this is the consequence of the fact, that nearest neighbour forces are underestimated as results from the comparison with BCM case in Tab. VI-8. The 0th shell force constant, being the sum of all other forces, gives roughly the estimation of how strong the interactions are and turns out to be about 8 % less than in BCM case.

The analogous to Fig. VI.2 picture for spectra obtained on the basis of RPA screening in the construction of force constants are presented in Fig. V-3. The accuracy of results is now much worse and the whole transverse acoustic branches become imaginary.

It is possible to sum up the interatomic force constants coming from the same plane to get the interplanar ones. This is interesting because recently a "direct" ab-initio calculation of interplanar force constants based on the same pseudopotential has been published [87]. Tab. VI-4 shows which of the interatomic force constants are involved in building the interplanar force constant for a given plane. In Tab. VI-10,11 we present our LDA interplanar force constants for (100) and (111) directions together with those of Ref. [87] and those we get from BCM [101]. We can state again, that as far as first planes are concerned, our forces are weaker. It seems as well, that the "direct" method gives overall better agreement with BCM results than our approach. We believe this is the effect of the high accuracy, which is needed in dielectric matrix calculations. As already discussed before, one should use a more representative set of mean-value points and calculate larger matrices specially in Λ direction.

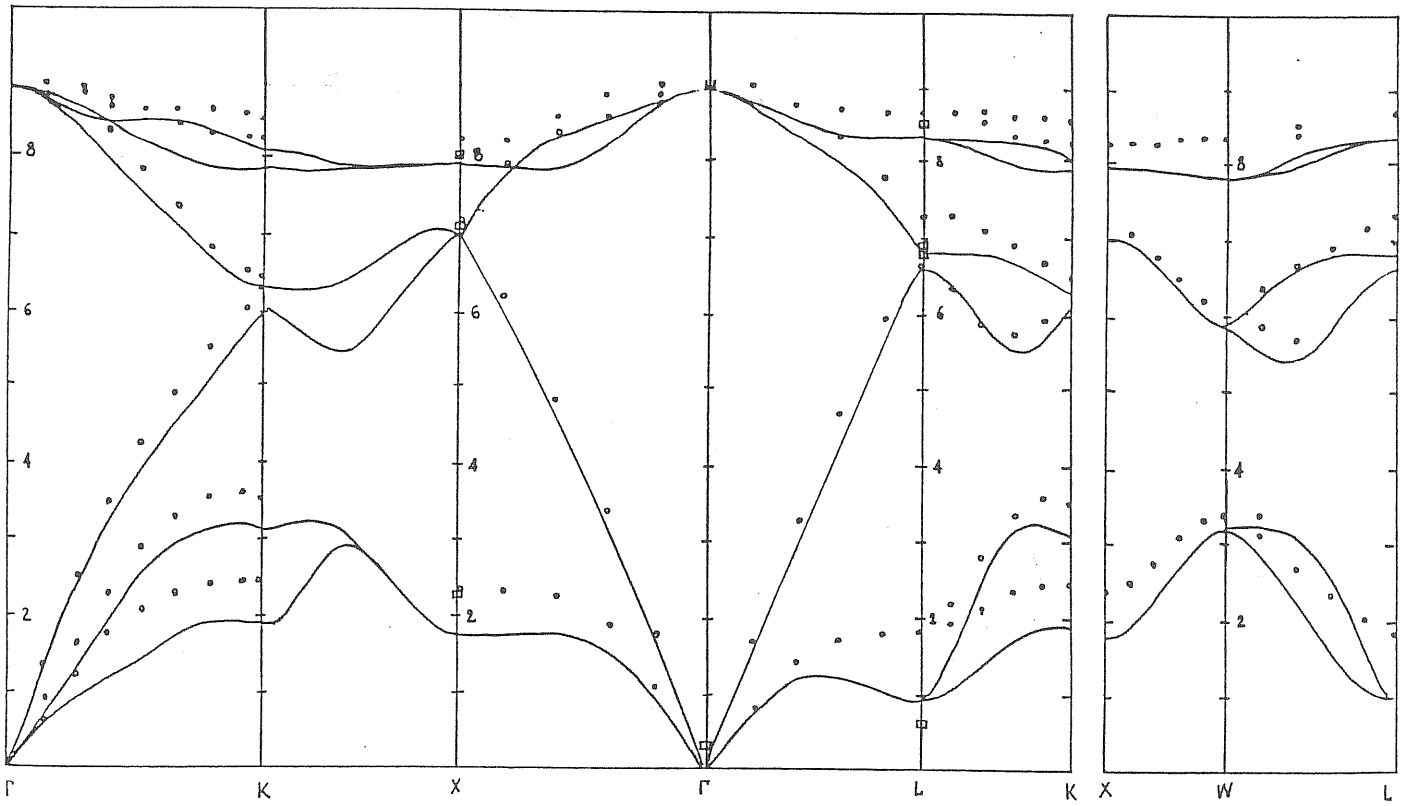

Fig.VI.4. Phonon dispersion curve in Ge obtained from ab-initio interatomic force constants. LDA dielectric matrices in the construction of force constants. Black dots indicate experimental values taken from Ref.106. White squares show the values obtained in chapter VI.2 from the diagonalization of dynamical matrices.

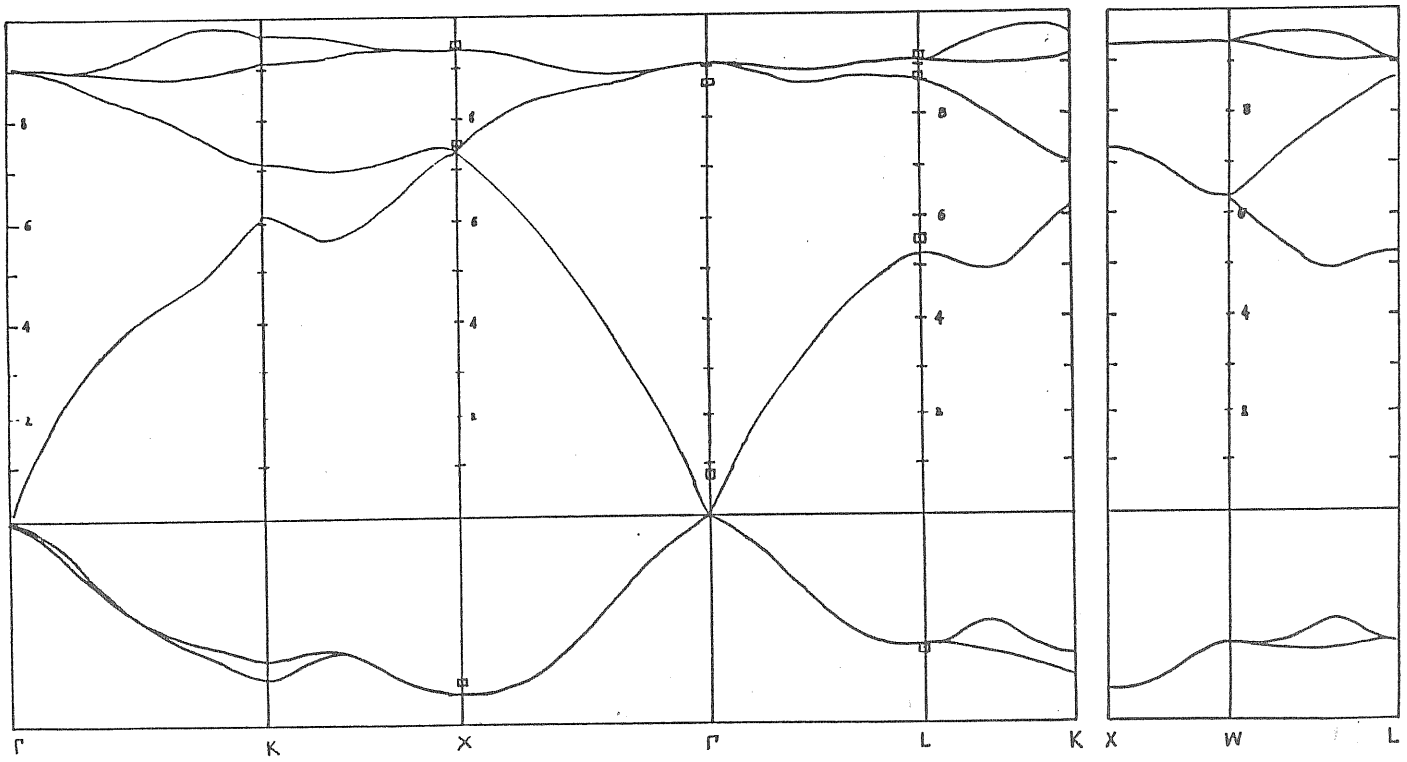

Fig.VI.5. Phonon dispersion curve in Ge from RPA interatomic force constants.

longitudinal			transverse		
LDA	Ref. [87]	BCM	LDA	Ref. [87]	BCM
2.0795	2.248	2.1812	1.6617	1.806	1.8485
-.9412	-1.050	-1.0103	-1.5434	-1.695	-1.6436
-.9412	-1.050	-1.0103	-.2502	-.203	-.2938
-.1192	-.083	-.0593	.083	.086	.086
.0202	-.006	-.0157	.0196	-.035	-.0137
.0202	-.006	-.0157	-.092	-.094	-.0841
.0159	.014	-.0041	.0348	.029	.0141
-.0266	...	-.0010	-.0288	-.007	-.0024
-.0266	...	-.0010	-.0064	-.023	-.0134
.0104	...	-.0002	-.0018	.015	.0022

Tab. VI-10. Interplanar force constants in 10^5 dyn/cm in (100) direction. LDA-our first-principle results; Ref. [87]-results of "direct" calculation of Ref. [87]; BCM-results from BCM[101]

longitudinal			transverse		
LDA	Ref. [87]	BCM	LDA	Ref. [87]	BCM
1.9347	2.161	2.0902	1.7541	1.931	1.9504
-.9983	-1.142	-1.1121	-.1304	-.101	-.1528
-.8427	-.900	-.8806	-1.7058	-1.899	-1.8452
-.0615	-.054	-.0172	.0579	.048	.0437
-.0243	-.020	-.0003	-.0447	-.044	-.0405
-.0261	-.029	-.0567	-.0030	-.024	-.0070
.037	.020	-.0009	.0115	.021	.0068
-.0066	...	.0	-.0039	...	-.0061
-.0493	...	-.0039	-.0074	...	-.0012
.0040	...	-.0001	.0004	...	.0010

Tab. VI-11. Interplanar force constants in 10^5 dyn/cm in (111) direction. LDA-our first-principle results; Ref. [87]-results of "direct" calculation of Ref. [87]; BCM-results from BCM[101]

CHAPTER VII

SCREENING OF IMPURITY POTENTIALS

This chapter is devoted to the study of polarization of electrons in semiconductors due to the presence of charged Coulombic-like impurities. The importance of this subject is determined by the enormous usefulness and practical applicability of electronic (or micro-electronic) devices, where the presence of impurities plays an essential role. The theoretical investigations of impurities in crystals are probably as old as the solid state theory itself and some of their performances belong to the most interesting achievements in that branch of physics. Let us mention here at least the famous effective mass theory [111-115] or the Koster and Slater approach [116].

There are different kinds of impurities or quantum electronic states due to impurities in semiconductors. According to their characteristics, they can be devided into shallow, deep, localized, delocalized, etc. Roughly speaking, strong and localized impurity potentials give rise to localized electron states with energies "deep" in the gap, while weak and slowly varying potentials produce weakly bound and distributed over many unit cells electronic states with "shallow" energies very close to band edges. In all these cases different mathematical tools are used to theoretically approach the problem. Particularly, in recent years, the theory of deep impurities has been dynamically developing reaching the precision and the beauty of the most modern selfconsistent band-structure calculations [117-121]. There are moreover several possible approches to the case of deep impurities, which can be used within the first-principle formalism. These are the Green functions techniques [117-121], the supercell technique [122-126] or cluster approach [127-128]. This is not the case with the theoretical description of shallow impurities. After the impressive successes of effective mass theory in fifties and sixties, the theoretical investigations of those impurities could not reach the ab-initio level of recent deep impurity

calculations. It is because on one hand the effective mass approximation does not take into account the microscopic structure of the crystal around the impurity, which turns out to be important for the most bound ground impurity state, and on the other hand, the just mentioned techniques used for deep states are inappropriate for slowly varying, long range potentials. The effective mass theory, which is very successful in describing shallow impurity excited states, usually fails when applied to the ground state. For this state the electron wave function has a substantial contribution inside a central cell region and the true shape of impurity potential is thus of a great importance.

There have been several attempts to treat the problem of shallow impurity ground state on the more microscopic ground [129-131]; in all of them however a model screened impurity potential has been used. In most cases it was a Coulomb potential screened with the diagonal, model dielectric function. Such a screening gives spherical, site-independent potential - a result different from reality particularly inside the central cell. A site-dependent potential having the same symmetry as the impurity site is obtained when the full, diagonal and off-diagonal screening is considered with the use of dielectric matrices.

The aim of the present chapter is to derive the microscopic polarization charge density around the impurity in germanium, on the basis of response matrix calculations presented in preceding chapters. Such a polarization charge determines the realistic form of the impurity potential, which should be used in the calculations of various physical problems. According to our knowledge, the only papers where a similar problem was dealt with are Ref. [39,132]. In Ref. [39] a model dielectric matrix fitted to ab-initio calculation at Γ point in silicon has been used to study the site dependence of impurity potentials in silicon. In Ref. [132] microscopically derived response matrices within somewhat different formalism than our have been applied to screen Coulomb impurities in diamond and silicon.

The question could arise, whether impurity potentials are weak enough to be treated within linear response. The deep impurities are obviously too strong for such an approach; as far as shallow ones are concerned, this question was positively answered by Baur et. al. [133], who have shown that Coulomb potentials in a periodic lattice with the atomic charge up to Z=1, screened with the linear response give rise to a polarization charge density which is very close to the one obtained from the full selfconsistent (i.e. non-linear !) calculation.

As in the previous chapter we are substituting the integral over the Brillouin zone by the discrete summation over the mesh of mean-value points:

$$\delta\varrho_\xi(\vec{r}) = \sum_{\vec{G}} \frac{\Omega_0}{(2\pi)^3} \int d\vec{q}\, d\varrho_\xi(\vec{q}+\vec{G})\, e^{-i(\vec{q}+\vec{G})\vec{r}} \longrightarrow \frac{1}{N_i} \sum_{\vec{q}_i} \sum_{\vec{G}} \delta\varrho_\xi(\vec{q}_i+\vec{G})\, e^{-i(\vec{q}_i+\vec{G})\vec{r}} \qquad \text{(VII-1)}$$

We have done calculations for a proton placed in the interstitial tetrahedral site and for arsenic in the substitutional position. In the latter case we have taken the difference between the arsenic and germanium pseudopotentials as the external perturbation. Summation in (VI-1) was done over the grid of (8,8,8) special points of Monkhorst and Pack [56].

In Fig. VII.1. the angular average of the polarization charge density for both cases is shown. The decomposition into the diagonal and off-diagonal response in (VI-1) is also presented. This figure is qualitatively very similar to the Figs. (10),(12) of Ref. [132](1983), which show charge polarization around the substitutional and interstitial positive point-like charge in silicon along (1,1,1) and (1,0,0) directions. (Note the inversion of vertical axis on these and on ours figurs. We present here the disturbance of electron density, while Mattausch et.al. give the change of charge density). As

expected, the essential difference between the substitutional arsenic and the interstitial proton case is inside the central cell region. The substitutional impurity induces the strongest polarization peak in the distance of about 1/4 of the bond-length, which rapidly decays to form - from about the nearest neighbour on - small and decreasing oscillations. The peak originates from the charge flux along the bond towards the impurity and results from the strong cancellation between the diagonal and off-diagonal contributions to screening.

It is evident, that in the central cell region the inclusion of the full dielectric matrix is essential. The diagonal response alone gives a very different picture of the screening behaviour of electrons: they are much more attracted to the positive impurity and their polarization does not show neither the just mentioned peak, nor the oscillations, but is monotonically decaying in the vicinity of the perturbing charge. It is the effect of the off-diagonal response to decrease the charge density on the impurity and to impose "tail" oscillations. These oscillations are around the value obtained from the diagonal screening.

The case of the interstitial proton presents some qualitative differences. Here charge disturbance has not any peak in the neighborhood of the impurity, but is monottonic. The polarization does not reach such high values as in the substitutional case, and spreads out over a sligthly greater distance. The diagonal contribution is - as it should be - very similar to the corresponding contribution in the substitutional case and again the final form of charge polarization comes from the cancellation of diagonal and off-diagonal responses. Here however, the absolute values at the impurity site of both these contributions are much greater. This is because the proton potential diverges at the origin and is much stronger than the "smooth" pseudopotential which we used in the substitutional case. Like previously, the decaying oscillations appear from about the nearest neighbour distance onwards.

It follows from the Fig. VII.1., that the impurity in the substitutional site is screened in a more effective way than in the interstitial site. The same conclusion has been drawn by the authors of Ref [132] for point-like impurities in diamond and silicon. This results stem from the fact that a substitutional impurity is surrounded by the charge of neighbouring bonds, which takes part in the screening, while the interstitial impurity stays in the centre of the region almost free of electrons.

It is possible to discuss the effectiveness of screening of impurities placed in different points in crystals displaying the total polarization charge contained in a sphere centred on the impurity. This is done in Fig. VII.2. The general form of the picture for both, substitutional and interstitial cases, is similar: the total polarization charge fastly grows with the increase of the sphere radius to pass then in quite slowly decaying oscillations around a value, which in principle should be determined by the macroscopic dielectric constant of germanium. While for the substitutional arsenic the first maximum of the curve is found a little bit farther than the nearest bond center, in the case of the interstitial proton it is reached at greater distance, roughly at one bond length from the impurity. This means then, that the charge in the substitutional case is more concentrated i.e. screens more effectively.

It could seem, that the Figs. VI.1. and VI.2. are not "compatible" with each other: the oscillations on the latter one are much more pronounced. We note however, that in Fig. VII.2. the integrated effect is shown, so the fluctuations of Fig. VII.1. are somehow multiplied by the value of the surface of the sphere - growing like the squere of its radius.

For large distances from impurity the oscillations in Fig. VII.2. should be around the value $1-1/\varepsilon_\infty$. Taking as the limit of total polarization charge for large r in Fig. VII.2. the value 0.93, we obtain for $\varepsilon_\infty=14.3$. This does not correspond to the value 22.4 we got for ε_∞ in chapter V, as it should for the sake of the consistency of calculations, in spite

of the fact that 22.4 is inaccurate. This is because ε_∞ in chapter V has been obtained taking the limit $\vec{q} \longrightarrow 0$ of the dielectric matrix, while response matrices used in this chapter have been calculated at the mesh of points all distant from $\vec{q}=0$.

It is interesting to look at the polarization charge in the (110) plane. This is shown on Fig. VII.3. for substitutional case and Fig. VII.4. for the interstitial one. The diagonal approximation to response matrices results in a charge disturbance which is almost spherical and very similar in both cases. (As was stated just above, the differences come from different potentials screened). The off-diagonal contribution is responsible for the directional character of screening and for the formation of the electrostatic dipoles or multipoles around the impurities. While in the case of substitutional arsenic most of the polarization charge is on the nearest bond, in the case of interstitial proton a charge transfer from the bonds into the interstitial region can be observed.

The results of this chapter concerning polarization charge around impurities can be easily transformed to the screended impurity potentials. These potentials should be used in principle in the calculation of impurity ground states. The main part of polarization charge around the substitutional arsenic is basically spherical. This cannot be said about the interstitial proton case. We conclude then that the detailed calculation of impurity ground states should be more difficult in the interstitial case, since there the non-spherical character of potential in the very central region can prove important.

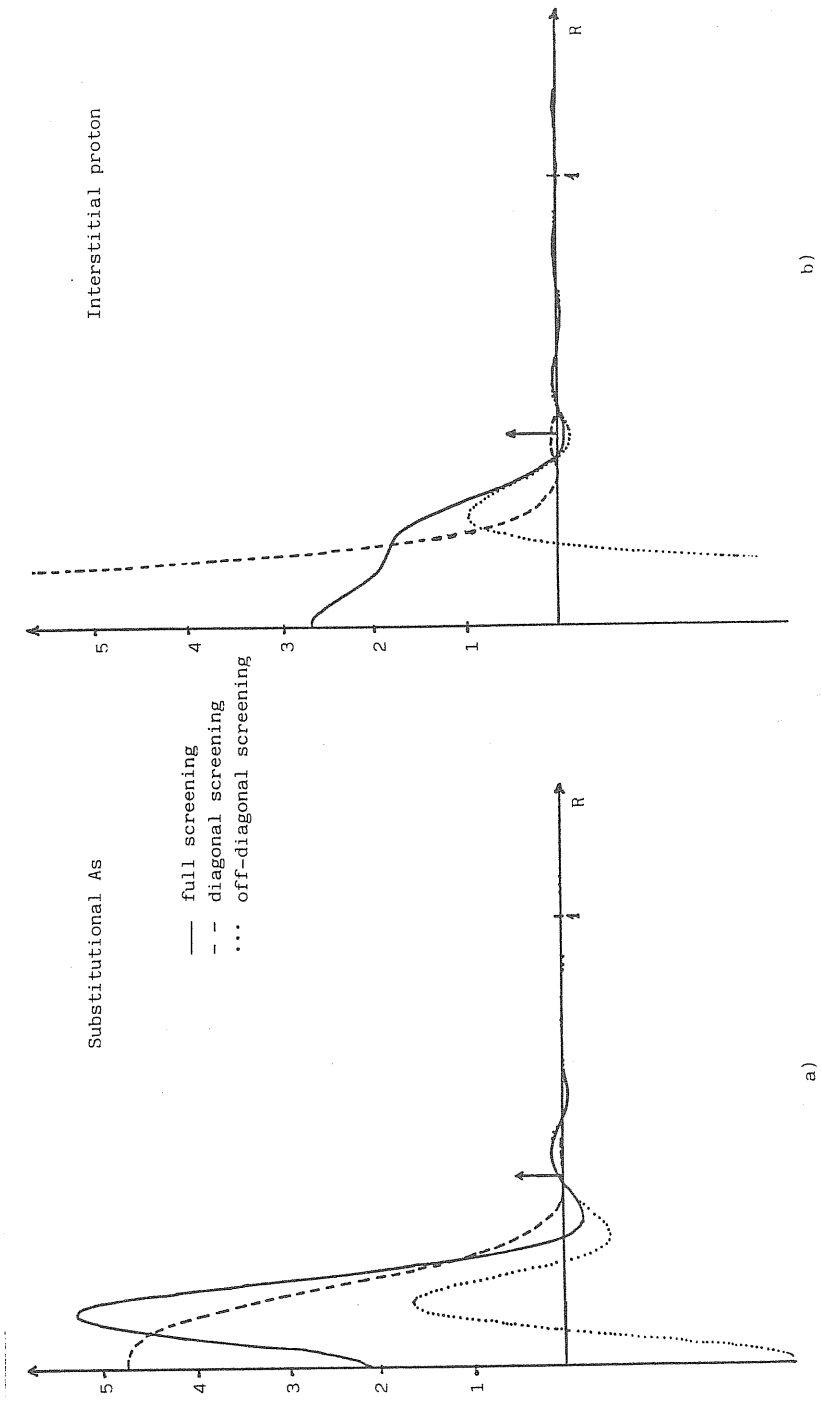

Fig. VII.1. Angular average of polarization charge (in electrons per cell) around an impurity in germanium : a) substitutional As; b) interstitial proton. The arrows indicate bond length distance. Solid line- full screening, dashed line - diagonal contribution to DM, dot line - off-diagonal contribution.

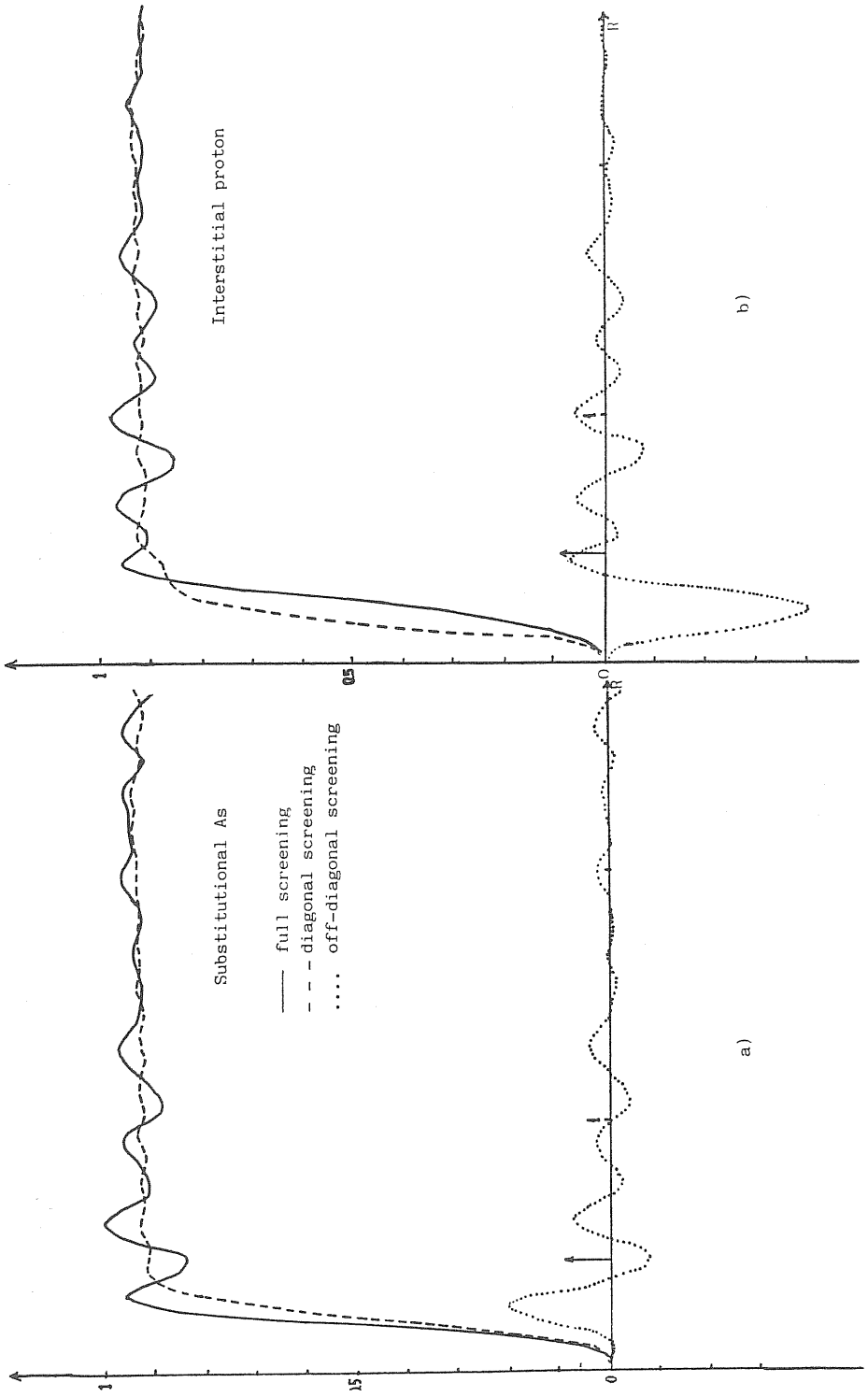

Fig. VII.2. Total electronic polarization inside a sphere of radius R around impurity; a) substitutional As; b) proton in the interstitial tetrahedral site. Arrows indicate bond length distance.

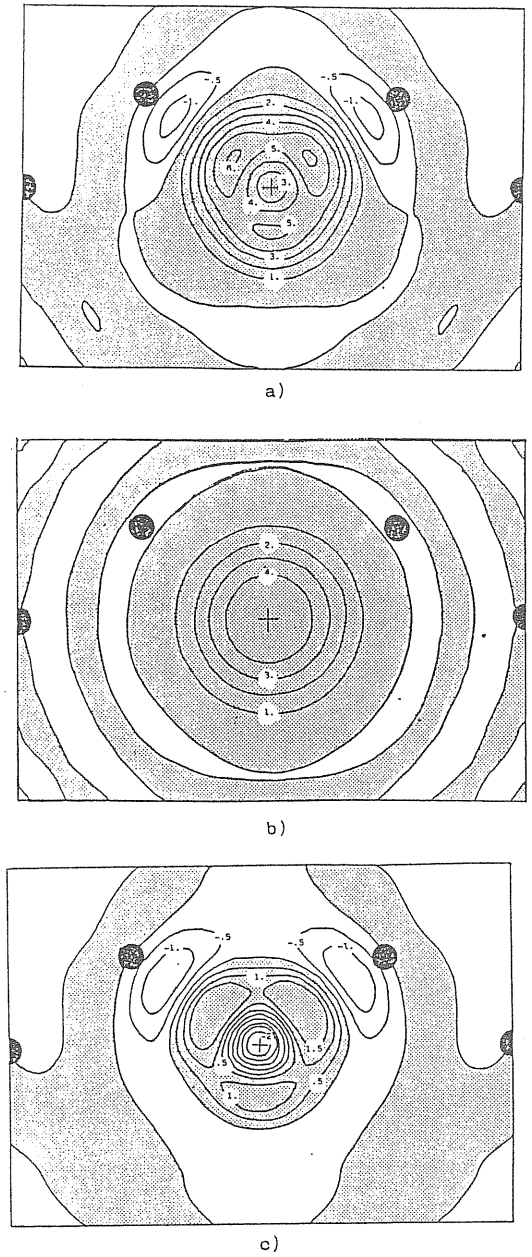

Fig. VII.3. Polarization of electrons in $(1\bar{1}0)$ plane (in electrons per cell) around the substitutional arsenic; a) full screening, b) diagonal screening, c) off-diagonal screening. Black dots indicate atoms, the cross shows the position of the impurity. Shaded areas indicate positive electron density.

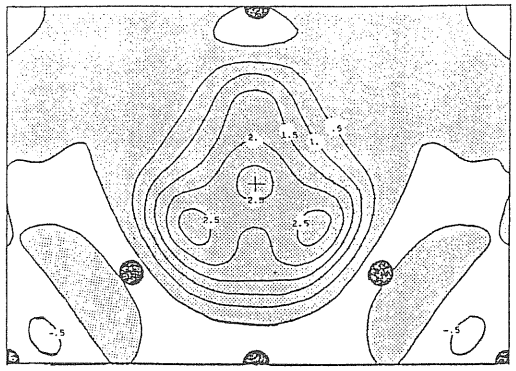

a)

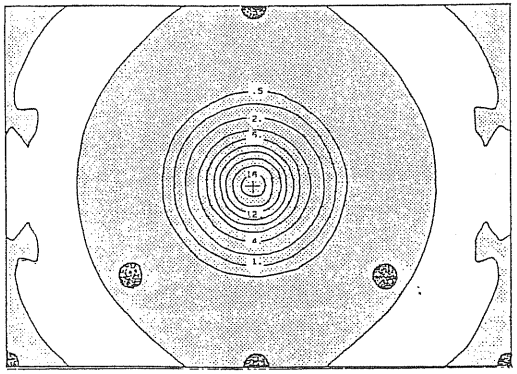

b)

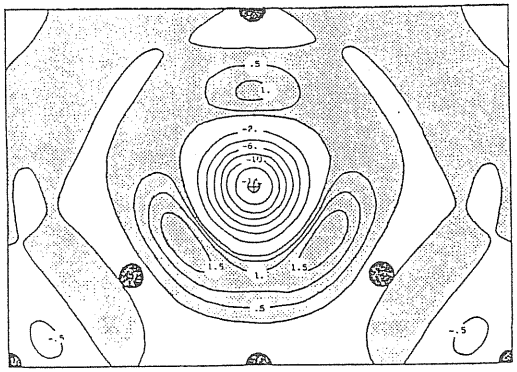

c)

Fig. VII.4. Polarization of electrons in $(1\bar{1}0)$ plane around a proton in the interstitial tetrahedral position. Symbols as in fig. VII.3.

VIII. CONCLUSIONS AND PERSPECTIVES

In this chapter we would like to summarize what was presented in this work giving at the end the discussion of other possible applications of dielectric screening theory in concrete physical problems.

The basic subject of the present work were first-principle calculations of dielectric matrices in semiconductors and their applications. As was noticed in chapter III, up to recently, this problem was solved by evaluation of "perturbative" expression of Adler and Wiser (I-40). The task proved to be very difficult so far and either response matrices have been calculated at $\vec{q}\longrightarrow 0$ limit only, or the accuracy of their evaluation was not satisfactory enough to the use in physical applications.

In chapter III new methods for dielectric matrix calculations are described. This is first of all the "direct" method of Ref. [14], which allows to obtain the whole columns of response matrices to all orders in perturbing potential without summing up over conduction bands. A second powerful tool introduced in this work is the application of Fast Fourier Transform technique in the evaluation of Eq. (I-40), useful when dealing with perturbation of a general $\vec{q}$-vector.

With the use the above efficient tools, we were able to calculate the dielectric matrices of germanium in Γ, X, L points and - for the need in physical applications - over the mesh of 10 mean-value points of Chadi and Cohen [55]. The matrices were of the order of 180~190, obtained within the local Berkeley selfconsistent pseudopotential scheme [60-62] with about 220 plane-waves in the basis set used to solve Kohn-Sham equations.

The dielectric matrix at the Γ point served us to accelerate

selfconsistency iterations according to the concept of Ho, Ihm and Joannopoulos [72]. We have performed in chapter IV a comparative study of different acceleration procedures.

On the example of the "head" of the dielectric matrix at $\vec{q}\longrightarrow 0$ limit we have reexamined the problem of the number of mean-value points needed in Brillouin zone integration in Eq. (I-40) to have convergent results. Our findings point out a stronger dependence on the number of special points than expected before (see chapter III and Ref. [10]). We have studied in detail the effect of exchange-correlation in screening. The results seem quite surprising. The dielectric matrices calculated within different pseudopotential schemes differ more because of exchange-correlation, than because of the details of band structure used. This is well visualized in Tab. V$_2$-5, where the largest eigenvalues of dielectric matrices at points Γ, X and L in germanium are reported. Exchange-correlation tends to reduce the diagonal elements of inverse dielectric matrix, while increases in absolute values the off-diagonal elements. This corresponds to the excitonic picture of those corrections. The effect of exchange-correlation in screening is studied also in physical applications throughout this work and in particular in lattice dynamics.

From the "head" and "wings" of the inverse dielectric matrix in the limit $\vec{q}\longrightarrow 0$ we obtained the macroscopic dielectric constant ε_∞ and Born effective charge Z^*. The value for ε_∞ we got (ε_∞=22.4) is quite far from experiment (ε_∞^{exp}=15.4) The Berkeley pseudopotential we use together with local density approximation give the gap between valence and conduction bands in germanium much too small and this fact is first of all reflected in the value of the "head" of dielectric matrix. The Born effective charge in germanium should be zero by symmetry. Our value for Z^* is -0.29 resulting in 7% violation of the acoustic sum rule. Better accuracy is difficult to achieve in the context of dielectric approach.

The first-principle calculations of lattice-dynamical properties of germanium were done within the "perturbative"

scheme i.e. with the inverse dielectric matrix used to construct the dynamical matrix at a given $\vec{q}$-point. We obtained phonon frequencies at Γ, X, L points and 10 special points of Chadi and Cohen as well as the polarization charge densities due to LTO phonon at Γ and TA phonon at X. The role of local-field effects and exchange-correlation in screening to lattice dynamics was examined in detail. Phonon frequencies at Γ and X turned out to be quite close to experiment, while those at L and on the Λ direction were much worse. The inclusion of exchange-correlation in screening was essential. Transverse acoustic phonon frequencies calculated with RPA response only have imaginary values for all $\vec{q}$-vectors (taking several symmetry lines), while the accuracy of most of other phonons is worse than if LDA response is used.

One of the most important results of the present work is the calculation of interatomic force constants According to our knowledge, it is the first ab-initio calculation of interatomic force constants in a covalent semiconductor. They could not be obtained within "direct" ab-initio techiques because of the necessity of using too big supercells. Our interatomic forces turn out to be of longer range than expected before (16'th neighbour forces are stronger than 3'th neighbour ones !) and those from coplanar bonding chains are the strongest ones. In Fig. VI-2 we have given the phonon spectra obtained from interatomic force constants up to 16 shells.

We have used the dielectric matrices calculated at the mesh of special points to obtain the polarization charge due to interstitial proton and substitutional arsenic in germanium. The shape of induced charge depends on where the impurity is placed in the crystal. The site dependence of polarization charge or the screened potential is strictly connected to the off-diagonal elements of dielectric matrix. We have analyzed in detail the shape of the polarization charge in (110) plane, the radial distribution of polarization as well as the total charge enclosed in a sphere around the impurity as a function of the radius of the sphere. The main effect turned out to be strongly localized roughly inside about the central cell. The differences in response between interstitial and substitutional cases are basically contained in this cell. The substitutional arsenic seems to be a bit more efficiently screened than interstitial proton; in the latter case the polarization disturbance around the impurity is more extended (see Fig. VII-1). The main effect in central cell results from a strong cancellation of the diagonal and off-diagonal screening - if the linear screening so close to impurity is assumed valid. Outside the first cell the off-diagonal screening imposes small and decaing oscillations in the polarization charge around the almost constant value obtained from the diagonal response.

We have proved in this work that first-principle calculations of the complete static dielectric properties of semiconductors are feasible nowadays. This can be achieved by the evaluation of large dielectric matrices over the (possibly fine) mesh of $\vec{q}$-points inside the Brillouin zone. By this method a great class of presently unsolved physical problems can be treated in a first-principle manner. This is specially important in the case of non-periodic perturbations to the crystal Hamiltonian, where selfconsistent supercell techniques could prove too difficult. In chapter VI and VII of this work we applied the above formalism to get interatomic force constants and polarization charge around an impurity with a Coulombic tail. The latter one can serve to calculate impurity ground states with central cell corrections and chemical shifts included in first-principle manner.

Numerous other applications are possible. As an interesting example let us mention here at least the problem of compositional order or disorder of an alloy. The silicon-germanium alloy, for instant, does not appear in any long-range ordered structure. To obtain the physical characteristics of its different structures (or even randomly generated disordered structure) probably the following method could be possible:

- calculate first a set of dielectric matrices over a sufficiently fine grid of $\vec{q}$-points in the BZ starting from, say, the virtual crystal approximation (VCA),
- impose on the top of VCA a given structure under consideration (possibly disordered) substituting the virtual-crystal atoms by the "true" atoms in any lattice site,
- treat the resulting difference potential within linear response approach, to get new charge density or - possibly - total energy of the structure.

The described above method can work certainly well in the case of compositional disorder, while would probably come into troubles in the case of structural disorder. When we relax the positions of atoms, the resulting perturbation could be not small enough to be dealt within linear response, if atomic displacements are too large. It is possible however, that from the response to small enough displacements of atoms we could have the indication of a correct relaxation. This could be then an useful guide to the surface reconstruction in particular and many other problems as well.

It was claimed in chapter VI, that the dielectric formalism is particularly suited in calculating electron-phonon interaction. It is because in this formalism the screened potential of phonons of any $\vec{q}$-vector can be obtained without the necessity of construction of supercells. For this reason then, the quantities averaged over $\vec{q}$ should be easy to evaluate.

We expect that together with the growing interest in the applications of dielectric screening theory, as described in this work, the theory itself will progress as well. The use of non-local pseudopotentials, so popular nowadays, will probably cause the generalization of dielectric matrix concept in order to give the response to non-local perturbations. It is possible also, that the dielectric operators will be treated as matrices not in the Fourier space, but in some other (say, localized) basis for compatibility reasons with some of the available

all-electron band structure schemes.

A small part of this work has been the object of three publications [14, 75, 101] which we reprint in Appendices C, D and E. Other publications reporting on different parts of this work are in preparation.

IX. APPENDICES

Appendix A: "Bare" perturbing potential due to phonon.

Suppose there is a phonon of wave-vector $\vec{q}$ in the crystal. The displacement of the atom in $\vec{R}_s$ position in lth unit cell is the following:

$$u_s^\alpha(l) = u_s^\alpha(\vec{q})\, e^{-i\vec{q}(\vec{R}_l+\vec{R}_s)+i\omega_q t} + c.c. \qquad (A-1)$$

where α stays for Carthesian coordinate.

Since to each atom is "attached" a (pseudo-)potential $V_s(r)$, the displacement pattern (A-1) will give rise to the following "bare" perturbation in the one-electron Hamiltonian:

$$\delta V_{ext}(\vec{r}) = \sum_{ls}\left[V_s(\vec{r}-\vec{R}_l-\vec{R}_s-u_s(l)) - V_s(\vec{r}-\vec{R}_l-\vec{R}_s)\right] \qquad (A-2)$$

Up to the first order in $\vec{u}$ this potential is:

$$\delta V_{ext}(\vec{r}) \cong \sum_{ls\alpha}\left[\frac{\partial}{\partial u_s^\alpha(l)}\, V_s(\vec{r}-\vec{R}_{ls}-\vec{u}_s(l))\right]\Big|_{\vec{u}_s(l)=0} u_s^\alpha(l) \qquad (A-3)$$

$$= \sum_{ls\alpha}\left[\frac{\partial}{\partial r^\alpha}\, V_s(\vec{r}-\vec{R}_{ls})\right] u_s^\alpha(l)$$

In Fourier space, after making use of (A-1), it takes the form:

$$\delta V_{ext}(\vec{k}) = \frac{1}{\Omega_0}\int d\vec{r}\;\delta V_{ext}(\vec{r})\, e^{i\vec{k}\vec{r}}$$

$$= -\sum_{ls\alpha}\int d\vec{r}\left[\frac{\partial}{\partial r^\alpha} V_s(\vec{r}-\vec{R}_{ls}) u_s^\alpha(\vec{q})\, e^{-iq\vec{R}_{ls}+i\omega_{\vec{q}}t} + c.c.\right] e^{i\vec{k}\vec{r}} = \qquad (A-4)$$

$$= i\sum_{ls\alpha}\left[u_l^{\alpha}(\vec{q})\vec{k}^{\alpha}e^{-i(\vec{q}-\vec{k})\vec{R}_{ls}+i\omega_{\vec{q}}t}V_s(\vec{k}) + u_s^{\alpha}(\vec{q})^{*}k^{\alpha}e^{i(\vec{q}+\vec{k})\vec{R}_{ls}-i\omega_{\vec{q}}t}V_s(\vec{k})\right]$$

$$= i\vec{k}\sum_{ls}\left[\vec{u}_s(\vec{q})e^{i(\vec{k}-\vec{q})\vec{R}_{ls}+i\omega_{\vec{q}}t} + \vec{u}_s^{*}(\vec{q})e^{i(\vec{k}+\vec{q})\vec{R}_{ls}-i\omega_{\vec{q}}t}\right]V_s(\vec{k})$$

Because of equality:

$$\sum_l e^{i\vec{k}\vec{R}_l} = \frac{(2\pi)^3}{\Omega_0}\sum_{\vec{G}}\delta(\vec{k}-\vec{G}) \qquad (A-5)$$

we obtain for $\delta V_{ext}(\vec{k})$ the following expression:

$$\delta V_{ext}(\vec{k}) = i\sum_{\vec{G}}\sum_s \vec{u}_s(\vec{q})(\vec{q}+\vec{G})V_s(\vec{q}+\vec{G})e^{i\vec{G}\vec{R}_s+i\omega_{\vec{q}}t}\frac{(2\pi)^3}{\Omega_0}\delta(\vec{k}-\vec{q}-\vec{G}) \qquad (A-6)$$

$$-i\sum_{\vec{G}}\sum_s \vec{u}_s^{*}(\vec{q})(\vec{q}+\vec{G})V_s^{*}(\vec{q}+\vec{G})e^{-i\vec{G}\vec{R}_s-i\omega_{\vec{q}}t}\cdot\frac{(2\pi)^3}{\Omega_0}\delta(\vec{k}+\vec{q}+\vec{G})$$

Remembering that a periodic function can be written in Fourier space as:

$$f(\vec{r}) = \sum_{\vec{G}} f_{\vec{G}}\, e^{-i\vec{G}\vec{r}} = \frac{\Omega_0}{(2\pi)^3}\int d\vec{k}\, f(\vec{k})\, e^{-i\vec{k}\vec{r}} \qquad (A-7)$$

which yields

$$f(\vec{k}) = \sum_{\vec{G}}\frac{(2\pi)^3}{\Omega_0} f_{\vec{G}}\,\delta(\vec{k}-\vec{G}) \qquad (A-8)$$

we have for δV_{ext} :

$$\delta V_{ext}(\vec{r}) = \sum_{\vec{G}}\delta V_{ext}(\vec{q}+\vec{G})e^{-i(\vec{q}+\vec{G})\vec{r}} + c.c. \qquad (A-9)$$

where

$$\delta V_{ext}(\vec{q}+\vec{G}) = i\sum_s \vec{u}_s(\vec{q})(\vec{q}+\vec{G})e^{i\vec{G}\vec{R}_s}V_s(\vec{q}+\vec{G})e^{i\omega_{\vec{q}}t} \qquad (A-10)$$

If $\vec{q}=0$, the $\vec{G}=0$ component of δV_{ext} vanishes because of the charge neutrality condition.

Appendix B: "Head" and "wings" of DM in the limit $\vec{q}\longrightarrow 0$.

According to $\vec{k}\cdot\vec{p}$ theory, the Bloch functions in the limit $\vec{q}\longrightarrow 0$ can be represented in the following way:

$$u_{c\vec{k}+\vec{q}} \longrightarrow u_{c\vec{k}} + \frac{\hbar\vec{q}}{m}\sum_{l\neq c}\frac{\langle u_{l\vec{k}}|\vec{p}|u_{c\vec{k}}\rangle}{E_c(\vec{k})-E_l(\vec{k})} \qquad (B-1)$$

Carefully bookeeping the limiting behaviour of different quantities in matrix element of (II-1), we arrive to the conclusion:

$$\langle\vec{k}v|e^{-i\vec{q}\vec{r}}|\vec{k}+\vec{q}c\rangle \longrightarrow \frac{\hbar\vec{q}}{m}\frac{\langle\vec{k}v|\vec{p}|\vec{k}c\rangle}{E_{c\vec{k}}-E_{v\vec{k}}} \qquad (B-2)$$

Putting (B-2) into (II-1,2) we obtain:

$$\epsilon(\vec{q},\vec{q}')\xrightarrow[\vec{q}\to 0]{} 1 + \frac{2e^2}{\pi^2|q|^2}\sum_{vc}\int_{BZ}d\vec{k}\frac{\hbar^2}{m^2}\sum_{\alpha\beta}\frac{q^{\alpha}q^{\beta}\langle c\vec{k}|p^{\alpha}|v\vec{k}\rangle\langle v\vec{k}|p^{\beta}|c\vec{k}\rangle}{(E_{c\vec{k}}-E_{v\vec{k}})^3} \qquad (B-3)$$

$$= 1 + \frac{2\hbar^2e^2}{\pi^2m^2}\sum_{\alpha\beta}\frac{q^{\alpha}q^{\beta}}{q^2}\int_{BZ}d\vec{k}\,A^{\alpha\beta}(\vec{k})$$

where

$$A^{\alpha\beta}(\vec{k}) = \sum_{vc}\frac{\langle c\vec{k}|p^{\alpha}|v\vec{k}\rangle\langle v\vec{k}|p^{\beta}|c\vec{k}\rangle}{(E_{c\vec{k}}-E_{v\vec{k}})^3} \qquad (B-4)$$

It can be realized that higher powers of energy denominators of Eq. II-1 appear in this way for $\vec{G}=0$ or $\vec{G}'=0$ or both. To

calculate the "head" of DM we must then integrate a function, which has the third power of band energies difference in the denominator; for "wings" this power is two, while for "body" elements one. The greater the power of energy difference in the denominator, the more rapidly the function varies. That is why for the calculation of the "head" of DM in $\vec{q} \longrightarrow 0$ limit one needs more special points than for "wings" and "body" elements.

Let us now derive the practical expressions for the calculation of the "head" and "wings" in diamond-structure semiconductors.

The BZ integral in (B-3) can be approximated by the discrete sum over special points:

$$\int_{BZ} d\vec{k}\, A^{\alpha\beta}(\vec{k}) \longrightarrow \frac{V_{BZ}}{N_j} \sum_{\vec{k}_j} A^{\alpha\beta}(\vec{k}_j) = \frac{V_{BZ}}{N_j} \sum_{R\in Oh} \sum_{i} \frac{N_i}{48} A^{\alpha\beta}(R\vec{k}_i) \qquad (B-5)$$

where N_j is the total number of special points in BZ, R are operations from the Oh group and Ni is the number of equivalent points to a given special point $\vec{k}_i$ from the irreducible part of BZ.

It is easy to prove the following property of $A^{\alpha\beta}(\vec{k})$:

$$A^{\alpha\beta}(R\vec{k}_i) = \sum_{\gamma\delta} R^{\alpha\gamma} R^{\beta\delta} A^{\gamma\delta}(\vec{k}_i) \qquad (B-6)$$

where $R^{\alpha\beta}$ are the 3x3 ortogonal $(R^{-1})=R^{T}$ matrices representing the operations of Oh group in real 3-dim space.

(B-6) inserted to (B-5) yields:

$$\int_{BZ} d\vec{k}\, A^{\alpha\beta}(\vec{k}) \longrightarrow \sum_{\vec{k}_i} \frac{V_{BZ}\cdot N_i}{48\cdot N_j} \sum_{\gamma\delta} A^{\alpha\beta}(\vec{k}_i) \sum_{R} R^{\alpha\gamma} R^{\beta\delta} \qquad (B-7)$$

Since $R^{\alpha\beta}$ form a three-dimentional irreducible representation of Oh group, the following ortogonality condition applies:

$$\sum_{R} R^{\alpha\gamma} R^{\beta\delta} = \frac{48}{3} \delta_{\alpha\beta} \delta_{\gamma\delta} \qquad (B-8)$$

With (B-8) and (B-7), (B-4) becomes:

$$\epsilon(\vec{q},\vec{q}) \longrightarrow 1 + \frac{2}{3} \frac{e^2\hbar^2 V_{BZ}}{m^2\pi^2} \sum_{\vec{k}_i} \frac{N_i}{N_j} T_2[\hat{A}(\vec{k}_i)] \qquad (B-9)$$

As far as a "wing" of a symmetrized DM is concerned, we have to calculate the following expression:

$$\tilde{\epsilon}(\vec{q}+\vec{G},\vec{q}) = \frac{2e^2}{\pi^2|\vec{q}+\vec{G}||\vec{q}|} \sum_{v,c} \int_{BZ} d\vec{k}\, \frac{\langle \vec{k}+\vec{a}_c | e^{i(\vec{q}+\vec{G})\vec{r}} | \vec{k}v\rangle \langle \vec{k}v | e^{-i\vec{q}\vec{r}} | \vec{k}+\vec{q}c\rangle}{E_c(\vec{k}+\vec{q}) - E_v(\vec{k})}$$

$$\longrightarrow \frac{2e^2}{\pi^2|\vec{G}||\vec{q}|} \sum_{v,c} \int_{BZ} d\vec{k}\, \frac{\langle \vec{k}c | e^{i\vec{G}\vec{r}} | \vec{k}v\rangle \frac{\hbar\vec{q}}{m} \langle \vec{k}v | \vec{p} | \vec{k}c\rangle}{E_c(\vec{k}) - E_v(\vec{k})} \qquad (B-10)$$

$$= \frac{2e^2\hbar^2}{m\pi^2|\vec{G}|} \sum_{\alpha} \frac{q^\alpha}{|q|} \int_{BZ} d\vec{k}\, B^{\alpha}_{\vec{G}}(\vec{k})$$

where

$$B^{\alpha}_{\vec{G}}(\vec{k}) = \sum_{v,c} \frac{\langle \vec{k}c | e^{i\vec{G}\vec{r}} | \vec{k}v\rangle \langle \vec{k}v | p^\alpha | \vec{k}c\rangle}{(E_c(\vec{k}) - E_v(\vec{k}))^2} \qquad (B-11)$$

Again replacing the integral by the summation over special points and manipulating with matrix elements, we get:

$$\int_{BZ} d\vec{k}\, B^{\alpha}_{\vec{G}}(\vec{k}) = \frac{V_{BZ}}{N_j} \sum_{R\in Oh} \sum_{i} \frac{N_i}{48} B^{\alpha}_{\vec{G}}(R\vec{k}_i) \qquad (B-12)$$

where

$$B^{\alpha}_{\vec{G}}(R\vec{k}_i) = \sum_{\beta} R^{\alpha\beta} B^{\beta}_{R^{-1}\vec{G}}(\vec{k}_i)\, e^{i\vec{G}\vec{f}_R} \qquad \text{(B-13)}$$

In the $\vec{q} \longrightarrow 0$ limit with $\vec{q} \parallel (100)$ we get:

$$\tilde{\epsilon}(\vec{q}_\Delta + \vec{G}, \vec{q}_\Delta) \xrightarrow[q_\Delta \to 0]{} \frac{2e^2\hbar}{48\pi^2 m} \frac{V_{BZ}}{|\vec{G}|} \sum_i \frac{N_i}{N_j} \sum_R \sum_\beta R^{\alpha\beta} B^{\beta}_{R^{-1}\vec{G}}(\vec{k}_i) e^{i\vec{G}\vec{f}_R} \qquad \text{(B-14)}$$

Appendices C, D, E : Related papers.

PHYSICAL REVIEW B VOLUME 31, NUMBER 8 15 APRIL 1985

Dielectric matrices in semiconductors: A direct approach

Andrzej Fleszar and Raffaele Resta*
Scuola Internazionale Superiore di Studi Avanzati, 34014 Trieste, Italy
(Received 19 March 1984; revised manuscript received 28 August 1984)

A new method for the evaluation of dielectric screening matrices in semiconductors is proposed. The present method is direct, in the sense that it avoids the use of slowly convergent perturbation sums, just by treating the crystal with a built-in perturbation as a new system. The several advantages of this approach with respect to previous ones are discussed. As a first application of the method, we calculate the random-phase approximation (RPA) dielectric matrices of Si and GaAs at the Γ, X, and L points; the results show the effectiveness and accuracy of the method. The possibility of extending beyond RPA is also discussed.

I. INTRODUCTION

The first-principles theory of the electronic dielectric response in real solids has attracted much interest in recent years.[1–4] The theory can be compared against experimental data—most directly in connection with phonons—but also gives a thorough understanding of basic (and nonmeasurable) features; for this reason, it is essential to the formulation of realistic models.

Within linear regimes, the response is described by the dielectric matrix.[1,3] Calculations for real materials have been possible only in recent times, starting from the Adler-Wiser[5] random-phase approximation (RPA) approach. Such calculations have proven to be quite elaborate,[6] even if a major simplification has been successfully reached[7] with the use of the mean-value point technique for Brillouin-zone (BZ) integration.[8–10] Two basic features which make such calculations extremely time consuming are the slow convergence of perturbation sums and the need of evaluating one by one the independent dielectric matrix elements. Because of the above reasons, numerical results are available for a few materials only[1–3,7,11] and mostly at the BZ center ($\vec{q}=0$ or $\vec{q}\to 0$).

In this work we present an alternative approach to the evaluation of dielectric matrices. We call it the "direct" RPA, by contrast with the "standard" RPA,[5] and by analogy with recent direct phonon calculations.[12–16] Within such an approach, one calculates a new ground state of the solid with frozen-in perturbation, and evaluates the response as the difference of perturbed minus unperturbed quantities. The use of perturbation theory and slowly convergent perturbation sums is avoided; furthermore, a whole column of the dielectric matrix is calculated at a time.

As a test, we apply our method to Si and GaAs. In order to get a quite accurate check of the present method, we have chosen to work within exactly the same framework as in Refs. 7 and 11, whose complete results are available to us in a computer-usable format. For this reason, our starting band structure is the Cohen-Bergstresser[17] one, obtained through the empirical pseudopotential method. This is the same as in Refs. 7 and 11, whose $\vec{q}=0$ standard RPA results we reproduce here almost identically with much smaller computational effort. Then we are able to go beyond and we calculate, at exactly the same level of accuracy, the dielectric matrices at the X and L points, thus supplementing the Γ results previously published.[7,11] In the case of Si, we compare the main screening features of our first-principle results against some of the available model dielectric matrices; this is done here using the concept of dielectric band structure (DBS), proposed some years ago by Baldereschi and Tosatti[18] and which proves very useful for the purpose.

The present method is indeed a way to evaluate the independent-particle polarizability; therefore it can be straightforwardly applied beyond RPA, to calculate the local-density-functional (LDF) dielectric response according to a well-known prescription.[13,19] Since LDF theory predicts quite good frozen-phonon frequencies,[13,14] we expect LDF dielectric matrices from self-consistent pseudopotentials to also be very accurate in lattice dynamics. In this paper, which is a method one, we prefer not to use such a pseudopotential, for the reasons explained above.

Section II contains the theory of the direct RPA method, as applied to the calculation of the dielectric matrix. In Sec. III, several features related to practical implementation are discussed. In Sec. IV we present numerical results for Si and GaAs. In Sec. V the DBS analysis is performed to compare with some models. In Sec. VI we analyze conclusions and perspectives.

II. DIRECT RPA METHOD

The response of a polarizable medium to a given bare electrostatic potential $\phi_0(\vec{r})$ is described, within the linear theory, by

$$\phi(\vec{r})=\int d\vec{r}\,\epsilon^{-1}(\vec{r},\vec{r}')\phi_0(\vec{r}')\,, \tag{1}$$

where ϕ is the screened electrostatic potential and the operator ϵ^{-1} contains all the information about the linear dielectric response of the medium. In compact notations we write Eq. (1) as

$$\phi=\epsilon^{-1}\phi_0\,. \tag{2}$$

We use a.u. ($e^2=m_e=\hbar=1$) throughout. The total self-consistent one-electron Hamiltonian is

$$H=H_0+\delta V\,, \tag{3}$$

where H_0 is the unperturbed one, and at the RPA level,

$$\delta V=-\phi\,. \tag{4}$$

The basic quantity to deal with is the independent-particle polarizability, which is the linear density response to the *total* potential acting on electrons:

$$n^{(1)}=\chi_0\delta V\,. \tag{5}$$

The RPA inverse of ϵ^{-1} is then in operator form:

$$\epsilon=1-v_C\chi_0\,, \tag{6}$$

where v_C is the Coulomb potential; since in a periodic solid v_C and χ_0 do not commute, ϵ is not Hermitian. For computational and displaying purposes it is better to refer to the Hermitian operator $\bar{\epsilon}$, simply related to ϵ by

$$\bar{\epsilon}=v_C^{-1/2}\epsilon v_C^{1/2}=1-v_C^{1/2}\chi_0 v_C^{1/2}\,, \tag{7}$$

which has been widely used in previous literature on the subject.[1,2,7,11]

We have summarized up to now the features which are common to the standard RPA and to the present approach. The basic difference is the way in which the independent-particle polarizability χ_0 is evaluated.

Within the standard RPA, first-order perturbation theory is used to obtain the wave functions of the perturbed Hamiltonian, Eq. (3), linearly in δV. With these wave functions the first-order change in the electron density is evaluated and an expression for χ_0 is found from Eq. (5); it only contains eigenvalues and eigenfunctions of the unperturbed Hamiltonian H_0.

The direct RPA we are proposing in this paper consists of directly solving for the eigenfunctions of the perturbed Hamiltonian, Eq. (3), without use of perturbation theory. The perturbation density is found by difference with the unperturbed case. The calculation is performed with a number of independent δV's sufficient to reconstruct the desired features of χ_0, through Eq. (5), and sufficiently small to ensure linearity. The present approach is inspired by recent direct solid-state calculations with built-in perturbations, such as frozen phonons[12] and other ones,[13–16,4] but at variance with them it does *not* require self-consistency in the perturbed case, since δV is already the total (screened) potential.

Now, we switch to reciprocal space. We use the following notations throughout for the Fourier transform of any function:

$$f(\vec{r})=(2\pi)^{-3}\sum_{\vec{G}}\int_{\mathrm{BZ}}d\vec{q}\,f(\vec{q}+\vec{G})e^{-i(\vec{q}+\vec{G})\cdot\vec{r}}\,, \tag{8}$$

where $\vec{G}$ are reciprocal-lattice vectors and $\vec{q}$ is within the BZ. In a periodic solid, the operators dealt with above are invariant under lattice translation and assume in reciprocal space a matrix form. The matrix indices are reciprocal vectors and the matrix elements depend parametrically on $\vec{q}$. For instance, Eq. (5) reads

$$n^{(1)}(\vec{q}+\vec{G})=\sum_{\vec{G}'}\chi_0(\vec{q}+\vec{G},\vec{q}+\vec{G}')\delta V(\vec{q}+\vec{G}')\,. \tag{9}$$

The Hermitian dielectric matrix (HDM) is obtained from Eq. (10), which reads

$$\bar{\epsilon}(\vec{q}+\vec{G},\vec{q}+\vec{G}')=\delta_{\vec{G},\vec{G}'}-\frac{4\pi}{|\vec{q}+\vec{G}||\vec{q}+\vec{G}'|}\times\chi_0(\vec{q}+\vec{G},\vec{q}+\vec{G}')\,. \tag{10}$$

The $\vec{G}\neq\vec{G}'$ HDM elements are responsible for "umklapp" effects in the response, which are generally referred to as local-field effects;[1] they are due to lattice periodicity, and are vanishing in a homogeneous system, such as the electron gas.

The starting point of all the previous HDM calculations, according to the best of the authors' knowledge, is the standard RPA expression for χ_0, first given by Adler and Wiser[5]

$$\chi_0(\vec{q}+\vec{G},\vec{q}+\vec{G}')=-\frac{4}{(2\pi)^3}\sum_{v,c}\int_{\mathrm{BZ}}d\vec{k}\,\frac{\langle\vec{k}+\vec{q},c\,|\,e^{i(\vec{q}+\vec{G})\cdot\vec{r}}\,|\,\vec{k},v\rangle\langle\vec{k},v\,|\,e^{-i(\vec{q}+\vec{G}')\cdot\vec{r}}\,|\,\vec{k}+\vec{q},c\rangle}{E_c(\vec{k}+\vec{q})-E_v(\vec{k})} \tag{11}$$

in terms of Bloch functions and band energies of H_0. Such calculations are quite lengthy, owing basically to the slow convergence of the summation in (11) over the conduction bands. This main problem is avoided within the present approach, where we only use valence wave functions of the perturbed and unperturbed crystal, as explained above. The authors of Refs. 7 and 11, who made full use of symmetry at the Γ point, found the standard RPA calculation still quite heavy. The symmetry benefit applies to our direct RPA calculation too, as explained below. Besides computer time, programming time is also important: The standard RPA requires *ad hoc* manipulation of matrix elements appearing in Eq. (11), which is avoided here.

The essence of our method is as follows: we switch on one monochromatic δV at a time, having a single nonvanishing component at the vector $\vec{q}+\vec{G}'$. We diagonalize the perturbed Hamiltonian and find the perturbation electron density; within the linear regime, this density has nonvanishing Fourier components only at the umklapp vectors $\vec{q}+\vec{G}$. Those components give us, from Eq. (9), one entire column of χ_0 for each monochromatic perturbation. The HDM is Hermitian (and real in centrosymmetric solids), as clearly appears in Eqs. (10) and (11). Within our scheme, it does not come out Hermitian by construction, so we have a very simple accuracy test for the method. For special $\vec{q}$ vectors the number of independent perturbations to be considered is greatly reduced by point symmetry (see below).

III. CALCULATIONS

Some features concerning the practical implementation of the above concepts to dielectric matrix calculations in semiconductors are separately discussed in the following.

A. Hermiticity

When the perturbation potential δV has a single Fourier component at $\vec{q}+\vec{G}'$, i.e., in real space

$$\delta V(\vec{r})=v e^{-i(\vec{q}+\vec{G}')\cdot\vec{r}} \tag{12}$$

the total Hamiltonian (3) is no longer Hermitian. This problem is easily circumvented by considering the density response to sine and cosine perturbations separately, each of which is real. The linear response to the perturbation (12) is then easily reconstructed. We notice at this point that in centrosymmetric materials a cosine perturbation always induces an even response, while a sine perturbation induces an odd response only within the *linear* regime. In a centrosymmetric material, the linear response to a cosine can be expanded as a Fourier cosine series and analogously for the sines, and this is the reason why we obtain a real symmetric χ_0. In noncentrosymmetric materials there are mixed sine-cosine responses, which are responsible for complex elements in the Hermitian matrix χ_0.

B. Linearity

Any linear response is, by definition, the linear term in the response to a vanishingly small perturbation. In other words, it is a functional derivative which we are evaluating in this work as a finite incremental ratio; we are therefore interested in choosing the strength of the perturbation v as small as possible. But since the (small) perturbation density is obtained as the difference of two large quantities, we are faced with a cancellation problem. It turns out that there is a large range of strengths which are small enough to induce linear response, although large enough to ensure cancellation causes no harm. This is in agreement with previous successful calculations for frozen *harmonic* phonons[12–14] where basically the same problem exists. Within this work, we have performed a preliminary study and we have chosen a value of $v=5\times10^{-5}$ hartree as the amplitude of our sine and cosine perturbations δV. The wisdom of this choice was assessed by several *a posteriori* checks on the results. Two of them have been already mentioned (Hermiticity of χ_0 or equivalently of $\tilde{\epsilon}$; odd response to odd perturbations in centrosymmetric crystals); others will be discussed below.

C. Supercells

The perturbed Hamiltonian, Eq. (3), when $\vec{q}=0$ has the same lattice periodicity as the unperturbed crystal; but when $\vec{q}\neq0$ this is no longer true. Since the one-electron states are easily obtained for a periodic Hamiltonian, we are forced to use some special $\vec{q}$ values, such that the perturbed Hamiltonian is periodic over a suitable supercell cal vectors of the new system (crystal plus perturbation). The feature is exactly the same as in the context of phonons[12–16] and will not be discussed further here. In the calculations presented in this work we deal with the Γ point (no supercell) and with the X and L points (supercell repeating twice the elementary cell in suitable directions).

A first comment concerns the zone-center case. A constant potential induces zero density response, of course, and our approach only gives the $\vec{G}\neq0$ *and* $\vec{G}'\neq0$ elements of χ_0 and ϵ; the missing elements are only defined in the $\vec{q}\to0$ limit and would require larger and larger supercells within the present scheme, while they are easily obtained within the standard RPA scheme.[7,11] An extension of the method of Ref. 4 could also possibly be implemented within the present approach.

A second comment concerns the zone-boundary cases, either X or L. We continue to use the $\vec{G}$ letter with the meaning of reciprocal vectors of the original lattice; then the reciprocal vectors of the superlattice can be partitioned in two sets: the $\vec{G}$ ones, and those having the form $\vec{q}+\vec{G}$. The unperturbed density has nonvanishing Fourier components only at the $\vec{G}$ vectors. If a monochromatic perturbation at $\vec{q}+\vec{G}'$ is switched on, the perturbed density has nonvanishing components at both sets, and the χ_0 matrix is obtained from the $\vec{q}+\vec{G}$ density components only. The $\vec{G}$ components of the perturbed density are equal to the unperturbed ones, within *linear* regime, but can be different because of quadratic and higher-order effects. So we obtain another accuracy check of the present method.

D. Brillouin-zone integration

The calculation of the electron density, for both the perturbed and unperturbed crystal, requires a BZ integration:

$$n(\vec{r})=2(2\pi)^{-3}\sum_{v}\int_{\mathrm{BZ}}d\vec{q}\,\langle\vec{r}\,|\,\vec{q},v\rangle\langle\vec{q},v\,|\,\vec{r}\rangle \tag{13}$$

and this is numerically performed with the mean-value points technique.[8–10] With an N-fold supercell, the BZ is folded back N times and the volume has a factor $1/N$, but there are N as many valence bands. The problem is that, in general, the set of special points depends upon the BZ shape and there is, in general, no guarantee that we will get the same accuracy for different N values. The choice of special points performed in this work does guarantee the same accuracy, and, even more, the doubled-cell results coincide exactly with the simple cell ones if a $\vec{q}=0$ perturbation is dealt with in both schemes.

To this aim we have used the reciprocal-space uniform orthogonal mesh of Monkhorst and Pack;[10] in their notation, we have chosen for the no-supercell case the (4,4,4) mesh. This gives 64 points in a cube but only 32 of them are not connected by a $\vec{G}$ vector and can be chosen in the fcc BZ. These are exactly the two Chadi-Cohen special points,[9] when all their symmetrically equivalent ones are separately considered (24 + 8). Of course, even at $\vec{q}=0$

tion is lower than the unperturbed crystal and the 32 points no longer reduce to two only. For the most unsymmetric perturbation, only time reversal can be invoked to reduce from 32 to 16.

When considering either the X or L supercells ($N=2$) simple geometrical considerations show that the new reciprocal vectors $\vec{q}+\vec{G}$ connect in both cases any of these 32 points to another point in the *same* set; therefore only 16 are now independent and can be chosen in the BZ of the superlattice; time reversal lowers this number further.

E. Independent elements

We use the same cutoff as in Refs. 7 and 11, i.e., all matrices (Hamiltonian, χ_0,ϵ) are set to zero when $|\vec{q}+\vec{G}|^2>21$ in $2\pi/a$ units. This gives a matrix size of 113×113 at Γ and of 108×108 at either X or L. But since the matrices are totally symmetric under the operations of the small point group of $\vec{q}$, the number of independent elements is reasonably small.

At the Γ point, the HDM is totally symmetric under all crystal symmetry operations and the body of it (i.e., $\vec{G}\neq0$ *and* $\vec{G}'\neq0$) has only 201 independent elements. These are separately evaluated within standard RPA in Refs. 7 and 11 using Eq. (11).[20] But according to the present method, we do *not* have to consider the response to 201 monochromatic perturbations, since each of them generates a whole column of χ_0, after Eq. (9). Looking more closely, the whole matrix can be built out of only one monochromatic perturbation per shell, i.e., 8 with the presently chosen cutoff (twice as many when separately considering sine and cosine, see Sec. III A).

At either the X or L points, the symmetry is lower and the number of independent elements higher. There are 468 of them at X and 598 at Γ; these can be built out of only 14 and 16 monochromatic perturbations, respectively.

IV. RESULTS

We present in this section the results obtained for the HDM's or Si and GaAs. For $\vec{q}=0$, standard RPA results to compare with have been obtained by Baldereschi and Tosatti[7] and by Resta and Baldereschi.[11] The problem of the BZ integration appearing in Eq. (11) has been widely discussed by these authors; the Chadi-Cohen two-point scheme[9] is the one to be chosen for the most meaningful comparison, being compatible with the scheme used here as explained in Sec. III D. We present in Table I the HDM elements calculated within direct and standard RPA for GaAs, with the same H_0 and the same cutoff. It is easily seen that the agreement between the two calculations is excellent, the absolute difference being of the order of 10^{-4}. Furthermore, from the several checks mentioned in the preceding section, we estimate the numerical accuracy of the present results to be at least 1 order of magnitude better. Therefore, we believe that most of the very small discrepancy is a convergence error of the standard RPA perturbation sums, which have been calculated in Refs. 7 and 11 summing over 90 conduction bands. For $\vec{q}$ at the zone boundary, at either X or L the standard

TABLE I. Hermitian dielectric matrix at $\vec{q}=0$ in GaAs. Only some of the independent elements are reported. The Resta and Baldereschi results, Ref. 11, shown in this table are those calculated with a two-point integration scheme (see text).

		This work		Resta and Baldereschi	
$\vec{G}$	$\vec{G}'$	Real	Imaginary	Real	Imaginary
111	111	1.6819	0.0000	1.6820	0
$\bar{1}11$	111	−0.0029	−0.0448	−0.0029	−0.0447
$1\bar{1}1$	$\bar{1}11$	−0.0142	0.0000	−0.0143	0
$1\bar{1}\bar{1}$	$\bar{1}11$	−0.1268	−0.0829	−0.1264	0.0830
200	111	0.1122	−0.0391	0.1123	−0.0390
200	$\bar{1}11$	0.0115	−0.0128	0.0112	−0.0128
200	200	1.5250	0.0000	1.5254	0
$\bar{2}00$	200	−0.0119	0.0000	−0.0117	0
020	200	−0.0093	0.0000	−0.0095	0

TABLE II. Hermitian dielectric matrix at the X point, $\vec{q}=(1,0,0)$ in units of $2\pi/a$. Only some of the independent elements are shown.

			GaAs	
G	G'	Si	Real	Imaginary
000	000	2.9484	2.8921	0.0000
$\bar{2}00$	000	0.0000	0.0000	0.4504
$\bar{1}1\bar{1}$	000	0.0829	0.1266	−0.0188
$\bar{1}1\bar{1}$	$\bar{1}1\bar{1}$	2.0860	2.0621	0.0000
002	$\bar{1}1\bar{1}$	−0.0022	−0.0006	0.0002
111	$\bar{1}1\bar{1}$	0.0185	−0.0010	0.0039
002	002	1.4198	1.4032	0.0000
022	002	−0.0065	−0.0038	0.0167
$1\bar{1}1$	$1\bar{1}1$	1.3305	1.3178	0.0000
111	$1\bar{1}1$	−0.0109	−0.0067	0.0192
200	$1\bar{1}1$	0.0532	0.0585	0.0181
022	022	1.1819	1.1796	0.0000
200	022	0.0146	0.0129	0.0048
$\bar{2}\bar{2}\bar{2}$	022	−0.0122	−0.0076	0.0094

TABLE III. Hermitian dielectric matrix at the L point, $\vec{q}=(\frac{1}{2},\frac{1}{2},\frac{1}{2})$ in units of $2\pi/a$. Only some of the independent elements are shown.

			GaAs	
G	G'	Si	Real	Imaginary
000	000	3.1683	3.0854	0.0000
$\bar{1}\bar{1}\bar{1}$	000	0.7425	0.6818	0.4391
$\bar{2}\bar{2}\bar{2}$	000	−0.1393	−0.1425	−0.0198
$\bar{1}1\bar{1}$	$\bar{1}1\bar{1}$	1.7969	1.7971	0.0000
$\bar{2}00$	$\bar{1}1\bar{1}$	0.1095	0.1443	−0.0543
111	$\bar{1}1\bar{1}$	0.0232	0.0083	0.0023
$\bar{1}11$	$\bar{1}11$	1.4290	1.4200	0.0000
002	$\bar{1}11$	0.0628	0.0739	0.0215
$\bar{2}02$	$\bar{1}11$	0.0551	0.0648	−0.0181
002	002	1.2775	1.2737	0.0000
111	002	0.0532	0.0617	0.0185
$\bar{1}\bar{1}\bar{3}$	002	−0.0087	−0.0018	−0.0047
111	111	1.2711	1.2693	0.0000
$\bar{2}\bar{2}\bar{2}$	111	−0.0197	−0.0064	0.0153
$\bar{2}02$	111	0.0157	0.0128	0.0027

RPA of Refs. 7 and 11 becomes computationally rather heavy, and we have no complete results to compare with. In this work, we have calculated the HDM of Si and GaAs both at the X and L points; some independent elements are shown in Tables II and III.

The diagonal elements $\bar{\epsilon}(\vec{q}+\vec{G},\vec{q}+\vec{G})$ are a smooth function of $\vec{q}+\vec{G}$, decreasing towards 1 with increasing $|\vec{q}+\vec{G}|$. The other HDM elements are numbers where trends and physical meanings are hardly detectable—a feature noticed several times.[1,3,7,11] Their significance becomes clear when applied to screen specific perturbations. An overall look is most meaningfully obtained with a DBS analysis, which is performed in Sec. V.

V. DIELECTRIC BAND STRUCTURE

Like any Hermitian operator, the HDM can be diagonalized. The eigenvectors at a given $\vec{q}$ point are a type of normal coordinates in the screening problem, and have no direct link to real physical perturbations. Nevertheless, this concept of DBS, proposed some years ago by Baldereschi and Tosatti[18] is a nice mathematical tool to extract some important trends from the HDM's. At high-symmetry $\vec{q}$ points the HDM eigenvalues can be classified according to the small group of $\vec{q}$, and the symmetry of the most screened perturbations is straightforwardly visualized. For instance, trends with increasing ionicity for the isoelectronic series Ge-GaAs-ZnSe have been identified and their origin has been understood[11] through a DBS analysis. When dealing with one material, but several different HDM models, the DBS gives a kind of fingerprint of the main screening features of each model. In the case of Si, a very detailed study has been published by Car *et al.*[22] with reference to some of the existing models.[22–24]

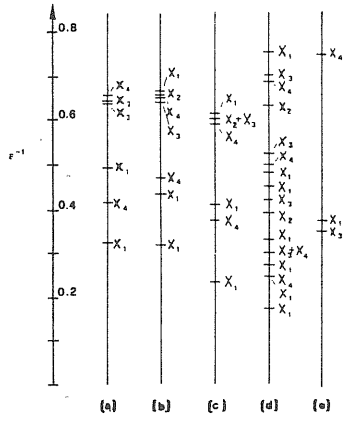

FIG. 1. Eigenvalues of the inverse HDM at the X point in Si. (a): Present work; (b): Car-Selloni (Ref. 24); (c): local-density model (Ref. 21); (d): Johnson model (Ref. 23); and (e): Sinha model (Ref. 22). Calculations (b), (c), (d), and (e) are taken from Ref. 21.

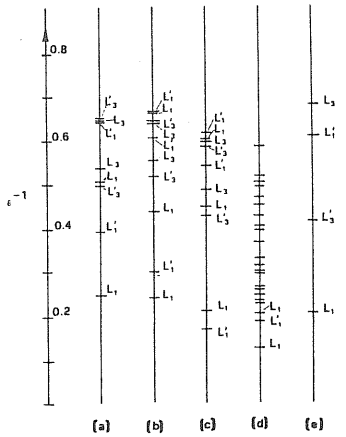

FIG. 2. Eigenvalues of the inverse HDM at the L point in Si. (a)—(e) represent different models as in Fig. 1.

Before this work, first-principles results were only available at $\vec{q}=0$ or $\vec{q}\to 0$; therefore at finite-q values Car *et al.* were only allowed to compare different models between themselves. In this section, we augment their analysis by comparing at the X and L points the model results with the present first-principle ones for Si. The results are presented in Figs. 1 and 2, where the most screened eigenvalues of $\bar{\epsilon}^{-1}$ are shown.

It can be seen that the model which looks overall most similar to the first-principle result is the Car-Selloni model,[24] even if the ordering of the eigenvalues is partly different. This is not surprising, since this model has been fitted after the first-principle HDM of Ref. 7, while the other ones have been proposed for a "specialized" use in lattice dynamics. In order to calculate phonon frequencies, only a limited amount of the information embedded in the HDM is used. Some models are able to predict good frequencies, although being strongly unsatisfactory for the physics of the screening process as a whole. The reasons why have been investigated in much detail by Car *et al.*,[21] to whom we refer to for a discussion on this point. In addition, we only wish to point out the fact that a typical fingerprint of local-field effects is the gap between the two most screened eigenvalues at the L point, since a diagonal HDM has an "empty lattice" DBS, and a closed gap. The Car-Selloni model gives the right ordering of levels, although it underestimates the L gap. In general, both the Car-Selloni and the local-density[21] models underestimate local-field effects, while Sinha's model[22] overestimates them. The Johnson model[23] is strongly unphysical, as already realized by Car *et al.*[21]

VI. DISCUSSION AND CONCLUSIONS

In this work we have presented a novel approach to calculate first-principle dielectric matrices in solids. The main limitations of the standard RPA, as applied to real

solids and realistic band structures, are overcome by our direct RPA methods, which allows much simpler computations without losing accuracy. One of the features making the present method very appealing is that we are able to get the fully converged perturbation sum without actually summing over empty states, while the standard RPA requires explicitly dealing with very high conduction bands.[7,11] The problem of slowly convergent perturbation sums, indeed, was recently circumvented also by Van Camp *et al.*[25] who used a moment expansion approach, but since their expansion is actually cut at a given order, the numerical results only approximate the RPA value.[6] On the contrary, we have shown here that we can easily obtain numerically the exact standard RPA results.

In this first application of the method, we have calculated the RPA dielectric matrices of Si and GaAs, with the use of Cohen-Bergstresser[17] band structure, in order to closely compare with previously published standard RPA calculations.[7,11,18] Besides reproducing them, we are now able to extend beyond; the results reported in Tables II and III and in Figs. 1 and 2, therefore, supplement those of Refs. 7, 11, and 18.

The shortcomings of the present approach are exactly the same as in any calculation based on supercell techniques.[13,14] The system (crystal plus perturbation) must have a periodicity which is commensurate to the unperturbed lattice. The supercell size cannot be arbitrarily large, but within the present computational possibilities, the attainable $\vec{q}$ points in the BZ form a mesh which is dense enough in order to interpolate or extrapolate[26] the HDM elements. There is presently a need for simple and yet realistic HDM models; *ab initio* calculations within the present methods can provide a reference frame for them.

Finally we briefly outline the possible extension of the method beyond RPA. Suppose we know the self-consistent one-electron potential obtained for the *unperturbed* crystal within the LDF scheme.[14–16] Then our approach yields the independent-electron polarizability χ_0; the LDF dielectric matrix is then related to this χ_0 by a relationship which is not the simple RPA one, but which is nevertheless tractable and easily implementable.[13,19] Notice that χ_0 is obtained here through ground-state calculations for the crystal with a frozen-in perturbation, but these must *not* be self-consistent. This is an important new feature of our method: To the best of our knowledge, all of the existing direct LDF treatments of perturbed crystals *do* require self-consistency for each perturbation considered. We are referring here to frozen phonons[12] and generalizations,[13–16] as well as to very recent work on dielectric screening.[4,26] A direct evaluation of the inverse HDM, having several features related to the present work but based on self-consistent LDF calculations, is presently being performed by Kunc and Tosatti.[27]

ACKNOWLEDGMENTS

We have benefited from discussions with A. Baldereschi, K. Kunc, and E. Tosatti. We also wish to thank K. Kunc and E. Tosatti for communicating to us some of their preliminary results.[27]

*To whom correspondence should be addressed.

[1] A. Baldereschi, in *Proceedings of the XV International Conference on the Physics of Semiconductors, Kyoto, 1980* [J. Phys. Soc. Jpn. 49, Suppl. A155 (1980)].
[2] *Ab-Initio Calculation of Phonon Spectra*, edited by J. T. Devreese, V. E. Van Doren, and P. E. Van Camp (Plenum, New York, 1983).
[3] A. Baldereschi and R. Resta, in Ref. 2, p. 1.
[4] K. Kunc and R. Resta, Phys. Rev. Lett. 51, 686 (1983).
[5] S. L. Adler, Phys. Rev. 126, 413 (1962); N. Wiser, *ibid.* 129, 62 (1963).
[6] P. E. Van Camp, V. E. Van Doren, and J. T. Devreese, in Ref. 2, p. 24.
[7] A. Baldereschi and E. Tosatti, Phys. Rev. B 17, 4710 (1978).
[8] A. Baldereschi, Phys. Rev. B 7, 5212 (1973).
[9] D. J. Chadi and M. L. Cohen, Phys. Rev. B 8, 5747 (1973).
[10] H. J. Monkhorst and J. D. Pack, Phys. Rev. B 13, 5188 (1976).
[11] R. Resta and A. Baldereschi, Phys. Rev. B 23, 6615 (1981).
[12] H. Wendel and R. M. Martin, Phys. Rev. B 19, 5251 (1979); Festkoerperprobleme 19, 21 (1979).
[13] R. M. Martin and K. Kunc, in Ref. 2, p. 49.
[14] K. Kunc and R. M. Martin, in Ref. 2, p. 65.
[15] K. Kunc and R. M. Martin, Phys. Rev. Lett. 48, 406 (1982).
[16] K. Kunc, Helv. Phys. Acta 56, 559 (1983).
[17] M. L. Cohen and T. K. Bergstresser, Phys. Rev. 141, 789 (1966).
[18] A. Baldereschi and E. Tosatti, Solid State Commun. 29, 131 (1979).
[19] P. E. Van Camp, V. E. Van Doren, and J. T. Devreese, Phys. Rev. B 24, 1096 (1981); Phys. Status Solidi B 110, K133 (1982).
[20] The independent elements evaluated in Refs. 7 and 11 in the $\vec{q}\to 0$ limit are actually 217. This figure comes out from nonanalytic "wing" ($\vec{G}=0$) elements. For an analytic matrix, the independent elements are $201+8+1=210$.
[21] R. Car, E. Tosatti, S. Baroni, and S. Leelaprute, Phys. Rev. B 24, 985 (1981).
[22] S. K. Sinha, Phys. Rev. 177, 1256 (1969).
[23] D. L. Johnson, Phys. Rev. B 9, 4475 (1974).
[24] R. Car and A. Selloni, Phys. Rev. Lett. 40, 1365 (1979).
[25] P. E. Van Camp, V. E. Van Doren, and J. T. Devreese, Phys. Rev. Lett. 42, 1224 (1979).
[26] J. B. McKitterick, Phys. Rev. B 28, 7384 (1983).
[27] K. Kunc and E. Tosatti, Phys. Rev. B 29, 7045 (1984).

Will appear in:
Proceedings of the 2nd Int. Conf. Phonon Physics (Budapest, August 1985)

CRUCIAL ROLE OF EXCHANGE AND CORRELATION IN LATTICE DYNAMICS OF GERMANIUM

A. Fleszar, K. Kunc*, R. Resta and E. Tosatti

Scuola Internazionale Superiore di Studi Avanzati
Strada Costiera 11, I-34014 Trieste
ITALY

ABSTRACT

We present and compare some results in first-principle lattice dynamics, obtained from both the direct and dielectric approaches, in order to get physical insight into the basic mechanisms. Our main result concerns the dominant role of exchange and correlation effects in electronic screening. When these effects are switched off, Ge is unstable against shear.

The first-principle theory of lattice dynamics in semiconductors is nowadays capable of providing both accurate numerical predictions and thorough physical understanding. In recent years, most of the results were obtained via the so-called "direct" approach[1,2], whose achivements are reported by one of us elsewhere[2] in this volume. An alternative, older way is the linear-response or "dielectric" approach[3], which also has been implemented and used by some research groups[4-6]. As far as harmonic phonons are concerned, the two approaches give - at least in principle - the same results, provided exchange and correlation (XC) effects are properly evaluated. On the other hand, the most popular approximation for evaluating dielectric matrices is the RPA[4], which does not include such XC effects. This suggests that a detailed study of phonons in semiconductors done both within direct and dielectric approaches could provide a useful physical insight into basic mechanisms.

The point we want to address here is the stability of a covalent semiconductor against shear. It is well known that TA phonons at the X point have a peculiar behaviour: while the sound velocity is resonably high, the TA branch quickly flattens out, reaching the X point with quite a low value of the frequency. It was pointed out very early[7] that in the

*Permanent address: CNRS,Tour 13,4 pl. Jussieu,75230 Paris-Cedex 05,France

approximation of homogeneous electronic screening this mode becoms unstable: this corresponds, in the dielectric matrix language, to a diagonal matrix. It was also found for Si that by inclusion of a suitably large off-diagonal screening by the (microscopically inhomogeneous) electron gas, the TA branch could be readily stabilized[8].

Here we are concerned particularly with Germanium, which is a somewhat more "metallic" semiconductor than Si and where off-diagonal screening is weaker. We have performed:

a) direct frozen phonon calculations for Ge at the Γ and X points[2]; the self-consistent local-density approximation (LDA) was used;
b) calculations of these same phonons via the dielectric approach, based on identically the same electronic structure, using the RPA expression for the dielectric matrix;
c) the same calculations as in (b), but including in the RPA dielectric matrix appropriate XC correction[9]. The dielectric matrix thus obtained is in principle the exact respons operator at the LDA level; the phonons calculated in (c) are therefore directly comparable to those calculated in (a).

The frequencies resulting from these calculations are presented in Table I. The experimental data are also shown.

Table I: calculated and experimental phonon frequencies (in Thz) for Ge; a)-frozen phonon; b)- RPA dielectric matrix method; c)- LDF dielectric matrix method.

	TO(Γ)	TA(X)	LA(X) LO(X)	TO(X)
a	9.12	1.61	....	....
b	9.15	3.25i	7.49	9.42
c	9.13	2.24	7.12	8.06
Exp.	9.12	2.40	7.21	8.26

We find that: i) The direct (a) and the dielectric LDA (c) calculations give rather similar results. They are not identical (as they should) probably because of the slight inaccuracies involved in the huge numerical cancellations[2] affecting particularly TA(X) mode in method (a). Other minor technical points, like basis set dimensions, could also affect the results. ii) The optical phonon at Γ, being essentially insensitive to off-diagonal screening[7], remains unchanged whether XC effects are

included (c) or not (b). iii) The TA phonon on the contrary, is found to be unstable (imaginary frequency in Tab.I) when using the RPA dielectric screening matrix (b). This means, therefore, that the soft TA(X) mode in Ge is stabilized precisely and only by the XC contributions to screening, while off-diagonal screening within the RPA contributes to stability but is not strong enough.

One way to understand this result is to note that XC has the main effect of reducing the average excitation energy of the system. This implies in turn an increase of off-diagonal dielectric matrix elements, as discussed earlier[10], which act as stabilizing agents.

More physically, this must have to do with the detailed behaviour of the electronic polarization charge upon TA shear. We are currently planing a study of this via the dielectric approach[11].

In closing we point out that, while XC effects prove to be crucial to the stability of Ge, their role has not so far appeared to be all that important in previous work. A narrow gap semiconductor in fact may turn out to be the casa where their importance is maximum. Simple metals, on one hand, and large gap insulators, on the other hand, appear to be systems where, for opposite reasons, the XC effects play only a minor role in phonon spectra.

REFERENCES

1) M.L. Cohen, Phys. Scr. T1, 5 (1982); R.M. Martin, Festkörperprobleme 25 (1985).

2) K. Kunc, this volume.

3) R.M. Pick, M.H. Cohen and R.M. Martin, Phys. Rev. B1, 910 (1970).

4) "Ab Initio Calculation of Phonon Spectra", edited by J.T. Devreese (Plenum N.Y., 1983).

5) A. Baldereschi and R. Resta, in Ref. 4), p.1 .

6) P.E. van Camp, V.E. van Doren and J.T. Devreese, in Ref. 4), p.24 .

7) R.M. Martin, Phys. Rev. 186, 871 (1969).

8) C.M. Bertoni, V. Bortolani, C. Calavdra and E. Tosatti, Phys. Rev. Lett. 28 , 1578 (1972).

9) P.E. van Camp, V.E. van Doren and J.T. Devreese, Phys.Rev.B24,1096 (1981).

10) K. Kunc and E. Tosatti, Phys. Rev. B29, 7045 (1984).

11) R. Resta, Phys. Rev. B27, 3620 (1983).

Will appear in:
Proceedings of the 2nd Int. Conf. Phonon Physics (Budapest, August 1985)

INTERPLANAR AND INTERATOMIC FORCE CONSTANTS IN SILICON AND GERMANIUM

A. Fleszar and R. Resta
Scuola Internazionale Superiore di Studi Avanzati
Strada Costiera 11, I-34014 Trieste
ITALY

ABSTRACT

The bond-charge (BC) model gives the most successful and the most realistic picture of lattice dynamics in covalent materials. In this work we perform a deconvolution of the BC model in terms of both interplanar and interatomic force constants. The main features of BC interplanar force constant (including their spatial extent) are discussed and compared to recent first principle calculations of the same quantities. Excellent agreement is found for Ge. As for the interatomic force constants, our main result is that long-range interactions mostly propagate along coplanar bonding chains.

1. INTRODUCTION

The phonon spectra of covalent semiconductors have been the subject of extensive theoretical work, at the level of both empirical models[1-6] and first-principle calculations[7-9]. While empirical models are fitted to the experimental spectra throughout the Brillouin zone, the first-principle calculations available so far predict phonon frequencies close ($\simeq$5%) to the experimental ones at some selected points or lines in the Brillouin zone.

The Weber adiabatic bond-charge (BC) model[5] is by far the most popular and the most realistic of the available models for diamond-structure materials; it accounts for the essence of ion-electron-ion interactions[4] in covalent solids and gives an excellent fit to phonon frequencies ($\simeq$2%), still using very few (4 in Si and Ge) empirical parameters. In this work, we assume the BC model as a paradigm and we compare to it some features of the existing first-principle calculations.

In the context of models, little interest has been paid to the

force constants themselves, since these are not the independent parameters in terms of which the dynamical matrix is usually built. But in some recent ab-initio work[8-13] force constants in real space are the most basic output of the calculations, since they can be directly evaluated through the Hellmann-Feynman theorem. One important question we address is the spatial extent of these forces. As for the BC model, it is qualitatively well known that the adiabatic interaction between bond charges is responsible for long-range forces, and that the long range forces are needed to account for the flat TA branches experimentally observed[14]. To the best of our knowledge, the present work is the first quantitative study of how far (and in which direction) do these long-range forces extend within the BC model. As for the first-principle calculations, they have been performed in a supercell geometry; in order to be computationally feasible, the supercell size could not be large at will; and the supercell size itself dictates the assumption of a cutoff in the range of interactions. The present study, therefore, also provides a guideline to first-principle calculations of forces, in the sense that the spatial extent of force constants obtained from BC suggests the optimum supercell size for calculations.

	Δ	
n	longit.	trans.
0	2.452	2.078
1	-1.128	-1.808
-1	-1.128	-0.367
±2	-0.074	0.093
3	-0.018	-0.013
-3	-0.018	-0.091
±4	-0.004	0.013
5	-0.001	-0.002
-5	-0.001	-0.012
±6	0.000	0.002
7	0.000	0.000
-7	0.000	-0.002
±8	0.000	0.000

Table I: Interplanar force constants for Si, after BC model (10^5 dyn/cm).

	Δ		Λ	
n	longit.	trans.	longit.	trans.
0	2.181	1.848	2.090	1.950
1	-1.010	-1.644	-1.112	-0.153
-1	-1.010	-0.294	-0.881	-1.845
±2	-0.059	0.086	-0.017	0.044
3	-0.016	-0.014	0.000	-0.041
-3	-0.016	-0.084	-0.057	-0.007
±4	-0.004	0.014	-0.001	0.001
5	-0.001	-0.002	0.000	-0.006
-5	-0.001	-0.013	-0.004	-0.001
±6	0.000	0.002	0.000	0.001
7	0.000	0.000	0.000	-0.001
-7	0.000	-0.002	0.000	0.000
±8	0.000	0.000	0.000	0.000

Table II: Interplanar force constants for Ge, after BC model (10^5 dyn/cm).

2. INTERPLANAR FORCE CONSTANTS

2.1 Bond-charge model

Let us consider phonons whose q-vector is along a given high symmetry line (Δ or Λ in diamond-structure materials). For these phonons, at any value of $|\vec{q}|$, atomic planes orthogonal to the $\vec{q}$-direction are displaced rigidly (either in the longitudinal or in the transverse directions). Therefore, the crystal vibrations can be described as those of a linear chain, whose equation of motion leads to a simple 2x2 secular equation. The basic ingredients are the one-dimensional force contants $\{k_n\}$. Different sets of force constants are needed for different choices of polarization and of propagation direction; they are in each case suitable combinations of interatomic force constants.

We have calculated the interplanar force constants, as resulting from the BC model, for longitudinal and transverse phonons, both along the Δ and Λ direction. The deconvolution was performed by one-dimensional fast-Fourier transform, starting from the BC dynamical matrix as provided by the Nielsen-Weber computer code[15]. Our results for these $\{k_n\}$ force constants are shown in Tab. I for Si and Tab. II for Ge.

2.2 First-principle calculations

The concept of interplanar force constants was introduced in the context of first-principle lattice dynamics by Kunc and Martin at the previous conference in this series[10]. To the aim of evaluating these force constants, the idea is to give a small (longitudinal or transverse) displacement to an atomic plane of the crystal, and to use the Hellmann-Feynman theorem in order to obtain the forces on all the other atoms from the self-consistent electronic density. For computational reasons, one uses supercells which repeat the elementary unit cell of the undistorted crystal m-times along the direction of phonon propagation. More details can be found elsewhere[9,12]; here it is important to stress that the method works properly only if the crystal planes which are neighbors of index m and larger are completely decoupled. At a first-principle level, the validity of this assumption is difficult to assess. For group IV materials, published calculations exist for Si and Ge.

The Si calculation[13] is for the Δ direction and makes use of norm-conserving pseudopotentials[16]. It is therefore very accurate in the description of the electronic ground state; the counterpart is that the supercell size is limited and only third-neighbor interplanar forces are attainable. We reproduce the Si results in Table III, after converting to our units.

n	Δ longit.	Δ trans.
0	2.226	1.791
1	-0.942	-1.495
-1	-0.942	-0.288
±2	-0.163	0.039
3	-0.008	-0.008
-3	-0.008	-0.078

Table III: Interplanar force constants for Si, after Ref. 13 (converted to 10^5 dyn/cm).

n	Δ longit.	Δ trans.	Λ longit.	Λ trans.
0	2.248	1.806	2.161	1.931
1	-1.050	-1.695	-1.142	-1.101
-1	-1.050	-0.203	-0.900	-1.899
± 2	-0.083	0.086	-0.054	0.048
3	-0.006	-0.035	-0.020	-0.044
-3	-0.006	-0.094	-0.029	-0.024
± 4	0.014	0.029	0.020	0.021
5		-0.007		
-5		-0.023		

Table IV: Interplanar force constants for Ge, after Ref. 12 (10^5 dyn/cm).

In the case of Ge, there are available calculations both for the Δ and Λ directions [10,12]; they make use of local pseudopotentials, thus allowing for large supercell size (m up to 8). We reproduce the Ge [10,12] interplanar force constants from the work of Kunc and Gomez Dacosta in Table IV.

2.3 Discussion

We start discussing the case of Ge, where more detailed data are available. The agreement between the BC force constants (Table II) and the first-principle ones (Table IV) is quite remarkable. The longitudinal forces have very short range and constant sign, while the transverse forces show features which are characteristic of covalent bonding, namely alternation in sign and long-rangeness [10,12]. The BC force constants rapidly decay for $|n| > 5$, thus supporting the fact that the first-principle calculations are converged for what concerns the supercell size.

Also we observe the presence of a sizeable n = -5 force for transverse phonons along Δ. This is a little bit surprising [12], since Valence-Force-Field (VFF) models [3] are able to fit quite accurately the phonon spectrum of Ge using shorter range forces only. More in detail, the longest-range interaction assumed in the VFF model is the so-called angle-angle interaction first proposed by McMurray et al. [3]. This force couples atoms along a bonding chain in the (110) plane, which are third neighbors along the chain but real fifth neighbors, like atoms A and D in Fig. 1. In term of planes (for phonons along Δ) this interaction only couples third-neighboring planes. Therefore both BC and first-principle results give support to the fact that some important interaction, missed by VFF

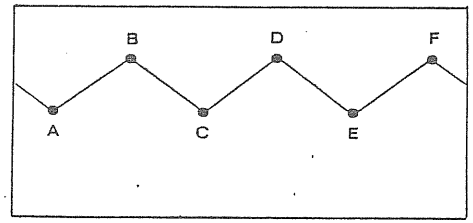

Figure 1: Bonding chain of atoms in the (110) plane.

models, couples neighboring planes of order four and five. This point will be further investigated in the next section.

The largest disagreement (9×10^3 dyn/cm) between the two sets of force constants is k_{-1} for transverse modes along the Δ direction. We conjecture here that this could well be due to a serious drawback of either the local pseudopotential or the local density approximation in describing this bond-bending shear displacement.

We now pass discussing the case of Si. An analysis of Table I and III shows rather important disagreement, which we interpret as due to the drastic decoupling assumed in the first-principle calculation. The BC model indicates sizeable interactions up to $|n| = 5$, which are missed in Ref. 13. Furthermore, with the chosen supercell size, the planes at $|n| = 4$ and $|n| = 5$ are 'folded back' over $|n| = 1$ and $|n| = 2$, thus giving spurious contributions even to the first-principle forces $k_{\pm1}$ and $k_{\pm2}$ calculated in ref. 13. Our interpretation is supported by the fact that the force constants k_3 and k_{-3}, which do not suffer from such a drawback, come out quite close ($\simeq10^3$ dyn/cm) from both BC and first-principles.

3. INTERATOMIC FORCE CONSTANTS

We do not publish here complete tables of interatomic force contants but we only discuss the most relevant physical features emerging from the calculations. The largest interatomic forces are, as expected, those involving first and second neighbors; the following one, in order of importance, involves atoms like A and D in Fig. 1, which only are fifth neighbors. Up to this point, we agree with the assumptions of VFF models [3]; besides these, VFF assumes complete decoupling, while our BC results also give sizeable interactions involving more distant neighbors. The next force in order of importance is a eight-neighbor one, which couples atoms like A and E in Fig. 1, which are fourth neighbors along coplanar bonding chains. The following ones, having both about the same magnitude, involve neighbors of order 3 and 13: the large extent of the latter seems

surprising, but it is worth noting that the 13-th neighbors involved are just the fifth neighbors along the bonding chain (atoms A and F in Fig.1).

In two very recent papers [6,17] Kane stressed the importance of the coplanar chains of bonds for propagating interactions in covalent material. Within BC model, such a mechanism is by no means explicitly assumed; nevertheless the results discussed in this Section show that BC predicts strong interaction between atoms which are rather far apart but lie on the same coplanar bonding chain. The present work, therefore, gives strong support to Kane's point of view.

REFERENCES

1) W. Cochran, Proc. R. Soc. A253, 260 (1959); F. Herman , J. Phys. Chem. Solids 8, 405 (1959.

2) P.N. Keating, Phys. Rev. 145, 637 (1966).

3) H.L. McMurray, A.W. Solbrig, J.K. Boyter and C. Noble, J. Phys. Chem. Solids 28, 2359 (1967); R. Tubino, L. Piseri and G. Zerbi, J. Chem. Phys. 56, 1022 (1972).

4) J.C. Phillips, Phys. Rev. 166, 832 (1968); R.M. Martin, Phys. Rev. 186, 871 (1969).

5) W. Weber, Phys. Rev. Lett. 33, 371 (1974); Phys. Rev. B15, 4789 (1977).

6) E.O. Kane, Phys. Rev. B31, 7865 (1985).

7) M.L. Cohen, Phys. Scr. T1, 5 (1982).

8) R.M. Martin, FestKörperprobelme XXV (1985).

9) K. Kunc, this volume.

10) K. Kunc and R.M. Martin, J. Phys. (Paris) 42, suppl. C6, 649 (1981).

11) K. Kunc and R.M. Martin, Phys.Rev. Lett. 48, 406 (1982).

12) K. Kunc and P. Gomez Dacosta, at this conference and to be published

13) M.T. Yin and M.L. Cohen, Phys. Rev. B25, 4317 (1982).

14) R. Sokel and W.A. Harrison, Phys. Rev. Lett. 36, 61 (1976).

15) O.H. Nielsen and W. Weber, Comp. Phys. Commun. 18, 101 (1979).

16) D.R. Hamann, M. Schluter and C. Chiang, Phys. Rev. Lett. 43, 1294 (1979).

17) E.O. Kane, Phys. Rev. B 31, 5199 (1985).

X. REFERENCES

[1] M. Born and J. R. Oppenheimer, Ann. Phys. 84, 457 (1927)

[2] J. C. Slater, "Quantum Theory of Atomic Structure" (McGraw-Hill, 1960)

[3] F. Bassani and G. Pastori Parravicini, "Electronic states and Optical Transitions in Solids", (Pergamon press, 1975)

[4] P. Hohenberg and W. Kohn, Phys. Rev. 136, B864 (1964)

[5] W. Kohn and L. J. Sham, Phys. Rev. 140, A1133 (1965)

[6] "Theory of the Inhomogeneous Electron Gas", ed. by S. Lundquist and N. H. March (Plenum, New York, 1983)

[7] L. J. Sham, Phys. Rev. 188, 1431 (1969)

[8] R. M. Pick, M. H. Cohen and R. M. Martin, Phys. Rev. B1, 910 (1970)

[9] "Dynamical Properties os Solids", ed. by G. K. Horton and A. A. Maradudin (North-Holland Publ. Comp., 1975)

[10] A. Baldereschi and E. Tosatti, Phys. Rev. B17, 4710 (1978)

[11] A. Baldereschi, R. Car and E. Tosatti, Solid St. Commun. 32, 757 (1981)

[12] R. Car, E. Tosatti, S. Baroni and S. Leelaprute, Phys. Rev. B24, 985 (1981)

[13] R. Resta, Phys. Rev. B27, 3620 (1983)

[14] A. Fleszar and R. Resta, Phys. Rev. B31, 5305 (1985)

[15] D. Bohm and D. Pines, Phys. Rev. 92, 609 (1953)

[16] P. Nozieres and D. Pines, Phys. Rev. 109, 762 (1958); Nuovo Cimento 9, 470 (1958)

[17] P. C. Martin and J. Schwinger, Phys. Rev. 115, 1342 (1959)

[18] J. M. Ziman: "Electrons and Phonons", (Oxford Univ. Press, 1960)

[19] R. Penn, Phys. Rev. 128, 2093 (1962)

[20] R. D. Grimes and E. R. Cowley, Can. J. Phys. 53, 2549 (1975)

[21] R. Resta, Phys. Rev. B16, 2717 (1977)

[22] H. Nara and A. Morita, J. Phys. Soc. Japan 21, 1852 (1966); P. K. W. Vinsome and D. Richardson, J. Phys. C4, 2650 (1971)

[23] A. Baldereschi and E. Tosatti, Solid St. Commun., 29, 131 (1979)

[24] J. C. Slater: "Quantum Theory of Molecules and Solids" (McGraw-Hill Book Company) Vols. 1-4

[25] E. Wigner, Phys. Rev. 46, 1002 (1934)

[26] J. C. Slater, Phys. Rev. 81, 385 (1951)

[27] D. N. Ceperley and B. J. Alder, Phys. Rev. Lett. 45, 566 (1980)

[28] J. Perdew and A. Zunger, Phys. Rev. B23, 5048 (1981)

[29] K. Kunc and E. Tosatti, Phys. Rev. B29, 7045 (1984)

[30] S. L. Adler, Phys. Rev. 126, 413 (1962)

[31] N. Wiser, Phys. Rev. 129, 62 (1963)

[32] J. Linghard, Kong. Danske Vid. Selsk. Mat.-Fys. Medd. 24, N° 8 (1954)

[33] H. Ehrenreich and M. H. Cohen, Phys. Rev. 115, 786 (1959)

[34] R. Resta and A. Baldereschi, Phys. Rev. B23, 6615 (1981)

[35] C. M. Bertoni, V. Bortolani, C. Calandra and E. Tosatti, Phys. Rev. B9, 1710 (1974)

[36] S. K. Sinha, Phys. Rev. 177, 1256 (1969)

[37] S. K. Sinha, R. P. Gupta and D. L. Price, Phys. Rev. B9, 2564, 2573 (1974)

[38] D. L. Johnson, Phys. Rev. B9, 4475 (1974)

[39] R. Car and A. Selloni, Phys. Rev. Lett. 40, 1365 (1979)

[40] R. Resta and A. Baldereschi, Phys. Rev. B24, 4839 (1981)

[41] H. Nara, J. Phys. Soc. Japan 20, 778 (1965); ibid, 20, 1097 (1965)

[42] J. P. Walter and M. L. Cohen, Phys. Rev. B2, 1821 (1970); ibid, 5, 3101 (1972)

[43] S. J. Sramek and M. L. Cohen, Phys. Rev. B6, 3800 (1972)

[44] J. A. Van Vechten and R. Martin, Phys. Rev. Lett. 28, 446 (1972)

[45] W. Hanke and L. J. Sham, Phys. Rev. Lett. 33, 582 (1974)

[46] N. E. Brener, Phys. Rev. B12, 1487 (1975)

[47] S. P. Singhal, Phys. Rev. B12, 564 (1975)

[48] S. G. Louie, J. R. Chelikowsky and M. L. Cohen, Phys. Rev. Lett. 34, 155 (1975)

[49] S. G. Louie and M. L. Cohen, Phys. Rev. B17, 3174 (1978)

[50] J. T. Devreese, P. E. Van Camp and V. E. Van Doren, Bull. Am. Phys. Soc. 23, 224 (1978)

[51] "Ab-initio Calculation of Phonon Spectra", ed. by J. T. Devreese, V. E. Van Doren and P. E. Van Camp, (Plenum Publishing, New York, 1983)

[52] J. T. Devreese, P. E. Van Camp and V. E. Van Doren, Phys. Rev. Lett. 42, 1224 (1979)

[53] P. E. Van Camp, V. E. Van Doren and J. T. Devreese, Phys. Rev. B24, 1096 (1981)

[54] A. Baldereschi, Phys. Rev. B7, 5215 (1973)

[55] D. J. Chadi and M. L. Cohen, Phys. Rev B8, 5747 (1973)

[56] M. J. Monkhorst and J. D. Pack, Phys. Rev. B13, 5188 (1976)

[57] Solid State Physics, Vol. 24, ed. by H. Ehrenreich, F. Seitz and D. Turnbull (Academic Press, 1970)

[58] W. A. Harrison: "Pseudopotentials in the Theory of Metals", (New York, Benjamin, 1966)

[59] M. L. Cohen and T. K. Bergstresser, Phys. Rev. 141, 739 (1966)

[60] J.R. Chelikowsky, M.L. Cohen, Phys. Rev. B13, 826 (1976)

[61] W.E. Pickett, S.G. Louie, M.L. Cohen, Phys. Rev. B17, 815 (1978)

[62] K. Kunc in: "Electronic Structure, Dynamics and Quantum Structural Properties of Condenced Matter", ed. by J.T. Devreese (Plenum Publishing, 1985)

[63] W. Hanke and L.J. Sham, Phys. Rev. B12, 4501 (1975); ibid 2, 4656 (1980)

[64] L.J. Sham in Ref. [9] Vol. 1

[65] K. Kunc and R. Resta, Phys. Rev. Lett. 51, 686 (1983)

[66] K. Kunc and R. Martin in Ref. [51]

[67] D.R. Hamann, M. Schluter, C. Chiang, Phys. Rev. Lett. 43, 1494 (1979)

[68] G.B. Bachelet, D.R. Hamann, M.L. Schluter, Phys. Rev. B26, 4199 (1982)

[69] G.P. Kerker, J. Phys. C13, L189 (1980)

[70] K. Kunc and R.M. Martin, Phys. Rev. Lett. 48, 406 (1982)

[71] D.G. Anderson, J. Assoc. Comp. Machinary 12, 547 (1965)

[72] Kai-Ming Ho, J. Ihm and J.D. Joannopoulos, Phys. Rev. B25, 4260 (1982)

[73] S. Baroni and R. Resta, to be published

[74] S. Baroni and R. Resta, to be published

[75] A. Fleszar, K. Kunc, R. Resta and E. Tosatti, Proc. of 2nd Int. Conf. on Phonon Physics, (Budapest, 1985); also to be published

[76] H. Wendel, R.M. Martin, Phys. Rev. Lett. 40, 950 (1978); Phys. Rev. B19, 5251 (1979); Festkorperprobleme 19, 21 (1979)

[77] K. Kunc, R.M. Martin, Phys. Rev. B24, 2311, 2081 (1981)

[78] M.T. Yin, M.L. Cohen, Phys. Rev. Lett. 45, 1004 (1980)

[79] B.N. Harmon, W. Weber, D.R. Hamann, Phys. Rev. B25, 1109 (1982)

[80] K. Kunc, R.M. Martin, Physica 117B, 118B, 511 (1983); "Trends in Physics" (ed. by J. Janta et al., JCMF Prague 1984)

[81] K. Kunc, Helvetica Phys. Acta 56, 559 (1983)

[82] M.L. Cohen, Physica Scripta T 1, 5 (1982)

[83] M.T. Yin in Proc. of 17th Int. Conf. Phys. Semiconductors, ed. by G.D. Chadi, W. Harrison (Springer 1985)

[84] K. Kunc, R.M. Martin, J. Phys. (Paris) 42, Suppl. C6, 649 (1981)

[85] M.T. Yin and M.L. Cohen, Phys. Rev. B25, 4317 (1982)

[86] K. Kunc, Proc. 2nd Int. Conf. Phonon Physics (Budapest 1985)

[87] K. Kunc, P. Gomes Dacosta, Phys. Rev. B32, 2010 (1985)

[88] M.T. Yin and M.L. Cohen, Phys. Rev. B26, 3259 (1982)

[89] O. H. Nielsen and R. M. Martin, Phys. Rev. Lett. 50, 697 (1983); Phys. Rev. B32, 3780, 3792 (1985)

[90] W. Cochran, Phys. Rev. Lett. 2, 495 (1959)

[91] S. K. Sinha, Crit. Rev. Solid State Sci. (USA) 3, 273 (1973); Phys. Rev. 177, 1256 (1969)

[92] J. R. Hardy, Phil. Mag. 6, 27 (1961)

[93] R. M. Martin, Phys. Rev. 186, 871 (1969)

[94] W. Weber, Phys. Rev. Lett. 33, 371 (1974); Phys. Rev. B15, 4789 (1977)

[95] H. L. McMurry, A. W. Solbrig, J. K. Boyter, C. Noble, J. Phys. Chem. Solids 28, 2359 (1967)

[96] R. Tubino, L. Piseri, G. Zerbi, J. Chem. Phys. 56, 1022 (1972)

[97] E. O. Kane, Phys. Rev. B31, 7865 (1985)

[98] M. Born and H. Huang: "Dynamical Theory of Crystal Lattices", (Oxford Univ. Press, 1954)

[99] A. A. Maradudin, E. N. Montroll, G. H. Weiss, I. P. Ipatova: "Theory of Lattice Dynamics in Harmonic Approximation", 2nd edition, Solid State Physics, Suppl. 3, (Academic Press, 1971)

[100] R. Resta and A. Baldereschi, to be published

[101] A. Fleszar and R. Resta, Proceedings of 2nd Int. Conf. Phonon Physics (Budapest 1985); also to be published

[102] M. Takeshima, Phys. Rev. B13, 5618 (1976)

[103] J. A. Appelbaum and D. R. Hamann, Phys. Rev. B8, 1777 (1973)

[104] K. Maschke and A. Baldereschi, Proc. XIV Int. Conf. on the Phys. of Semicon., Edinburgh, 1978 (Inst. Phys. Conf. Ser. 43, 673 (1979))

[105] P. E. Van Camp, V. E. Van Doren and J. T. Devreese, Phys. Rev. B31, 4089 (1985)

[106] G. Nilsson and G. Nelin, Phys. Rev. B3, 364 (1971)

[107] O. H. Nielsen, W. Weber, Comp. Phys. Commun. 18, 101 (1979)

[108] F. Herman, J. Phys. Chem. Solids 8, 405 (1959)

[109] A. W. Solbrig, J. Phys. Chem. Solids 32, 1761 (1971)

[110] E. O. Kane, Phys. Rev. B31, 5199 (1985)

[111] G. Wannier, Phys. Rev. 52, 191 (1937)

[112] C. Kittel and A. H. Mitchell, Phys. Rev. 96, 1488 (1954)

[113] W. Kohn and J. M. Luttinger, Phys. Rev. 97, 1721 (1955); ibid, 98, 915 (1955)

[114] W. Kohn in Solid State Physics, Vol. 5 (Acad. Press 1957)

[115] S. T. Pantelides, Rev. Mod. Phys. 50, 797 (1978)

[116] G. F. Koster and J. C. Slater, Phys. Rev. 95, 1167 (1954)

[117] G. A. Baraff and M. Schluter, Phys. Rev. Lett. 41, 892 (1978); Phys. Rev. B19, 4965 (1979)

[118] J. Bernholc, N. O. Lipari and S. T. Pantelides, Phys. Rev. Lett. 41, 895 (1978); Phys. Rev. B21, 3545 (1980); Proc. 15th Int. Conf. Phys. Semicon., Kyoto (1980), p. 235

[119] G. A. Baraff, E. O. Kane and M. Schluter, Proc. 15th Int. Conf. Phys. Semicon., Kyoto (1980), p. 231

[120] M. Scheffler, Festkorperprobleme 22, 115 (1982)

[121] R. Car, P. J. Kelly, S. T. Pantelides, Proceedings of the 17th Int. Conf. Phys. Semicon., ed. by G. D. Chadi, W. A. Harrison (Springer 1985) p. 713

[122] S. G. Louie, M. Schluter, J. R. Chelikowsky and M. L. Cohen, Phys. Rev. B13, 1654 (1976)

[123] U. Lindefelt, J. Phys. C11, 85 and 3651 (1978)

[124] W. E. Pickett, M. L. Cohen and C. Kittel, Phys. Rev. B20, 5050 (1979)

[125] D. Vanderblit and J. D. Joannopoulos, Phys. Rev. Lett. 49, 823 (1982)

[126] P. Boguslawski, G. Papp and A. Baldereschi, Proc. 17th Int. Conf. Phys. Semicon., ed. by G. D. Chadi, W. Harrison, (Springer 1985) p. 939

[127] L. A. Hemstreet, Phys. Rev. B15, 834 (1977); L. A. Hemstreet and J. O. Dimmock, Phys. Rev. B20, 1527 (1979)

[128] G. G. DeLeo, G. D. Watkins and W. B. Fowler, Phys. Rev. B23, 1851 (1981); ibid, B25, 4962 (1982)

[129] A. Baldereschi, Phys. Rev. B1, 4673 (1970)

[130] L. Resca and R. Resta, Solid St. Commun. 29, 275 (1979);

Phys. Rev. Lett. 44, 1340 (1980)

[131] M. Altarelli, W. Y. Hsu, Phys. Rev. Lett. 43, 1346 (1979); M. Altarelli, W. Y. Hsu, R. A. Sabatini, J. Phys. C10, L605 (1977)

[132] H. J. Mattausch, W. Hanke and G. Strinati, Phys. Rev. B26, 2302 (1982); ibid, B27, 3735 (1983)

[133] J. Baur, K. Maschke and A. Baldereschi, Phys. Rev. B27, 3720 (1983)